Mechanism of CFTR Dislocation During Endoplasmic Reticulum-associated Degradation

by

Eric J. Carlson

A DISSERTATION

Presented to the Department of Cell & Developmental Biology

and the Oregon Health & Science University

School of Medicine

in partial fulfillment of

the requirements for the degree of

Doctor of Philosophy

2006

School of Medicine
Oregon Health & Science University

CERTIFICATE OF APPROVAL

This is to certify that the Ph.D. dissertation of

Eric J. Carlson

has been approved

[redacted]
Mentor

[redacted]
Member

[redacted]
Member

[redacted]
Member

[redacted]
Member

Table of Contents

Table of Figures

ACKNOWLEDGEMENTS

To my wife and children for their patience all these years, and to everyone who helped along the way. Many thanks.

Abstract

Cystic fibrosis is a lethal recessive disorder caused by inherited mutations in the cystic fibrosis transmembrane conductance regulator (CFTR). Sixty to eighty percent of wild type CFTR is degraded, and the most common mutation, deletion of F508, leads to essentially complete degradation by the proteasome. Therefore, a detailed understanding of the degradation pathway would provide useful information for developing therapeutics. To identify components in CFTR degradation, two compartments were examined: membrane-localized components and cytosolic components. Inactivation of membrane proteins had no effect on CFTR degradation suggesting that either membrane proteins were not sensitive to treatment or that cytosolic proteins with redundant functions exist. In contrast, affinity depletion of rabbit reticulocyte lysate (RRL) using nonhydrolyzable ubiquitin fusion proteins containing E2 ubiquitin conjugating enzymes (Ub-UbcH5a (uu5) and Ub-Ubc6 (uu6)) decreased CFTR degradation significantly. Adsorbed proteins eluted from uu5 beads were identified by liquid chromatography-tandem mass spectrometry (LC-MS-MS), and the most abundant protein identified was the AAA-ATPase, p97. Adaptor proteins mediate the diverse functions of p97, which range from membrane fusion to degradation. The heterodimer ufd1/npl4 binds ubiquitinated substrates and directs p97 to the degradation pathway where p97 has been proposed to segregate components of protein complexes, provide the driving force for dislocation and serve as an intermediary in presenting substrates to the proteasome. Given its proposed role in ERAD, p97 was chosen for further characterization in CFTR degradation. Depletion of RRL p97 resulted in a 50% reduction in both the rate and extent of CFTR degradation. However, p97 depletion had no effect on the degradation of

cytosolic domains but specifically stimulated degradation of transmembrane domains (TMDs). Moreover, the stimulatory effect was dependent on TMD hydrophobicity and stability. This effect was also correlated with the rate of degradation, suggesting that p97 functions as an accessory factor to the proteasome and enhances the rate and efficiency of thermodynamically stable transmembrane domain dislocation and degradation.

CHAPTER 1

Introduction

Note: Strategy section derived from the introduction of *Carlson, et al, Methods in Molecular Biology, 301: 185-205. 2005.*

I. Cystic fibrosis

Many diseases, including cystic fibrosis (CF), result from protein misfolding. The cellular quality control machinery recognizes misfolded proteins, which are then targeted for degradation by the cytosolic ubiquitin-proteasome system. The disruption in processing and trafficking of the substrate leads to disease phenotypes. Cystic fibrosis is a recessively inherited genetic disease characterized by fibrosis of the pancreas and viscous mucus production leading to infection and inflammation in the lung, pancreas, gut, and vas deferens (Chillon et al., 1995; Lowe et al., 1949; Quinton, 1999). CF patients secrete sweat with high salt, and cystic fibrosis was proposed to result from impaired electrolyte transport when it was shown that Cl^- could not be absorbed in CF sweat glands (Quinton, 1983). A systematic search of the disease locus resulted in the identification in 1989 of a regulated chloride channel called the cystic fibrosis transmembrane conductance regulator (CFTR) (Riordan et al., 1989; Rommens et al., 1989). CFTR is localized to the apical membrane of polarized epithelial cells with primary expression in the gut, lungs, pancreas, and sweat glands. It functions to regulate epithelial Cl^-, salt, and water transport, thus providing a mechanistic explanation for the diverse phenotypes observed in CF.

A puzzling aspect of CF is that genotype and phenotype are weakly correlated except in the case of pancreatic insufficiency. In the pancreas, chloride secretion is required for bicarbonate secretion, and without bicarbonate secretion, the decreased fluid volume and pH result in inefficient clearance of the digestive enzymes from the pancreas leading to early enzyme activation and autolysis of the ducts (Choi et al., 2001; Quinton,

1986; Steward et al., 2005). By contrast, lung disease is much more complex. Thick mucus, decreased mucus clearance, and increased infection by pathogens including *Pseudomonas auruginosa* and *Haemophilus influenza* lead to increased inflammation (Gibson et al., 2003; Rowe et al., 2005). Although not entirely explained, a major part of this appears to be related to airway surface liquid (ASL) (Matsui et al., 1998). ASL is a thin film of water, typically 7-10 μm in depth, coating the luminal surface of bronchi and small airways that covers cilia. ASL provides a liquid interface between cilia and the mucus layer (Knowles and Boucher, 2002). The depth of the ASL is determined by coordinated regulation of Na^+ absorption by the epithelial Na^+ channel (ENaC) and Cl^- secretion by CFTR and the Ca^{2+} activated chloride channel (CaCC) (Stutts et al., 1995; Tarran et al., 2005a). Recent findings suggest that the ratio of nucleotide/nucleoside and shear stress caused by breathing regulate chloride secretion, and CF patients rely only on the shear stress activation of Cl^- making them more susceptible to disruption in ASL regulation (Tarran et al., 2005a; Tarran et al., 2005b). Inability to clear mucus efficiently leads to recurrent pneumonia infections and inflammation causing progressive lung damage, and ultimately death by asphyxiation. The median age of survival has risen from 1-2 years to over 30 years largely due to antibiotics and aggressive maneuvers to clear airway secretions (CFF, 2004; Gibson et al., 2003).

CFTR

CFTR is a member of the ABC transporter family and contains two transmembrane domains (TMD) with six TM segments each, two nucleotide binding domains (NBD), and an additional cytosolic regulatory domain (R domain) (Riordan et al., 1989). The ATP binding sites are thought to be sandwiched within the interface of the

NBD dimer, analogous to bacterial ATP transporters (Figure 1-1) (Locher et al., 2002). Site 1 has the Walker A motif in NBD1 and signature sequence in NBD2, while site 2 consists of the Walker A and the signature sequence in NBD2 and NBD1, respectively. Thus, NBD dimerization is critical for ATP binding and hydrolysis (Locher et al., 2002). In CFTR the Site I ATPase is inactive because a critical glutamate residue in the site 1 Walker B motif is mutated to serine (E573S) (Lewis et al., 2004; Sheppard and Welsh, 1999). ATP bound to site I has been proposed to prime CFTR where ATP binding at site II opens the channel and hydrolysis closes the channel (Riordan, 2005). Thus, the Cl^- channel is rapidly inactivated by a single hydrolysis event.

By analogy to cyclic nucleotide gated channels, CFTR can be considered a hydrolysable ligand gated channel with ATP as ligand (Kaupp and Seifert, 2002; Riordan, 2005). Additional regulatory constraints are imposed by the R domain (Ostedgaard et al., 2001), which contains numerous sites for phosphorylation by both PKA and PKC (Riordan et al., 1989). Intriguingly, a recent study suggests that phosphorylation of the R domain promotes association with other CFTR domains (Chappe et al., 2005). Both ATP binding and phosphorylation are required for channel activity; however, phosphorylation can both activate and inhibit Cl^- channel activity (Gadsby and Nairn, 1999).

Additionally, CFTR associates with and regulates many other proteins (Amaral, 2005). The N-terminus both regulates CFTR function via interactions with the R domain and also associates with syntaxins 1A and 8 (Bilan et al., 2004; Naren et al., 1997). In contrast, the C-terminus contains a PDZ-binding motif (TDRL) which mediates interactions with ezrin binding protein (NHERF) (Hall et al., 1998) and thereby couples

CFTR to the plasma membrane scaffolding protein ezrin which coordinates interactions with kinases, phosphatases and the cytoskeleton (Short et al., 1998). Thus the C-terminus of CFTR is important in regulating CFTR localization and activity (Moyer et al., 1999). ENaC, the epithelial sodium channel, and the bicarbonate/chloride antiporter are regulated by CFTR and control airway surface liquid and pancreatic secretion, respectively (Choi et al., 2001; Stutts et al., 1995). Thus, CFTR plays a key role in regulating other proteins, although the precise mechanism and tissue specificity of this process is not fully understood.

Over 1,000 inherited mutations have been identified throughout the CFTR gene (CF Genetic Analysis Consortium://www.genet.sickkids.on.ca/cftr/) and have been variably grouped into six different classes (Welsh et al., 2001; Zielenski, 2000; Zielenski and Tsui, 1995). Class I mutations result in an absence of CFTR synthesis; Class II mutations disrupt processing and intracellular trafficking (and include ΔF508); Class III have disordered regulation, Class IV have defective conductance or gating, and Class V are splicing mutants. Finally, Class VI mutants show decreased stability at the plasma membrane, probably due to decreased recycling from the early endosomal compartment. The most common mutation, deletion of Phe508 (ΔF508, a Class II mutant), is found in 70% of all disease alleles and >90% of CF patients. ΔF508 CFTR fails to exit the endoplasmic reticulum (ER) for further processing in the Golgi and is degraded via the ER-associated degradation (ERAD) pathway. 60-80% of wild type CFTR is also inefficiently processed in most cell types studied (Cheng et al., 1990; Jensen et al., 1995; Meacham et al., 2001; Ward et al., 1995), although recent evidence suggests that native epithelia may process endogenous CFTR more efficiently (Varga et al., 2004). As a

prototype for studying folding disorders, broad insight for other disorders has been gained from studying the folding, recognition, and degradation of CFTR. Additionally, because CFTR is a clinically important substrate, an increased understanding of maturation and degradation has potential therapeutic applications.

II. Endoplasmic reticulum-associated degradation

Secretory and membrane proteins that are misfolded in the endoplasmic reticulum (ER), undergo degradation via a specialized degradation pathway ERAD. Targeting misfolded proteins to the ubiquitin-proteasome pathway involves many steps including substrate recognition, ubiquitination, presentation to the proteasome, unfolding and translocation into the proteolytic core, and finally degradation of the substrate into TCA (trichloroacetic acid) soluble peptides. This process also requires dislocating the substrate from either the lumen or the lipid bilayer to the cytosol where the ubiquitin-proteasome system is located.

Folding

CFTR is a glycoprotein with 12 TMs and three large cytosolic loops. Its complex architecture is characterized by a kinetic folding defect that results in ERAD for both wild type and mutant proteins (Du et al., 2005; Kleizen et al., 2005; Qu et al., 1997; Thibodeau et al., 2005). Both intradomain (helical packing) and interdomain (TMD and NBD association) interactions occur both co- and posttranslationally (Figure 1-2), and this process is enabled by chaperones (Lu et al., 1998). Since CFTR is an integral membrane protein, both luminal and cytosolic chaperones participate in the folding process.

Cytosolic chaperones important in CFTR maturation include Hsp70 that, together with the J domain containing cofactor Hsp40/DnaJ, is important in early CFTR biogenesis (Meacham et al., 1999). ATP-bound Hsp70 binds hydrophobic patches, thereby decreasing aggregation. Hsp40 associates with Hsp70, promoting ATP hydrolysis which stabilizes Hsp70 binding (Minami et al., 1996). GrpE then promotes ADP release, and upon rebinding ATP, Hsp70/Hsp40 dissociate from the substrate (Packschies et al., 1997). The binding and release cycle may occur repeatedly. During CFTR folding, Hsp70/DnaJ2 bind to NBDs, and later recruit Hsp90 (Loo et al., 1998; Youker et al., 2004). Another cofactor, Hip, a tetratricopeptide repeat (TPR) protein, can displace Hsp40, stabilizing Hsp70 binding to substrate (Hohfeld et al., 1995). After Hip binding, an additional TPR-containing cochaperone, Hop, recruits Hsp90 to the growing complex (Chan and Smith, 1998). Hip, Hop, and Hsp70 are displaced from the complex by p23 and an immunophilin, FKBP8 in the case of CFTR, form the final maturation complex (Frydman and Hohfeld, 1997; Wegele et al., 2004) before export from the ER. When CFTR fails to fold efficiently (Wang et al., 2004), both wild type and mutant protein are targeted for degradation.

Substrate recognition

As proteins fold they interact with the cellular quality control system including chaperones, which play the dual role promoting both maturation and degradation depending on the associated cofactors (Zhang et al., 2001). For CFTR, Hsp70 appears to be critical in this process. An important question in the field, therefore, is how cochaperones determine the pathway- profolding or shunt to degradation. Hsp70 may function as a clock with prolonged interaction causing the substrate to be directed into the

degradation pathway. Consistent with this, Hsp70 cochaperones such as the TPR-containing ubiquitin ligase, CHIP (Meacham et al., 2001) and J domain cysteine string protein (CSP) (Zhang et al., 2002) promote degradation. In contrast, the cofactor HspBP1 inhibits CHIP activity, and thus promotes maturation (Alberti et al., 2004).

As a glycoprotein, CFTR is subject to arguably the best understood quality control chaperones, the calreticulin/calnexin cycle (Pind et al., 1994). Similar to cytosolic chaperones, prolonged cycling with these chaperones results in substrates being targeted to ERAD via mannosidase trimming of the mannose core carbohydrates and recognition by another lectin called EDEM (Gnann et al., 2004). However, the luminal loops of CFTR are very small (2-30 residues), and luminal chaperones such as calnexin/calreticulin, protein disulfide isomerase, and the Hsp70 and Hsp90 homologs (BiP/kar2 and Grp94, respectively) appear to be relatively unimportant in CFTR degradation. In summary, cytosolic chaperones appear to be critical in the decision between the folding and degradation of CFTR, whereas chaperones in other compartments do not.

Ubiquitination

Proteins are targeted for degradation by a cascade of enzymes called ubiquitin activating enzyme (E1), ubiquitin conjugating enzymes (E2s), and ubiquitin ligases (E3s) (Ciechanover, 1994; Hershko and Ciechanover, 1998). E1 activates ubiquitin by forming a high energy thioester bond. The activated ubiquitin is then transferred to an E2 enzyme. E3s interact with E2s to transfer ubiquitin to lysine residues on specific substrates via an isopeptide bond. In some cases ubiquitin is transferred directly by the E2 while in other cases, it is transiently transferred to the E3. A single E1, about a dozen

identified E2s- perhaps more in mammals, and hundreds of E3s have been identified in cells. Importantly, different combinations of E2s and E3s confer specificity to the reaction (Glickman and Ciechanover, 2002).

E3s are comprised of both single proteins and protein complexes. HECT (homologous to E6AP carboxyl-terminus) domain ligases represent the prototypical E3 family (Schwarz et al., 1998), and the canonical cascade of ubiquitin transfer is based on their function (Huang et al., 1999). However, a much larger group contains RING (Really Interesting New Gene) domains, which are modified zinc fingers (Borden, 2000). RING E3 ligases are also made up of either single proteins or protein complexes, such as SCF (Skp1, cullin1, F box), VHL (von Hippel Lindau complex), and APC/ C (Anaphase Promoting Complex/cyclosome) (Deshaies, 1999). SCF ligases are multiprotein ligases consisting of a backbone of cullin1 that binds Skp1 which in turn binds the substrate binding module (the F box protein) and predominantly utilizes the E2 cdc34/ubc3 (yeast) (Deshaies, 1999). Membrane-localized ligases include the Doa10 (MARCH VI (membrane associated ring CH) in mammals) ligase (Bartee et al., 2004; Gnann et al., 2004), the Hrd1/Hrd3 complex (Wilhovsky et al., 2000), and gp78 (Zhong et al., 2004). Finally, the U-box family of ligases are single protein RING ligases (Hatakeyama et al., 2001).

Four E3 ligases have been implicated in CFTR degradation. The first is a ligase that binds cytosolic domains of CFTR and contains Hsp70, the U-box protein CHIP, and the E2 ubcH5 (Meacham et al., 2001). Second, SCF^{FBX2} binds glycosylated proteins located in the cytosol after dislocation, including CFTR (Yoshida et al., 2002). Third, Doa10 and Hrd1/Hrd3 have been implicated in CFTR degradation in yeast, which does

not have CHIP (Gnann et al., 2004). The mammalian homolog of Doa10, MARCH VI, has been identified and contains fourteen transmembrane segments (Bartee et al., 2004). However, the structural feature that this ligase recognizes has yet to be identified, and a role in CFTR degradation in mammalian systems has not been established. Lastly, a complex containing derlin-1 (der1-like protein) was recently proposed by Cyr et al to recruit tail-anchored proteins to the ER membrane including VIMP (Ye et al., 2004) and Rma1. Rma1 has been proposed to function as an ER membrane sensor that recognizes misfolded TM domains (D. Cyr, personal communication). In summary, both cytosolic and membrane-localized ligases are involved in CFTR degradation and recognize cytosolic and transmembrane segment cues during the protein folding process.

Dislocation

A unique feature of ERAD is that substrates in the endoplasmic reticulum compartment must be dislocated into the cytosol where the ubiquitin-proteasome system is located. Two things appear to be required for this to occur: a translocation channel and a driving force. Both luminal and membrane ERAD substrates including CPY* and Pdr5 appear to use the sec61 translocon channel (Huyer et al., 2004; Plemper et al., 1998). However, yeast sec61 mutants had little effect on the degradation of the ABC transporter Ste6 (Huyer et al., 2004), or the tail-anchored E2 ubc6 (Walter et al., 2001), suggesting the existence of a novel channel for partitioning TMs into the aqueous environment. Alternatively, membrane proteins may be directly extracted from the lipid bilayer.

One area that has received considerable recent attention is the driving force for dislocation. ERAD substrates and the proteasome system reside in distinct compartments, and dislocation from the ER into the cytosol requires crossing or

extraction from a hydrophobic barrier, the ER membrane. Two AAA-ATPases (ATPases Associated with various cellular Activities) (Ogura and Wilkinson, 2001) have been implicated in this process: p97 and the 19S regulatory complex (RC) of the proteasome (Mayer et al., 1998; McCracken and Brodsky, 2003; Pickart and Cohen, 2004; Plemper et al., 1998; Ye et al., 2001). Both ATPases associate with the 20S proteasome, bind directly to polyubiquitinated proteins and facilitate degradation of both ER and cytosolic substrates (Bays and Hampton, 2002; Dai et al., 1998; Pickart and Cohen, 2004). Both localize to the ER, although by different mechanisms. The 19S directly interacts with the Sec61 (Kalies et al., 2005) translocon, whereas p97 binds indirectly via interaction with ubiquitin ligases, derlin-1, and ubx2 (Lilley and Ploegh, 2004; Neuber et al., 2005; Schuberth and Buchberger, 2005; Ye et al., 2004; Zhong et al., 2004).

Despite evidence implicating the 19S RC and p97 in ER-associated degradation (ERAD), their precise role remains unknown and somewhat controversial. The AAA-ATPases (Rpt1-6) collectively open the gate into the 20S core (Kohler et al., 2001), exhibit chaperone-like activity (Braun et al., 1999; Liu et al., 2002) and facilitate assembly and disassembly of the 26S proteasome during the degradation cycle (Babbitt et al., 2005). Thus it is possible that 19S unfolding activity might play a direct role in dislocating ERAD substrates from the ER lumen and/or bilayer. Consistent with this, functional proteasomes are required for the tight coupling of membrane extraction and proteolytic cleavage during degradation of ER membrane proteins (Mayer et al., 1998; Xiong et al., 1999). Moreover, purified 19S RC is sufficient for ATP-dependent dislocation of the luminal substrate, pro-alpha factor (Lee et al., 2004).

Accumulating evidence has suggested that p97 rather than the 19S regulatory subunit is primarily responsible for ER dislocation. Functioning together with its cofactors, Ufd1 and Npl4, p97 exhibits unfolding/segregating activity and plays an important role in presenting substrates to the proteasome (Richly et al., 2005; Verma et al., 2004). Inactivation of p97 or its adaptor proteins reduces the degradation of ubiquitinated ERAD substrates including PDR5, Ste6, CFTR, HmgCoA, Spt23, Mga2, and CPY* (Bays et al., 2001; Elkabetz et al., 2004; Gnann et al., 2004; Hitchcock et al., 2001; Huyer et al., 2004; Jarosch et al., 2002; Rabinovich et al., 2002; Rape et al., 2001). p97 inhibition or addition of dominant negative p97 also decreases reduces US11-dependent dislocation and degradation of MHC I (Ye et al., 2001) and stabilizes a mutant form of CFTR (ΔF508) (Dalal et al., 2004). Thus, understanding the precise role of p97 has broad and significant implications for the function and regulation of cellular degradation and is the primary focus of this dissertation (Figure 1-3).

Presentation to the proteasome

Tetraubiquitin is the minimal signal for binding to the 19S proteasome (Thrower et al., 2000), and both Rpn10 and Rpt5 have been shown to bind directly to polyubiquitinated substrates (Ferrell et al., 2000; Lam et al., 2002). However, adaptor proteins containing UBL domains also facilitate substrate presentation (Hartmann-Petersen and Gordon, 2004). Rad23 and dsk2 (hPLIC), contain both UBA (ubiquitin associated) domains, which bind ubiquitin, and UBL (ubiquitin like) domains that can present ERAD substrates including Sic1,CPY* and HmgCoA to the proteasome (Richly et al., 2005; Verma et al., 2004). p97 has been proposed to coordinate substrate presentation by protecting the substrate from deubiquitinating enzymes while the

polyubiquitin chain is elongated before the transfer of substrate to UBA/UBL domain proteins (Richly et al., 2005). As there are many UBA and UBL domain proteins, multiple presentation pathways to the proteasome may exist (Buchberger, 2002; Hartmann-Petersen and Gordon, 2004; Verma et al., 2004). These pathways are predicted to be broadly overlapping, but do have some substrate specificity. Doa10, a membrane-localized E3, likely utilizes the p97 pathway (Gnann et al., 2004). However, cytosolic E3 ligases such as SCF complexes (SCF^{Fbx2}) can interact directly with the proteasome in a nucleotide-dependent manner (Verma et al., 2000). Additionally, the Hsp70 cochaperone Bag-1 contains a UBL domain and thus may facilitate presentation of CFTR via the CHIP ligase complex (Luders et al., 2000).

Unfolding and degradation

Degradation of a substrate into TCA soluble peptides is the final step of the quality control process. Before translocation into the catalytic 20S chamber can occur, the substrate must be unfolded (Pickart and Cohen, 2004). For ERAD, this includes dislocation and membrane extraction. Substrate unfolding is initiated near the site of ubiquitination, and local instability enables degradation to proceed rapidly (Lee et al., 2001; Prakash et al., 2004). However, ERAD substrates are problematic in two regards. First. ubiquitination machinery is in the cytosol or on the cytosolic face of the ER membrane, so lumenal proteins must be dislocated in order to be ubiquitinated. This problem appears to be overcome in part by the coordination of substrate, E3 ligase, and dislocation driving force by the UBA protein, ubx2 (Neuber et al., 2005; Schuberth and Buchberger, 2005). The second problem is that membrane proteins are integrated into the lipid bilayer and are likely stable, but transmembrane segments with polar residues

may introduce instability where unraveling of the substrate could begin. Unfolding of substrates also appears to be rate limiting, and degradation of folded substrate is slower and energetically costly (1 ATP/residue) compared to the degradation of denatured substrate (Kenniston et al., 2003). This is consistent with ATP-independent degradation by PA28-capped proteasomes. Membrane proteins pose a particular problem in that hydrophobic TMs in the lipid bilayer must be extracted prior to unfolding. Overcoming this energy barrier may result in inefficient partitioning of substrate into degradation (Kenniston et al., 2005), and a second unfolding activity (p97) would likely enhance the process.

The proteasome

The proteasome is a multicatalytic protease present in the cytosol and nucleus consisting of a 20S core particle and capped by regulatory particles, the best described being the 19S regulatory subunit (PA700) and PA28 (11S, REG) (Pickart and Cohen, 2004; Rechsteiner and Hill, 2005). Proteolytic activity is located within the chamber formed by the subunits of the 20S core, and access is gained by translocation through the axial pores (Voges et al., 1999). The core is formed of a stack of four heptameric rings ($\alpha\beta\beta\alpha$) consisting of seven alpha subunits in the outer rings and seven beta subunits in the inner rings. Three beta subunits have catalytic activity: β1 has peptidylglutamyl peptide hydrolyzing-like activity, β2 has trypsin-like activity, and β5 has chymotrypsin-like activity (Dick et al., 1998). Together these proteases cleave substrates such that the end products of degradation are TCA soluble fragments (4-22 a.a.) (Emmerich et al., 2000; Kisselev et al., 1999b). The proteasome is the only known cellular protease described that degrades substrates with this property.

To control the spatial regulation of degradation, access to the 20S core is regulated by "caps." The 19S particle consists of at least 18 subunits that include a hexameric ring of AAA-ATPases (Rpt1-6) in the base, and a lid comprised of Rpn (non-ATPase) subunits (Ferrell et al., 2000). Rpn 10 can bind polyubiquitinated proteins directly and therefore facilitate substrate recruitment (Wilkinson et al., 2000). Additionally, Rpn1and 2 bind UBL domains and may serve as docking sites to facilitate presentation by linker proteins such as Rad23, dsk2, and Bag1 (Elasser et al., 2002; Saeki et al., 2002). Rpn11 deubiquitinates substrates which is required for translocation into the 20S core (Verma et al., 2002). ATPases bind polyubiquitinated substrate, gate the 20S particle and have chaperone-like activity, unfolding and threading substrate into the catalytic chamber (Braun et al., 1999; Kohler et al., 2001; Lam et al., 2002; Liu et al., 2002). PA28, an alternative cap, gates entry into the catalytic core in an ATP-independent manner but does not directly bind ubiquitinated proteins (Dubiel et al., 1992). Release of cleaved fragments may be facilitated by both dissociation of the 19S regulatory particle from the 20S core (Babbitt et al., 2005; Voges et al., 1999) and by PA28 recruitment.

III. Strategy

Much of our early knowledge of the ubiquitin proteasome pathway originated from biochemical characterization of cytosolic extracts such as rabbit reticulocyte lysate (RRL). While early studies focused primarily on cytosolic degradation substrates (Hershko and Ciechanover, 1998), RRL also contains the necessary factors to carry out ERAD and has recently been used to identify and dissect various components and steps involved in degrading secretory (Gusarova et al., 2001; Qu et al., 1996) and membrane

proteins (Sato et al., 1998; Wilson et al., 1995; Xiong et al., 1999). One approach that has proven particularly useful is to combine the capacity of RRL for both membrane protein biogenesis and degradation. When supplemented with ER-derived microsomal membranes, RRL retains newly synthesized membrane proteins in a functional ER compartment that is readily amenable to biochemical manipulation.

The strategy employed in this dissertation entailed the use of RRL for reconstitution, quantitation, and manipulation of the ERAD pathway. The methods described use rough microsomes derived from canine pancreas (CRM) as a source of functional ER membranes, although other sources such as *Xenopus laevis* oocytes (Kobilka, 1990; Lu et al., 2000), semi-permeabilized cells (Wilson et al., 1995), or yeast (Brodsky et al., 1993) could potentially be used. The RRL system has a robust degradation activity that likely reflects the terminally differentiated state of reticulocytes in which cellular organelles and most cytosolic proteins are being degraded.

A major advantage of this system is that the substrate is synthesized *in vitro*, and is thus the only protein that contains significant incorporated radioisotope (Jackson and Hunt, 1983). It is therefore possible to quantitatively measure substrate entry into the degradation pathway (ubiquitination) and its progressive conversion into TCA soluble peptide fragments. Release of substrate from the ER membranes can also accomplished by simple fractionation techniques, and both microsomes and lysate are directly accessible to pharmacological and/or biochemical modification prior to or during the degradation reaction. Utilizing this system, we were able to address the roles of two AAA-ATPases in the dislocation of the polytopic membrane protein CFTR.

Figure 1-1. ABC transporter structure (from Lochor, K.P. et al, Science, 296:1091-1098. 2002). **A.** A side view of the *E. coli* vitamin B_{12} transporter showing the arrangement of TMDs (purple and red) and NBDs (green and blue). Cyclotetravanadate (ball and stick) is located in the ATP binding pockets, which are sandwiched between the two NBDs. The black lines indicate approximate boundaries of the membrane bilayer. CFTR is unique among ABC transporters in that it can hydrolyze ATP at only one site. **B.** A bottom view of the BtuCD NBDs that more clearly indicates how ATP binding sites are comprised of regions on both NBDs with the Walker A motif (ATP binding) and Walker B (ATP hydrolysis) contributed from one NBD and the signature sequence (ATP binding) from the other NBD.

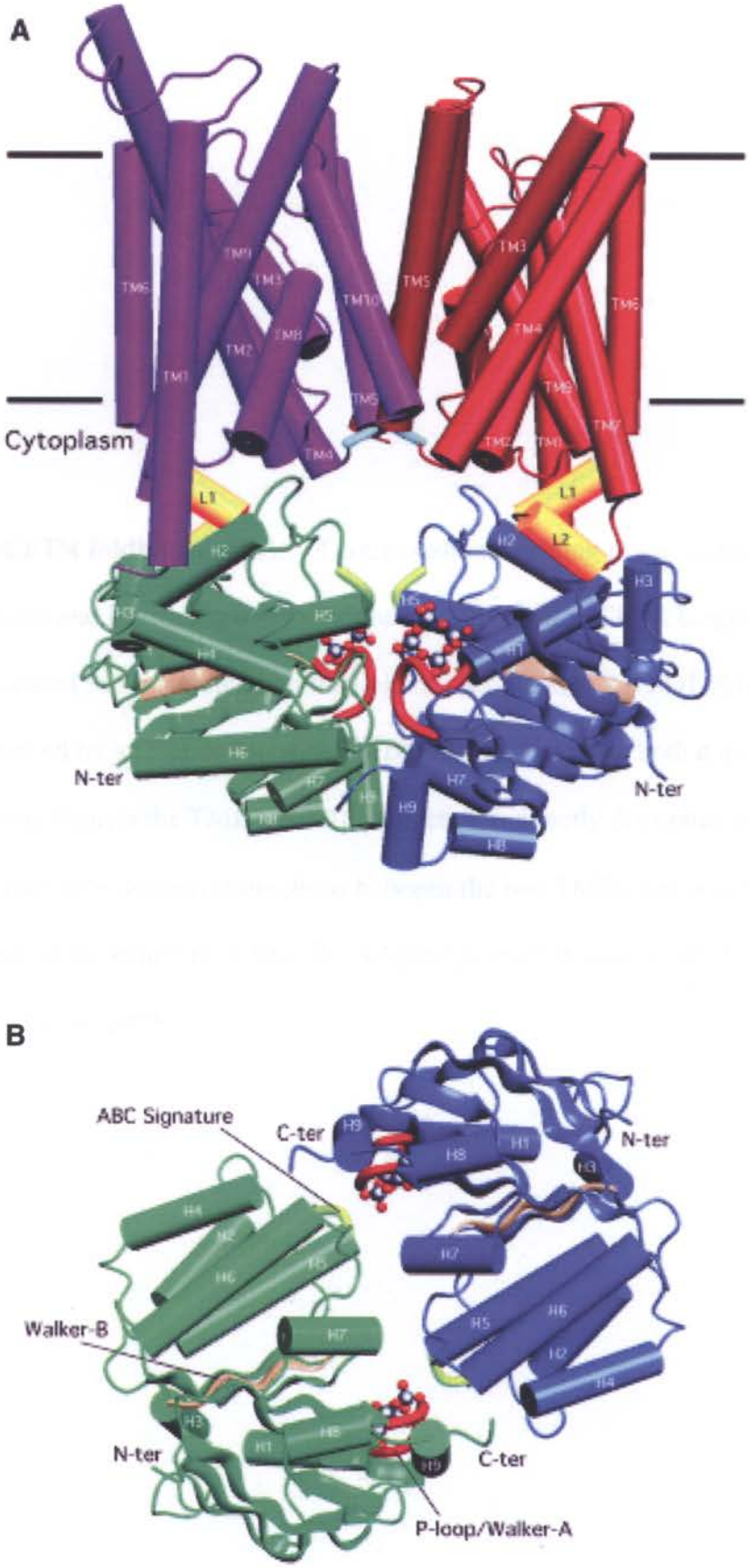
A
Cytoplasm
TM1
TM2
TM3
TM4
TM5
TM6
TM7
TM8
TM9
TM10
L1
L2
H1
H2
H3
H4
H5
H6
H7
H8
H9
N-ter
N-ter
B
ABC Signature
C-ter
N-ter
Walker-B
N-ter
C-ter
P-loop/Walker-A

Figure 1-2. CFTR folding. A model of cotranslational folding events indicating that both intradomain and interdomain associations are important in CFTR biogenesis. First TMD1 is translated and integrated into the lipid bilayer. In step 2 NBD1-R is translated and folds followed by an interaction with TMD1 that may stabilize both domains. The ΔF508 mutation disrupts the TMD1/NBD1 interaction indirectly disrupting downstream steps, particularly interdomain interactions between the two TMDs and two NBDs. The model is based on the structure of BtuCD. *Adapted from Thibodeau et al, Nat. Struct. Mol. Biol. 12: 10-16, 2005.*

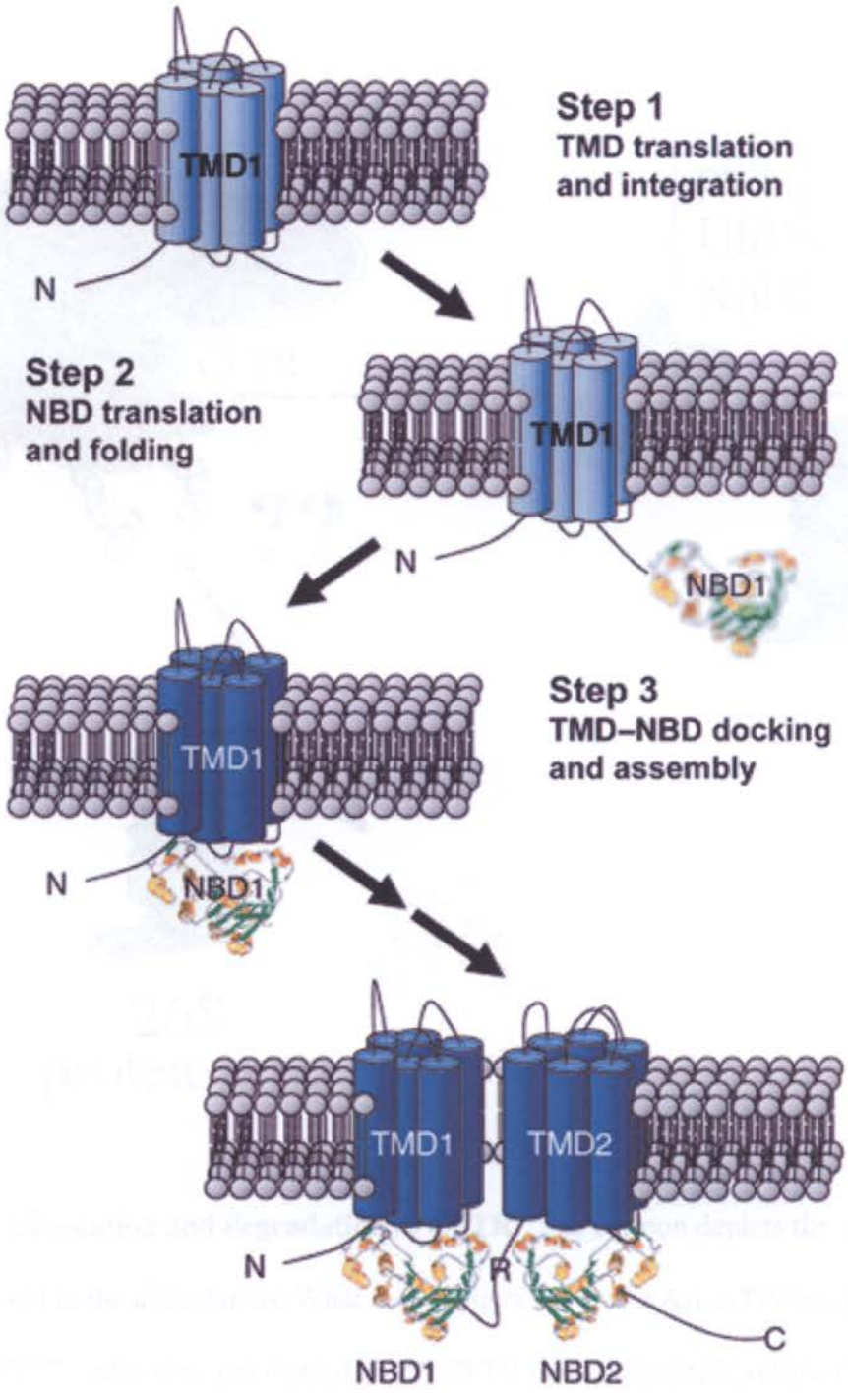
Step 1
TMD translation
and integration
TMD1
N
Step 2
NBD translation
and folding
TMD1
N
NBD1
Step 3
TMD–NBD docking
and assembly
TMD1
N
NBD1
TMD1
TMD2
N
C
NBD1
NBD2

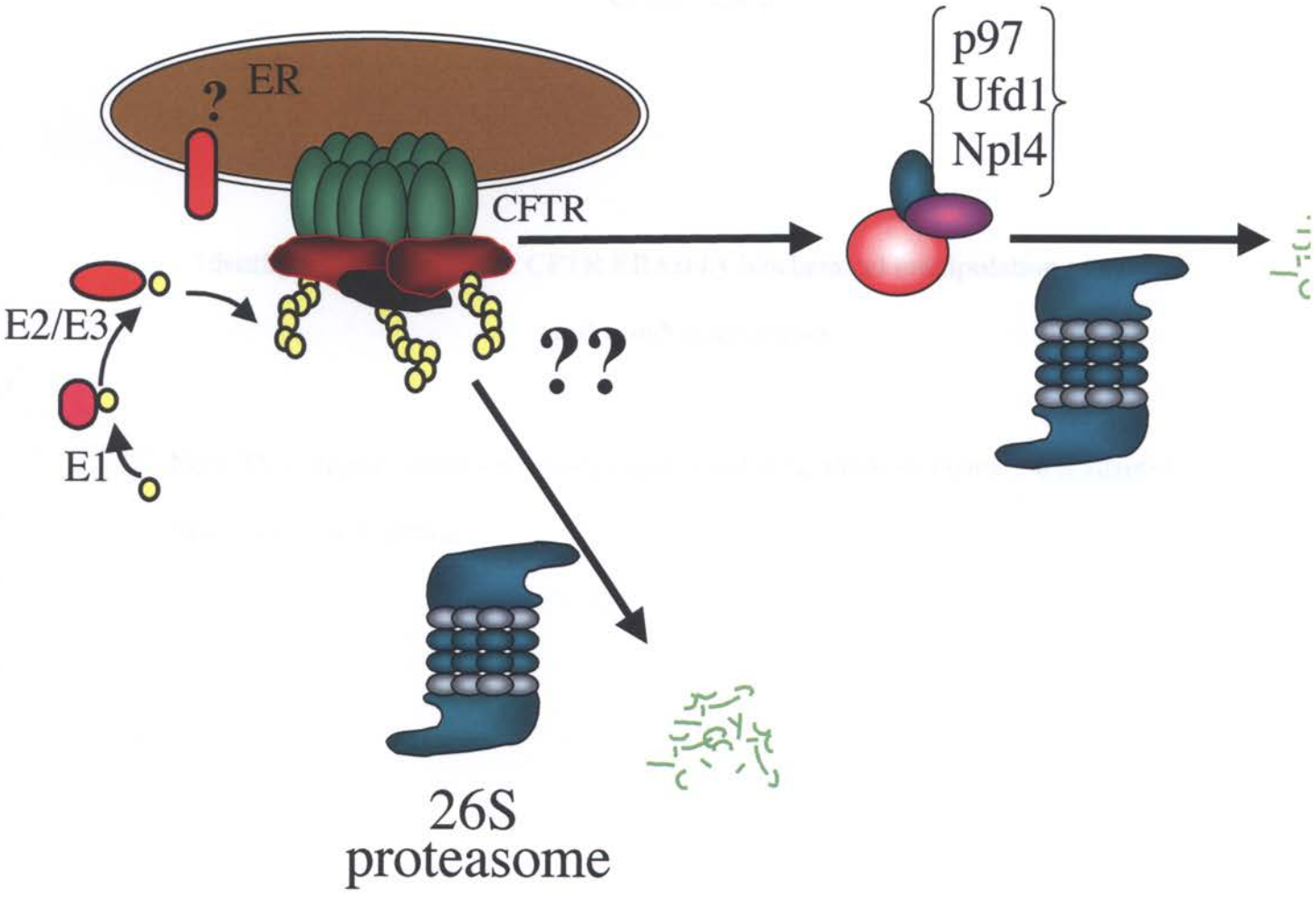

Figure 1-3. Dislocation and degradation of CFTR. The cartoon depicts the question being addressed in the dissertation: What is the role of the two AAA-ATPases, p97 and 19S RC, in CFTR extraction and degradation? CFTR is ubiquitinated (yellow circles). This tag is required for interaction with both ATPases. Although only a cytosolic E3 ligase is shown, membrane-localized ligases are likely involved in CFTR ubiquitination (represented by red cylinder).

CHAPTER 2

Identifying components of CFTR ERAD by biochemical manipulation of cytosol and rough microsomes

Note: This chapter contains primarily unpublished data, although Figure 2-8 is adapted from Chapter 4, Figure 2.

CHAPTER 2

Identifying components of CFTR ERAD by biochemical manipulation of cytosol and rough microsomes

Note: This chapter contains primarily unpublished data, although Figure 2-8 is adapted from Chapter 4, Figure 2.

Abstract

Membrane proteins reside in three distinct compartments: the endoplasmic reticulum (ER) membrane, the ER lumen, and the cytosol. To determine which of these compartments house quality control machinery we used an *in vitro* rabbit reticulocyte lysate (RRL) system to analyze rough microsomes and lysates for components of CFTR ERAD. Remarkably, protease stripping or alkylation of microsomes with N-ethylmaleimide had no effect on CFTR degradation. However, affinity depletion of RRL with His-tagged recombinant nonhydrolyzable ubiquitin fusion proteins (UFP) markedly reduced CFTR degradation (~50%). LC-MS-MS analysis of eluate from UFP loaded beads identified chaperones, deubiquitinating enzymes, E3 ubiquitin ligases, and 19S ATPases. Strikingly, the predominant component of the eluate was the AAA-ATPase, p97. By refining the depletion strategy using a specific p97 adaptor protein, p47, we were able to deplete >99% of p97 from the cytosolic lysate. This enabled us to study the role of p97 in CFTR degradation and membrane extraction in detail (see Chapter 4).

Introduction

The cystic fibrosis transmembrane conductance regulator (CFTR) is inefficiently processed in the endoplasmic reticulum (ER) and subsequently degraded by the 26S proteasome. Although many ERAD components have been identified a unique set of overlapping proteins appears to be required for many of the substrates examined to date. Attempts to generalize which proteins will be needed based on cytosolic or luminal mutation has proven a difficult task and definite rules have thus far been elusive.

Yeast genetic screens have provided a powerful tool to identify ERAD components (Nishikawa et al., 2005). Degradation of luminal substrates, not surprisingly involves the luminal chaperones, BiP/Kar2 and protein disulfide isomerase (PDI). Membrane-localized components such as the E3 ligases, Hrd1/Hrd3 and Doa10, are utilized for the ubiquitination of both luminal and membrane proteins, including PDR5, HmgCoA, Ste6 and CFTR (Gnann et al., 2004; Plemper et al., 1998; Wilhovsky et al., 2000). Membrane proteins, however, do not appear to require luminal chaperones, but rather mutagenesis of cytosolic chaperones Hsp70/Ssa1 and Ssa2 and Hsp40/Ydj1 and Ydj2 reduce degradation (Huyer et al., 2004; Youker et al., 2004; Zhang et al., 2001). Dislocation may also occur differently for various substrates. The sec61 translocon appears to be utilized for CPY*, MHCI, and PDR5, but a sec61-independent pathway has been demonstrated for ubc6 and ste6 (Huyer et al., 2004; Plemper et al., 1998; Walter et al., 2001; Ye et al., 2004). The latter pathway is undefined, but may involve a novel channel to facilitate partitioning of hydrophobic TM segments out of the lipid bilayer. However, genetic screens are limited in that effects are often indirect and analysis of

identified proteins may not be possible if the protein is essential. Temperature sensitive mutants are similarly limited because complete depletion may not be possible during the short incubation times at nonpermissive temperatures. Finally, while many pathways are highly conserved, mammalian ERAD pathways likely exhibit additional layers of redundancy and/or complexity. Thus, it is highly desirable to use mammalian systems to identify and/or verify key ERAD components.

Rabbit reticulocyte lysate (RRL) provides a powerful system for identifying and characterizing ERAD components involved in CFTR degradation. In this system CFTR is translated *in vitro* using canine rough microsomes (CRMs) such that it is the only radiolabeled protein translated, thus allowing for direct analysis of degradation by quantitating conversion of full-length CFTR into TCA soluble peptides. Also, both microsomes and lysate are directly accessible to pharmacological and/or biochemical modification prior to or during the degradation reaction.

Results

Biochemical manipulation of membrane proteins

Protease digestion of microsomes and analysis of the released peptides has proven to be a powerful tool for identifying ER components involved in nascent chain translocation (Walter et al., 1979). In the case of the signal recognition particle receptor (SRPR), translocation can be restored by addition of the purified alpha subunit or by *in vitro* translation of SRPRα (Andrews, 1989). In preliminary experiments we showed that proteolysis similarly cleaved ER-localized proteins ubc6, an E2 enzyme, and cue1, a ubc7 binding protein, from the membrane (Appendix F, Figure F-1). We therefore

hypothesized that proteolysis might provide a means to identify ER membrane proteins involved in the CFTR degradation pathway.

Trypsinized ER membranes were assayed for translocation competence using the secretory protein, preprolactin, which was used because it is relatively small (~30kD) with a cleavable signal sequence. A trypsin titration was carried out on microsomes and assayed by loss of signal sequence cleavage (Figure 2-1A). 0.9 mg/ml trypsin completely disrupted translocation, but still allow efficient reconstitution of translocation (~80%) by addition of recombinant SRPRα (1μg/ μl membranes) or *in vitro* translation of SRPRα (Figures 2-1B and 2-1C). This concentration of trypsin also degraded ubc6 and cue1 (Appendix E, Figure E-2). CFTR translations were therefore performed using trypsinized membranes with and without added SRPRα. CFTR was integrated and glycosylated in mock treated and reconstituted membranes, but not in trypsinized membranes. (Figure 2-2). Similar results were observed for proteinase K (data not shown).

Since many E2 enzymes have active site cysteines, membrane proteins were also treated with the alkylating reagent, N-ethylmaleimide (NEM). This reagent also inactivates SRPRα (Gilmore, 1982), and translocation can be restored by the addition of recombinant SRPRα allowing the effectiveness of the treatment to be monitored (data not shown). Both membrane treatments were then tested for an effect on CFTR degradation.

Membrane manipulation does not affect CFTR degradation

CFTR was synthesized *in vitro* in the presence of microsomes and ^{35}S-methionine yielding a ~150kD core glycosylated membrane-integrated protein. Membranes were isolated by centrifugation, resuspended, and added to degradation reactions containing

RRL (70% of reaction volume), an ATP regenerating system, and the reducing agent, DTT (3mM). Degradation was monitored by two separate parameters. Loss of full-length CFTR was assessed by SDS-PAGE and conversion of CFTR into TCA soluble peptides was monitored by liquid scintillation counting. Upon incubation, CFTR was converted into a high molecular weight complex (HMW), which gradually disappears over 4 hours (Figure 2-3A, mock). Similarly, ~65% CFTR became TCA soluble in 4 hours (Figure 2-3B, mock). When translation and degradation were done with proteolyzed, alkylated, or doubly-treated membranes, only a small amount of CFTR was pelleted with microsomes, and this material was rapidly and completely degraded in 30-60 minutes (Figure 2-3B, trypsin). Thus, misfolded and nonintegrated CFTR is readily targeted to the ERAD pathway. By contrast, CFTR degradation in SRPR-reconstituted membranes resulted in a rate and extent of degradation similar to mock treated membranes (Figure 2-3). Thus, proteolysis and biochemical inactivation of ER membrane proteins did not affect CFTR degradation, suggesting that redundant proteins exist in the cytosol.

Biochemical manipulation of cytosol

Cytosolic components such as Hsp70/Hsp40 and CHIP contribute to CFTR degradation (Meacham et al., 2001; Zhang et al., 2001), and thus we devised a strategy to identify candidates for CFTR ERAD in the cytosol. Recombinant His-tagged proteins including CHIP, ubc6, Ub-ubc6, ubcH5a, and Ub-ubcH5a were immobilized on Ni-NTA and used as bait to bind RRL factors. The depleted RRL was then assayed in a degradation reaction to determine whether any hypothetical depleted proteins affected

CFTR ERAD. This approach allowed a single adsorption step, and any proteins bound to beads could be eluted and identified by mass spectrometry.

Initially, baits including an E3 ligase (CHIP) and two E2 enzymes (Ubc6 and ubcH5a) did not affect degradation (Figure 2-4). We therefore attempted "on column" *in vitro* ubiquitination of immobilized ubc6 in the presence of E1, ubiquitin, and ATP-Mg^{2+}. However, this proved to be inefficient (data not shown) as the ubiquitin could be transferred to an E3 or substrate in RRL. Therefore, ubiquitin fusion proteins (UFP) consisting of an N-terminal nonhydrolyzable ubiquitin (Ub G76V) and a C-terminal E2 (either ubc6 or ubcH5a) were constructed (Figure 2-5A and B). RRL depleted with UFPs markedly decreased CFTR degradation (Figure 2-5C and D). Ub-ubcH5a was slightly more effective than Ub-ubc6.

To identify candidate ERAD components, RRL proteins were eluted from uu5-loaded beads with 1M NaCl, separated by SDS-PAGE, silver stained and excised (Figure 2-6). Following in-gel trypsin digestion, samples were analyzed by liquid chromatography tandem mass spectrometry (LC-MS-MS). Proteins were identified in seven bands including E3s, Ub hydrolases, co-chaperones, AAA-ATPases, and 19S subunits (Figure 2-6).

Affinity depletion of RRL p97

The most abundant RRL protein eluted from uu5 beads was the AAA-ATPase, p97/VCP/cdc48. Immunoblots of serially adsorbed RRL revealed that uu5 depleted only ~50% of RRL p97 (Figure 2-7A). In ERAD, p97 functions in a heterotrimeric complex with the adaptor proteins, ufd1 and npl4. Consistent with this, an immunoblot showed

that ufd1 was reduced to below detection following a single adsorption (Figure 2-7B). Thus, it is likely that uu5 effectively depleted the p97/ufd1/npl4 complex.

In order to definitively determine whether p97 is required for ERAD, complete depletion was necessary. Thus, two additional strategies were employed. First, an antibody was made against the C-terminus of p97. This was previously shown to be effective in depleting cell lysates of p97 (Dai et al., 1998). However, we found that although this antibody could recognize recombinant p97 by immunoblotting, it did not recognize RRL p97 (data not shown). Thus, it is likely that RRL p97 is modified by tyrosine phosphorylation, and the major tyrosine phosphorylation site is located in the epitope (Egerton and Samelson, 1994). The second strategy was to use p47, an alternate binding partner of p97, as a bait for affinity depletion (Figure 2-8A) (Kondo et al., 1997). p47 competes with the ufd1/npl4 heterodimer for binding to p97. This proved to be highly effective, and had the additional benefit of not depleting ufd1 (and presumably npl4) (Figure 2-8B). p47-mediated depletion of p97 resulted in ~50% decrease in CFTR degradation which was partially restored upon the addition of recombinant p97 (2-8C). In contrast, depletion of both ufd1 and p97 resulted in a similar decrease in CFTR degradation with no recovery upon p97 add-back (Figure 2-8D). This is consistent with genetic data that ufd1 is required for p97-mediated ERAD effects (Jarosch et al., 2002).

Discussion

CFTR is a prototypical ERAD substrate, and here we described several parallel biochemical approaches to identify candidate proteins involved in the CFTR degradation pathway. A variety of treatments aimed at inactivating potential membrane protein components failed to have any effect on degradation in the *in vitro* RRL system. In

contrast, affinity depletion of RRL using UFPs decreased CFTR degradation and removed a population of proteins that were identified by mass spectrometry. Of these proteins, p97 was chosen for further study. Refinement of the depletion strategy using the p97 cofactor, p47, depleted >98% of RRL p97. These techniques can now be extended to other substrates for analysis of various protein-protein interactions.

Inactivation of microsome translocation activity yielded membranes that could be functionally reconstituted by recombinant SRPRα. Although, no effect was observed on the degradation of full-length CFTR because different ligases likely recognize different features of CFTR. For example, CHIP is a cofactor of Hsp70 that binds to the cytosolic NBDs, but not TMDs. Thus, CFTR truncations expressed in protealyzed membranes would be predicted to be stabilized. Alternatively, depletion of Hsp70 and/or CHIP from RRL would indicate whether membrane-localized ligases play a role in CFTR degradation. Many E3s may ubiquitinate CFTR including the cytosolic ligases CHIP and SCF^{FBX2}, a lectin ligase, and the as yet untested, ER-localized ligases, MarchVI and Rma1 (Bartee et al., 2004; Meacham et al., 2001; Yoshida et al., 2002). The cytosolic ligases may use p97-independent presentation to the proteasome as SCF complexes and a co-chaperone of Hsp70, BAG-1, can interact directly with the proteasome (Luders et al., 2000; Verma et al., 2000). By contrast, the ER-localized ligases are likely part of pathway that converges at p97 (Gnann et al., 2004).

Affinity depletion using p47 effectively removed p97 from RRL. This approach could also be used to analyze and compare the proteins bound to different E2s and UFPs such as ubc6 vs. ubcH5a or ubcH5a vs. Ub-ubcH5a. Separating the eluates on sizing columns might allow different complexes to be isolated. Alternatively, BN-PAGE could

be used to analyze complexes eluted from UFP beads. This would begin to address how degradation is organized and whether just one large complex exists or multiple smaller complexes cooperate at different steps in the ERAD pathway.

Now that p97 has been selectively depleted from RRL, its specific role in CFTR degradation can be dissected (see Chapter 4). p97 is involved in many cellular functions ranging from post-mitotic membrane fusion to ERAD. The *in vitro* system established here therefore provides very important tools to dissect effects that impinge directly on ERAD as opposed to other cellular effects following p97 depletion such as mistrafficking or mitotic arrest. Moreover, the reduction in degradation observed in yeast and cells has been interpreted to mean that p97 is essential for ERAD. Thus, "complete" depletion in a reconstituted biochemical system will allow this hypothesis to be tested in a manner not possible *in vivo*.

Methods

Note: Many of these methods are described in detail in Appendices A-F.

Reagents: Reagents are from Sigma unless otherwise indicated. RRL and microsomes were made as described previously (Appendices A and B; (Carlson et al., 2005))

Cloning: Plasmid Constructs. Plasmids pSPCFTR are described elsewhere (Xiong et al., 1997). PTrc-p47, and pQE-p97 were generously provided by Dr. Hemmo Meyer. Coding sequences for p97 and p47 were subcloned into Nco1 and BamH1 sites of pET15b (EMD Biosciences, San Diego, CA) for heterologous expression.

Plasmid pETUb^{G76V} was made by amplifying the human ubiquitin cDNA coding sequence (gift of Dr. M. Hochstrasser) with sense primer (AAGACTTCATGATG

CAGATCTTCGTCAAC) and antisense primer (AACCAGCCATGGCCACACCTCTT AGTCTTAAGAC), digesting with NcoI and BspHI, and ligating into an NcoI digested pET15b vector. The antisense primer also introduced a G to V mutation at Ubiquitin codon 76. Plasmid pETUb-ubcH5a was then made by amplifying ubcH5a (gift of Dr. Peter Howley) with sense primer (TGACCCATGGCGCTGAAGAGGATT) and antisense primer (TCCGGCGGATCCTTAGTGATGATGATGATGATGCATTGC ATATTTCTGAGT), digesting with NcoI and BamHI and ligating between the NcoI and BamHI sites of pET15ub^{G76V}. The resulting in pET15Ub-ubcH5a vector encodes a non-cleavable ubiquitin fusion protein with a His_6 tag at the C-terminus of ubcH5a. The ubcH5a insert was also ligated between the NcoI and BamHI sites of pET15b to produce plasmid pET15b ubcH5a.

Plasmids pET15b ubc6 and pET15bUb-ubc6 were made by amplifying yeast ubc6 (gift of A. Weissman) with sense primer (ATTTAGGTGACACTATAG) and antisense primer (CGGTACAGATCTCAATGGTGGTGATGATGGTGATGGCCATCATTAGG TTCTTTGCC) , digesting with NcoI and BamHI, and ligating into NcoI/BamHI digested pET15b or pET15bub^{G76V}, respectively.

Recombinant proteins: Recombinant protein expression was induced in transformed BL21(DE3) cultures using 0.4mM isopropyl β-D-1-thiogalactopyranoside (IPTG; Fisher Scientific, Pittsburgh, PA) as previously described (Carlson et al., 2005). Cell lysates were loaded onto a 5 ml Ni-NTA column (Qiagen, Inc., Valencia, CA), washed with 10 bed volumes of 300mM NaCl, 1mM βME, 5% glycerol, 0.4mM PMSF, 25mM imidazole, and 50mM Tris-HCl, pH 7.5, and eluted with a 25mM-500mM linear gradient

of imidazole. Fractions were pooled, dialyzed against 100mM NaCl, 1mM βME, and 25mM Tris-HCl, pH 7.5 (Buffer A), then concentrated, and stored at –80°C. Aliquots were thawed once and discarded.

Affinity Depletion of RRL and CRM: Rabbit reticulocyte lysate (RRL) and canine pancreatic rough microsomes (CRMs) were affinity depleted using Ni-NTA beads containing near saturating amounts His-tagged recombinant proteins at a ratio of 5:1 (RRL:Ni-NTA). RRL was incubated at least 4 hr at 4°C with continuous mixing. Supernatants were removed and frozen in liquid nitrogen. Mock depletions were performed using equal volumes of empty Ni-NTA beads. Following depletion, RRL or CRMs were separated by SDS-PAGE, transferred to nitrocellulose or PVDF, and blotted with mouse α–p97 (1:500; BD Transduction Laboratories, San Jose, CA) or mouse α-ufd1 (1:1,000; BD Transduction Laboratories) followed by α-mouse- HRP secondary Ab (1:20,000. Biorad, Hercules, CA). The blots were imaged on Kodak film using Pierce west pico supersignal substrate according to the manufacturer's directions (Pierce Biotechnology, Inc., Rockford, IL).

Identification of eluted proteins*:* To identify adsorbed proteins, remaining supernatant was removed, and beads were washed with 6-8 x 1 ml of 100mM NaCl, 20mM imidazole, 1mM β-mercaptoethanol, 25mM Tris-HCl, pH 7.5. Bound proteins were eluted with 1 M NaCl, 1 mM β-mercaptoethanol, 25 mM Tris-HCl, pH 7.5. To prepare samples for analysis by mass spectrometry, the eluted proteins were concentrated by TCA precipitation (20% TCA, centrifuged at 16,000 x g for 10 min, washed with 50%

acetone, and resuspended in SDS-LB, analyzed by SDS-PAGE and silver stained according to the modified Blum method (REFS). Briefly, gels were fixed in 40% (v/v) ethanol and 10% (v/v) acetic acid, then washed three times in 30% ethanol and once in ddH_2O. Gels were sensitized in 0.02% sodium thiosulfate then washed three times with ddH_2O. Incubation in 0.1% silver nitrate was done at 4 ^{o}C for 20 minutes. Following three rinses in ddH_2O, gels were developed in 3% sodium carbonate and 0.05% formalin. Gels were scanned, and images were processed using Adobe Photoshop. Selected protein bands were manually excised from the gel and minced, washed twice in mH_2O, followed by two washes in 50mM ammonium bicarbonate, 50% acetonitrile. Gel slices were then dried, reduced by addition of 10mM DTT, 100mM ammonium bicarbonate, and then alkylated in 55mM iodoacetamide, 100mM ammonium bicarbonate. Following two washes in 50mM ammonium bicarbonate, 50% acetonitrile, gel pieces were dried. Samples were rehydrated in 10ng/μl trypsin (Sequencing grade modified trypsin, Promega, Madison, WI) in 100mM ammonium bicarbonate. After 15 min, excess solution was removed and 100mM ammonium bicarbonate was added. Samples were incubated overnight at 37 °C. Peptides were eluted from the gel by removing the supernatant, and washing/sonicating the remaining gel pieces, first in 12.5mM ammonium bicarbonate, 25% acetonitrile, then in 2.5% formic acid, 25% acetonitrile. The combined supernatant/wash solutions were then dried in preparation for mass spectrometric analysis. Samples were analyzed by LC-MS-MS or MALDI-TOF MS and identified by mass fingerprinting. MS analysis was done by L. David (OHSU, Portland, OR) and G. Hilliard (Univ. of Tennessee Health Science Center, Memphis, TN).

Membrane proteolysis and alkylation: CRMs were diluted 10-fold into 1 mM DTT, 50 mM triethanolamine-acetate, pH 7.5 containing 0.9 μg/ml trypsin or 25 μg/ml Proteinase K and incubated on ice for 1 hr. Proteolysis was stopped by addition of 0.5mM PMSF (final concentration). KoAc was adjusted to 0.5M, and membranes were then pelleted through 0.5M sucrose, 0.5M K0Ac, 5mM $MgCl_2$, 1mM DTT, 0.5mM PMSF, 50mM HEPES, pH 7.5. Microsomes were resuspended and pelleted a second time through 0.5M sucrose, 100mM KCl, 5mM $MgCl_2$, 1mM DTT, 50mM HEPES, pH 7.5 to remove traces of PMSF. Membranes were resuspended in 0.25 M sucrose, 1 mM DTT, 50 mM triethanolamine-acetate, pH 7.5. For NEM treatment, microsomal membranes were pelleted through 0.5M sucrose, 100mM KCl, 5mM $MgCl_2$, 50mM HEPES, pH 7.5, and the pellet was resuspended in the original volume in Buffer C (-DTT). 2mM NEM was added followed by incubation at 24°C for 30 minutes. The reaction was quenched with 10-fold excess DTT (20 mM). SRα repopulation of treated microsomal membranes was done either by *in vitro* translation of SRα or by addition of recombinant SRα (preferred method). Briefly, membranes were incubated on ice for at least 30 min with 1μg SRα/ μl of membranes, pelleted, resuspended in the original volume in 0.25 M sucrose, 1 mM DTT, 50 mM triethanolamine-acetate, pH 7.5 and stored at –80°C. Mock treated membranes were made by following the indicated procedures without protease or NEM.

In vitro transcription/translation: mRNA was transcribed with SP6 RNA polymerase for 1 hour at 40°C and translated in a transcription-linked reaction for 1-2 hr at 24°C as described in detail elsewhere (Carlson et al., 2005). RNAse-free H_2O was substituted for DNA in mock transcription reactions. Endogenous RRL and CRM mRNAs were digested

prior to translation (Carlson et al., 2005). Canine pancreatic rough microsomal membranes (A_{280}= 4) were added at the start of all translations. Aurin tricarboxylic acid (25 - 50μM) was added after 15-20 minutes to synchronize translation. Following translation, CRM containing *in vitro*-synthesized protein were isolated by centrifugation, 180,000 x g for 10 min, through 0.5M sucrose, 100mM KCl, 5mM $MgCl_2$, 1mM DTT, 50mM HEPES, pH 7.5 and resuspended in 1/2 original volume in 0.1M sucrose, 100mM KCl, 5mM $MgCl_2$, 1mM DTT, 50mM HEPES, pH 7.5.

Degradation Assay: Isolated CRMs were added to RRL supplemented with 1mM ATP, 12mM creatine phosphate, 5mM $MgCl_2$, 3mM DTT, 10mM Tris-Cl, pH 7.5 and 4μg creatine kinase/50μl reaction (Carlson et al., 2005) and incubated at 37°C. Recombinant p97 (200ng/μl RRL) (Oberdorf et al., 2006) was also added to p97-depleted RRL where indicated. Samples were removed at indicated times (T_n), precipitated in 20% TCA and centrifuged at 16,000 x g for 10 min. TCA supernatants (TCA Sol) were then counted in ScintiSafe (Fisher Chemicals) using a Beckmann LS6500 scintillation counter. Total [^{35}S] present in each sample was determined by directly counting an aliquot of the degradation reaction. Mock reactions were used as a control to correct for small amounts of nonspecific, ATP-independent association of [^{35}S] with the membranes (Carlson et al., 2005). The percent of protein converted to TCA soluble fragments at each time point was determined using the following formula:

$$\% \text{ of total counts} = \{(CFTR(T_n\text{-}T_0) - Mock(T_n\text{-}T_0))/(CFTR(total - TCA\ sol\ T_0) - Mock(total - TCA\ sol\ T_0))\}*100$$

Where T_n = TCA soluble counts at T=n and T_0 = TCA soluble counts at T=0 for indicated CFTR and Mock translation reactions.

Carbonate extraction: CRMs containing translation products were added to 1 ml 0.25M sucrose, 1μg BSA, and 0.1M Tris-Cl, pH 7.5 or 1 ml 0.1M Na_2CO_3, pH 11.5, 1μg BSA and incubated on ice for 30 min, followed by centrifugation at 180,000 x g for 30 min. Pellets were solubilized in 30 μl SDS-PAGE loading buffer. Supernatants were precipitated in 20% TCA, and the resulting pellets were solubilized in 30 μl SDS-PAGE loading buffer. Aliquots of resuspended membrane pellets were analyzed by SDS-PAGE. Samples were analyzed by SDS-PAGE and EN^{3}HANCE (Perkin Elmer, Boston, MA) fluorography and imaged on Kodak film.

Endoglycosidase H treatment: Aliquots of CFTR translation reactions were incubated in 1M sodium citrate, pH 5.5, 0.1% SDS and Endoglycosidase H, and incubated at 37 ^{o}C for 1 hr. Samples were analyzed by SDS-PAGE with EN^{3}HANCE fluorography.

Figure 2-1. Reconstitution of SRP-dependent translocation in proteolyzed membranes. (**A**) Microsomal membranes were digested as indicated, and translocation competence was assayed using the secretory protein preprolactin (pPrl). Processing is indicated by signal sequence cleavage to Prl. (**B**) Mock-treated and trypsinized microsomes were incubated in an *in vitro* translations programmed with SRα mRNA, collected by pelleting and reincubated in a second translation reaction expressing preprolactin. (**C**) A His-tagged cytoplasmic fragment of SRα was affinity purified from *E. coli* lysate and incubated (1μg SR/μl CRM) with proteolyzed microsomes. Repopulated membranes were then pelleted and used in cell free translations. The efficiency of prolactin translocation in repopulated microsomes was equal to that in non-proteolyzed (mock-treated) microsomes (compare lanes 2 and 3 to lane 6).

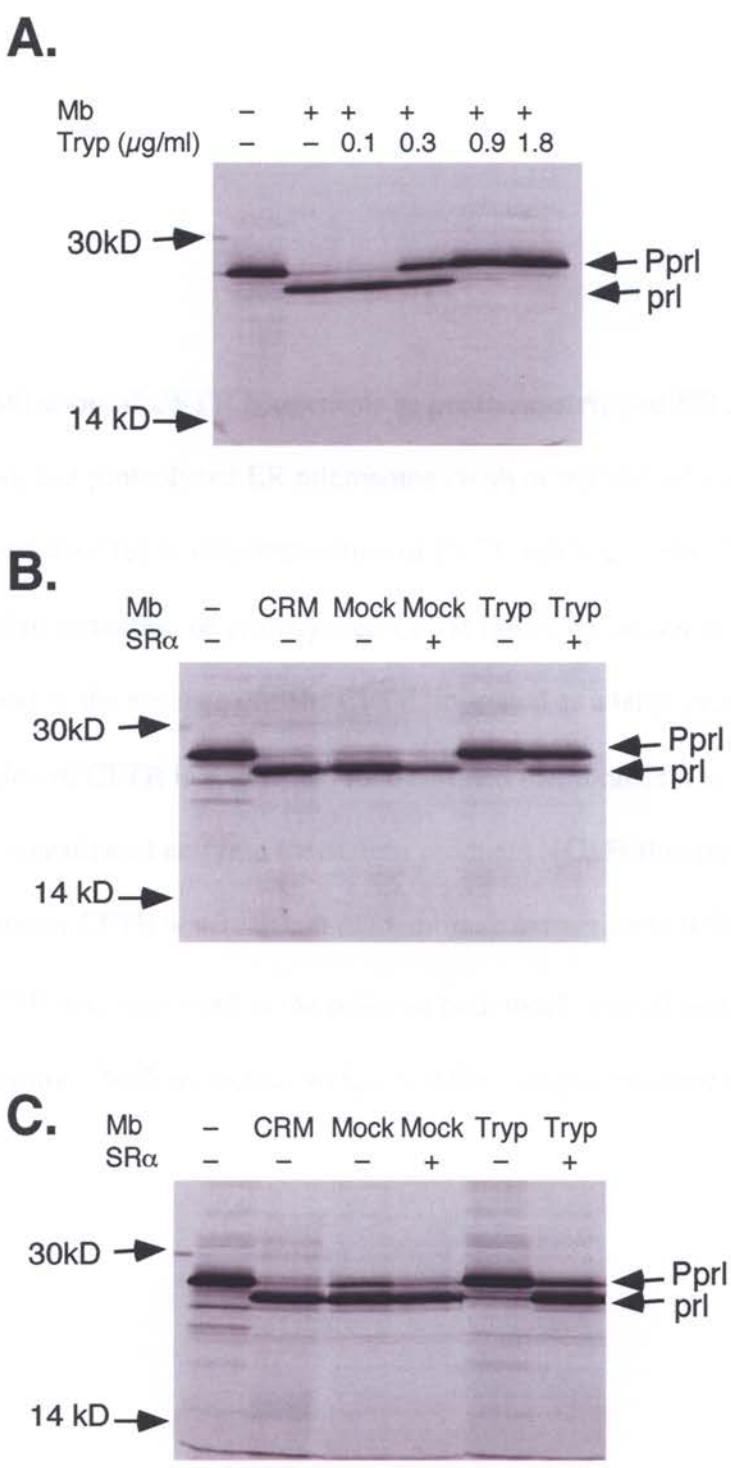
A.
Mb – + + + + +
Tryp (μg/ml) – – 0.1 0.3 0.9 1.8
30kD
14 kD
Pprl
prl
B.
Mb – CRM Mock Mock Tryp Tryp
SRα – – – + – +
30kD
14 kD
Pprl
prl
C.
Mb – CRM Mock Mock Tryp Tryp
SRα – – – + – +
30kD
14 kD
Pprl
prl

Figure 2-2. Reconstitution of CFTR Biogenesis in protease-stripped ER membranes. (**A**) CRMs, mock-treated, and proteolyzed ER microsomes with or without adsorbed cytoplasmic fragment of SRα were used for *in vitro* translation of CFTR mRNA. SRα reconstituted microsomes resulted in formation of glycosylated CFTR (gCFTR) similar to mock-treated and native CRMs, whereas in the absence of SRα CFTR migrated as a large protein aggregate. (**B**) N-linked glycosylation of CFTR in native and reconstituted membranes was verified by Endoglycosidase H digestion of cell free translation products. (**C**) Following translation in reconstituted membranes CFTR was resistant to membrane extraction in 0.5M KoAc (A) and 0.1M Na_2CO_3 as CFTR was recovered in the pellet in both mock-treated and reconstituted CRMs. In trypsinized microsomes, high molecular weight (HMW) complexes were recovered in the supernatant.

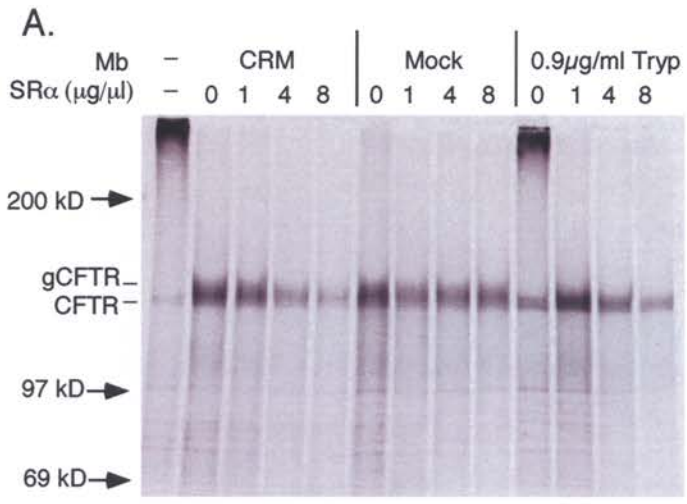
A.
Mb – CRM Mock 0.9μg/ml Tryp
SRα (μg/μl) – 0 1 4 8 0 1 4 8 0 1 4 8
200 kD
gCFTR
CFTR
97 kD
69 kD

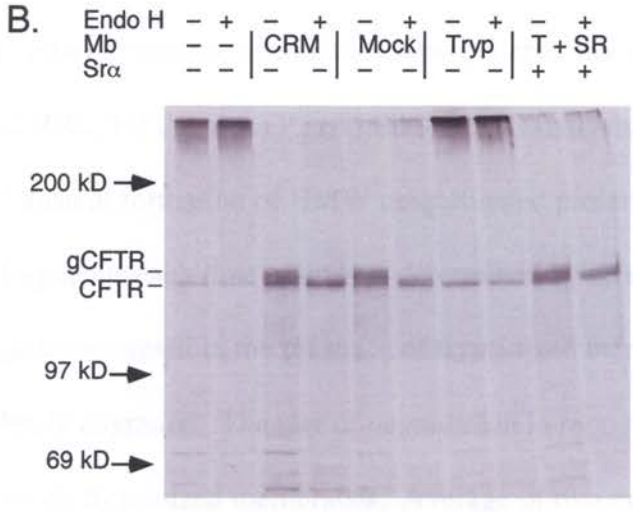
B.
Endo H – + – + – + – + – +
Mb – – CRM Mock Tryp T + SR
Srα – – – – – – – – + +
200 kD
gCFTR
CFTR
97 kD
69 kD

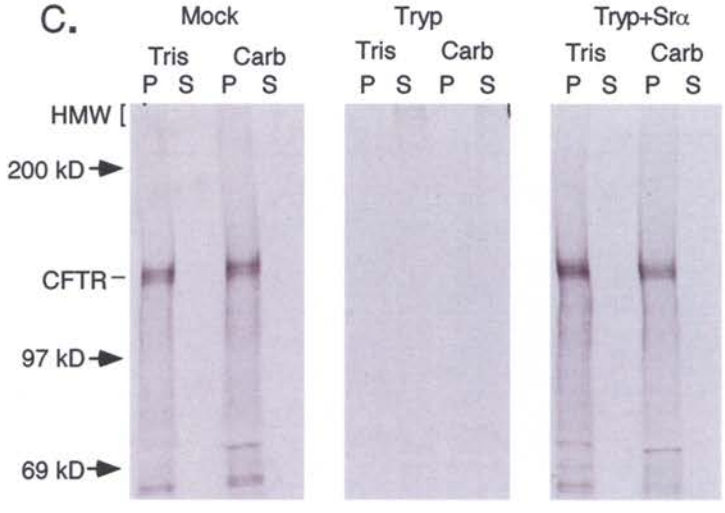
C.
Mock
Tryp
Tryp+Srα
Tris Carb
P S P S
HMW
200 kD
CFTR
97 kD
69 kD

Figure 2-3. CFTR degradation into TCA soluble fragments. CFTR synthesized in the presence of mock treated, trypsinized, NEM-treated or PK-treated membranes that were reconstituted with SRα. After synthesis, membranes were pelleted and added to a degradation reaction containing fresh RRL, DTT and ATP. (**A**) SDS-PAGE analysis shows disappearance of full-length protein and transient formation of HMW ubiquitinated proteins. (**B**) Conversion of CFTR to TCA soluble fragments each time point was determined by scintillation counting. Cytosolic CFTR aggregates generated in the presence of trypsinized membranes lacking SRα were rapidly and completely degraded. The rate of degradation in repopulated membranes was indistinguishable from mock trypsinized membranes. Average of two experiments shown.

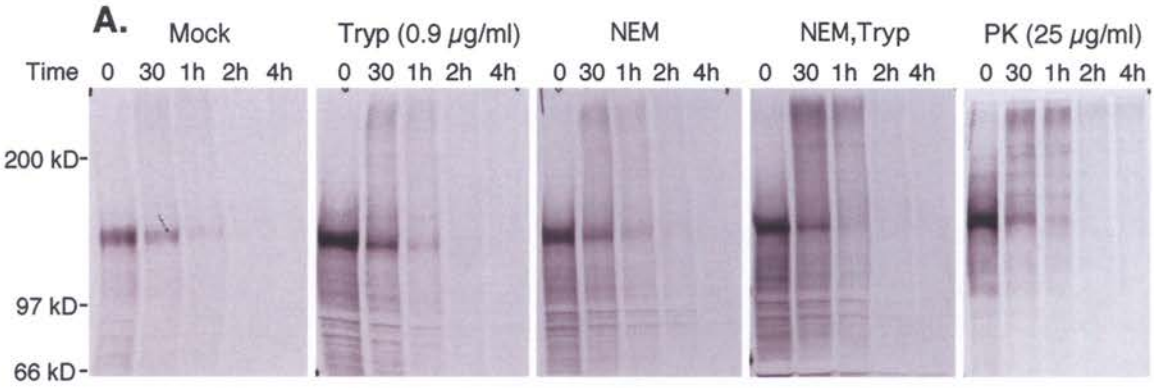
A.
Mock
Tryp (0.9 μg/ml)
NEM
NEM,Tryp
PK (25 μg/ml)
Time 0 30 1h 2h 4h
200 kD-
97 kD-
66 kD-

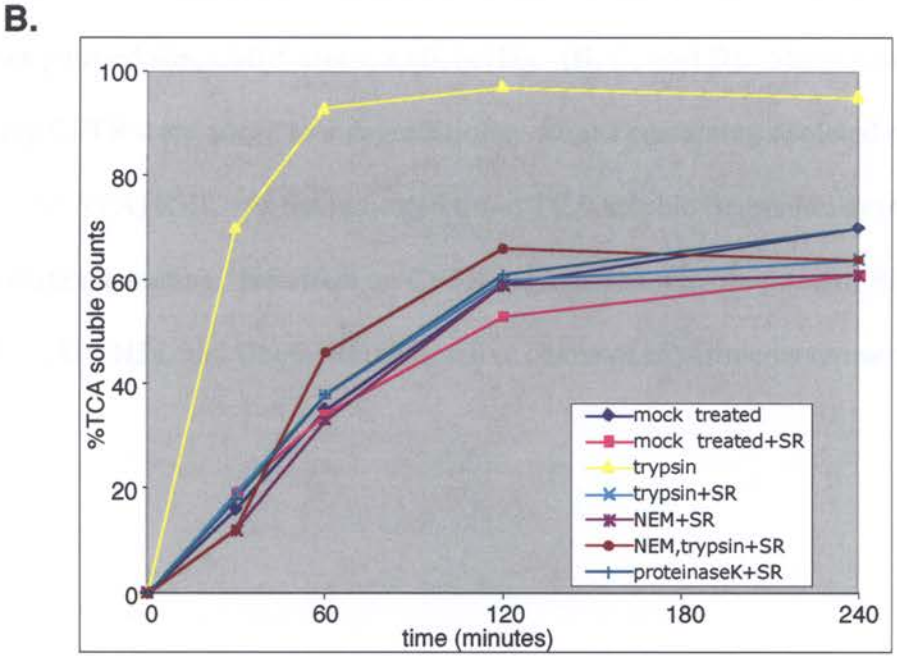
B.
%TCA soluble counts
time (minutes)
mock treated
mock treated+SR
trypsin
trypsin+SR
NEM+SR
NEM,trypsin+SR
proteinaseK+SR

Figure 2-4. CFTR degradation in affinity depleted RRL. **(A)** A Coomassie stained gel shows purified His_6 CHIP, Ubc6, andUbcH5a. **(B, C, and D).** Microsomes containing CFTR were added to a degradation reactions containing depleted or mock depleted (Ni NTA) RRL. At the indicated times TCA soluble fragments were quantitated by scintillation counting. No effect on CFTR degradation was observed in RRL adsorbed with CHIP, UbcH5a, and Ubc6. Representative charts of experiments repeated twice.

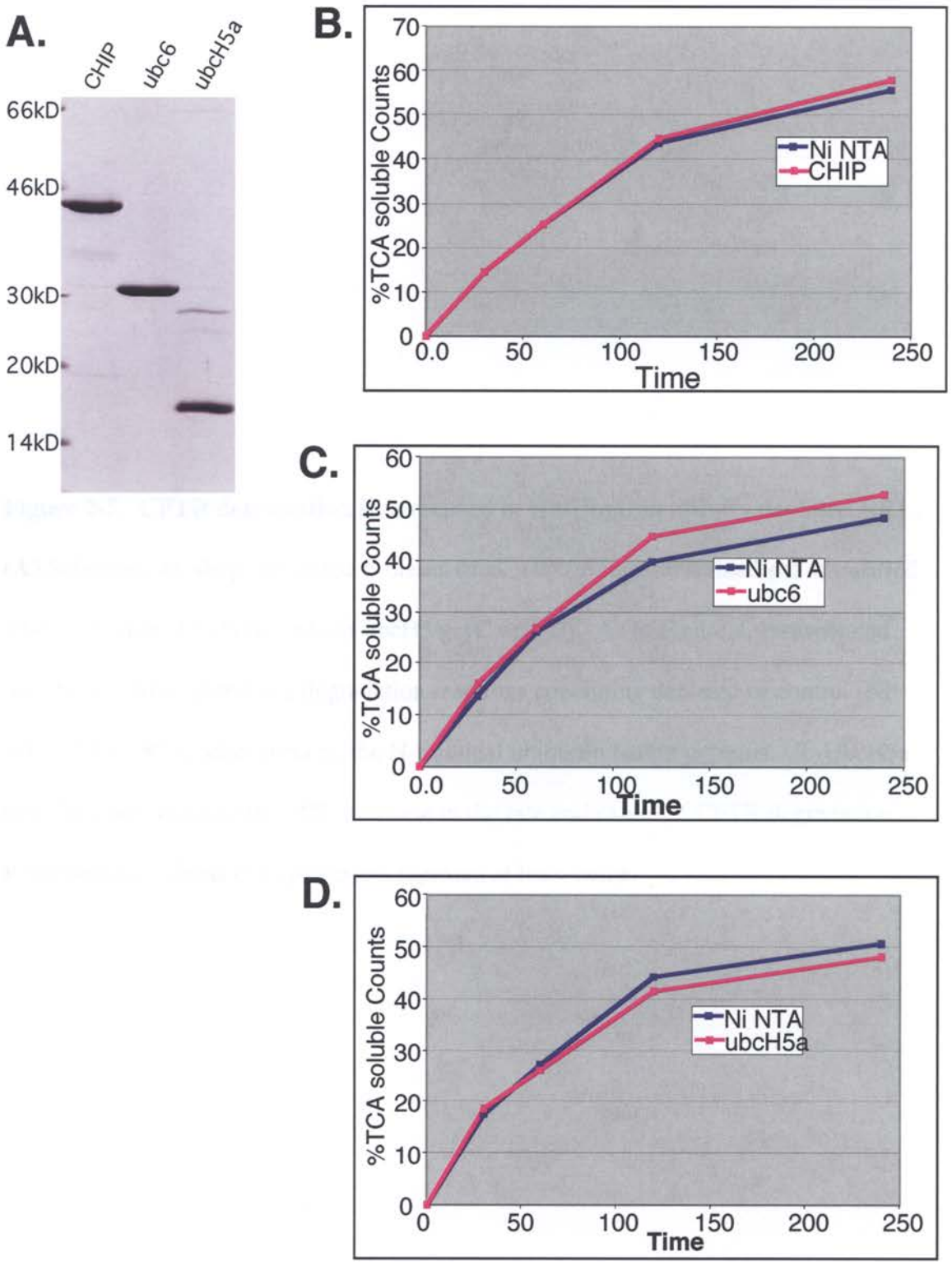
A.
CHIP
ubc6
ubcH5a
66kD
46kD
30kD
20kD
14kD
B.
%TCA soluble Counts
Time
Ni NTA
CHIP
C.
%TCA soluble Counts
Time
Ni NTA
ubc6
D.
%TCA soluble Counts
Time
Ni NTA
ubcH5a

Figure 2-5. CFTR degradation is decreased in Ub-UbcH5a affinity depleted RRL. **(A)** Schematic of ubiquitin fusion proteins used. **(B)** Coomassie stained gel of purified Ubc6, Ub-ubc6, UbcH5a, and Ub-ubcH5a. **(C and D).** As in Figure 4, resuspended membranes were added to a degradation reactions containing depleted or control (Ni NTA) RRL. RRL adsorption by the N-terminal ubiquitin fusion proteins, Ub-UbcH5a and Ub-Ubc6, resulted in ~30% decrease in the rate and extent of CFTR degradation. Representative charts of experiments repeated at least twice.


A.
Ub G76V
Ubc (E2)

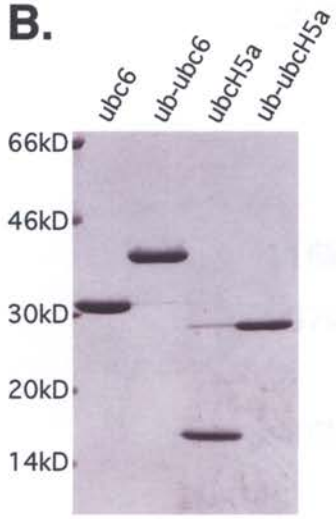
B.
ubc6
ub-ubc6
ubcH5a
ub-ubcH5a
66kD
46kD
30kD
20kD
14kD

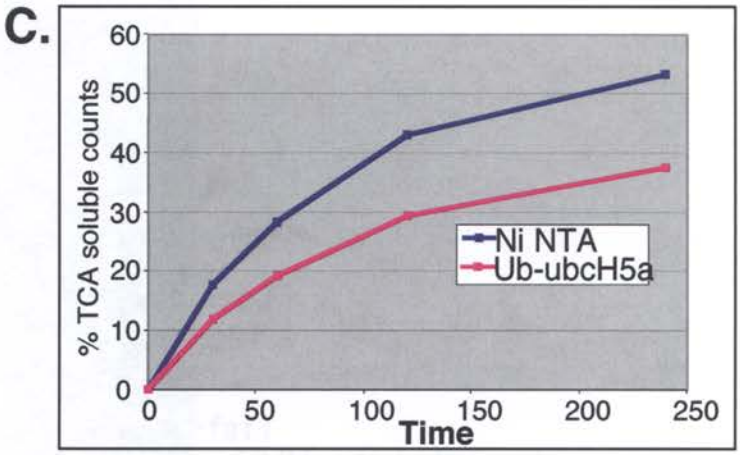
C.
% TCA soluble counts
60
50
40
30
20
10
0
0
50
100
150
200
250
Time
Ni NTA
Ub-ubcH5a

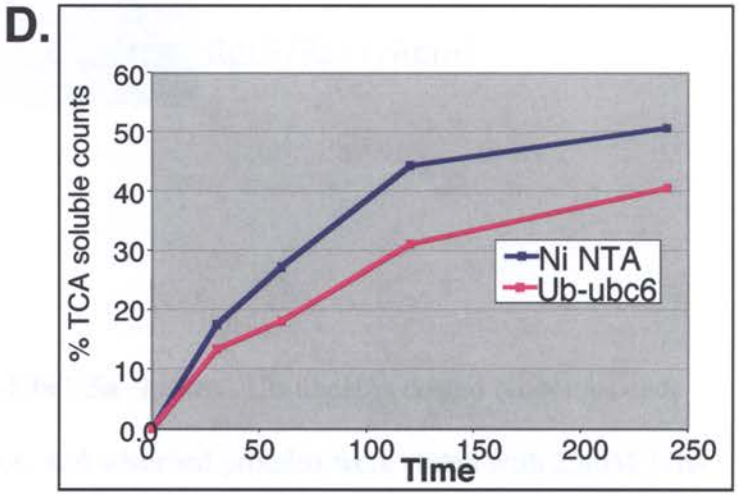
D.
% TCA soluble counts
60
50
40
30
20
10
0.0
0
50
100
150
200
250
TIme
Ni NTA
Ub-ubc6

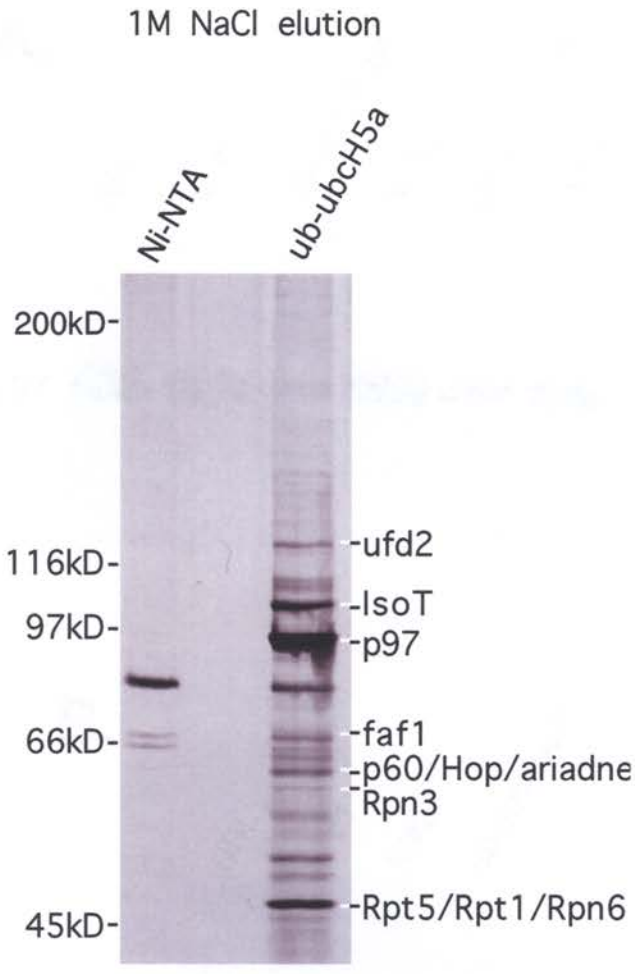

Figure 2-6. LC-MS-MS of Ub-UbcH5a eluates. Ub-ubcH5a coated Ni-NTA beads were incubated with RRL, washed, and adsorbed proteins were eluted with 25mM Tris-Cl, pH 7.5, 1M NaCl, and 1mM 2-mercaptoethanol. Eluates were separated by SDS-PAGE, and silver stained eluted proteins were excised and analyzed by MALDI-TOF MS fingerprinting or LC-MS/MS. Identified bands are indicated.

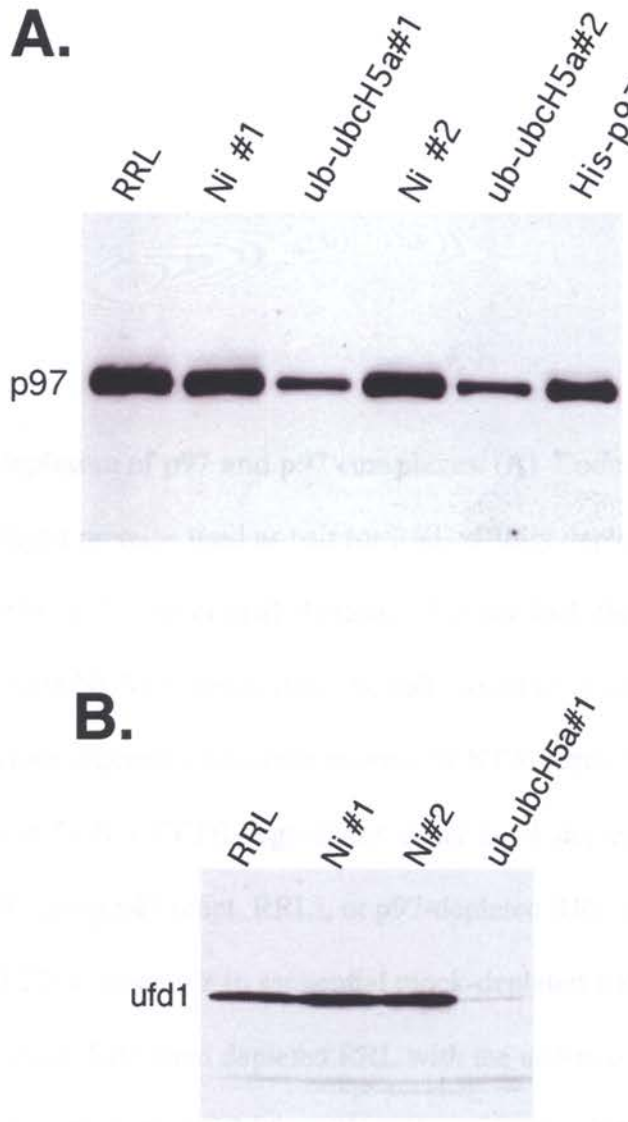

Figure 2-7. RRL depletion by Ub-UbcH5a. RRL was incubated with Ub-UbcH5a beads. Aliquots were separated by SDS-PAGE, transferred to nitrocellulose, immunoblotted with (**A**) p97 antibody (BD Bioscience) and reprobed with (**B**) Ufd1 antibody (BD Bioscience). Of note, only ~50% of p97 was removed from RRL by serial adsorptions, whereas the p97 adaptor protein, ufd1, was depleted after a single adsorption step.

Figure 2-8. RRL depletion of p97 and p97 complexes. (**A**) Coomassie stained gel of recombinant His-tagged proteins used as bait for RRL affinity depletion. (**B**) Immunoblots for either p97 (top) or ufd1 (bottom) of intact RRL (lane 1), RRL following a single adsorption with Ni-NTA beads (lane 2), uu5 coated beads (lane 4) or p47 coated beads (lane 6), and two sequential adsorptions with Ni-NTA beads (lane 3) or uu5 followed by p47 (lane 5). (**C**) CFTR degradation using mock depleted RRL (Ni RRL), RRL depleted of p97 using p47 (depl. RRL), or p97-depleted RRL plus recombinant p97 (depl.+p97). (**D**) CFTR degradation in sequential mock-depleted RRL (Ni-Ni), ufd1 and p97-depleted RRL (depl. RRL) and depleted RRL with the addition of recombinant p97 (depl.+p97). Error bars represent SEM from three experiments. **Note:** This figure is adapted from Figure 4-2, Chapter 4.

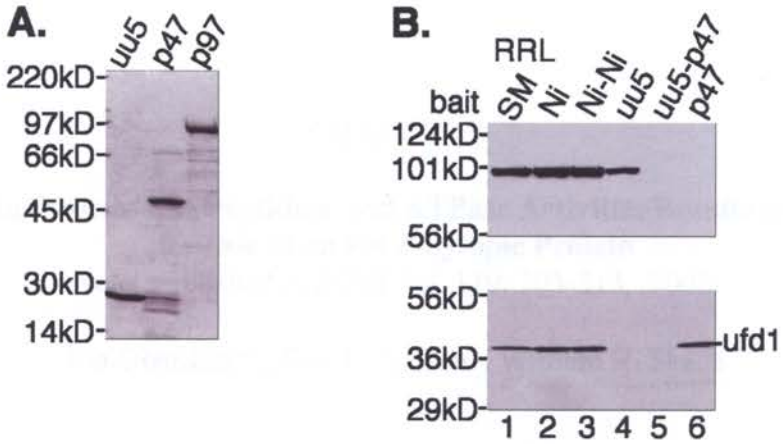
A.
uu5
p47
p97
220kD
97kD
66kD
45kD
30kD
14kD
B.
RRL
bait
SM
Ni
Ni-Ni
uu5
uu5-p47
p47
124kD
101kD
56kD
56kD
36kD
29kD
ufd1
1 2 3 4 5 6

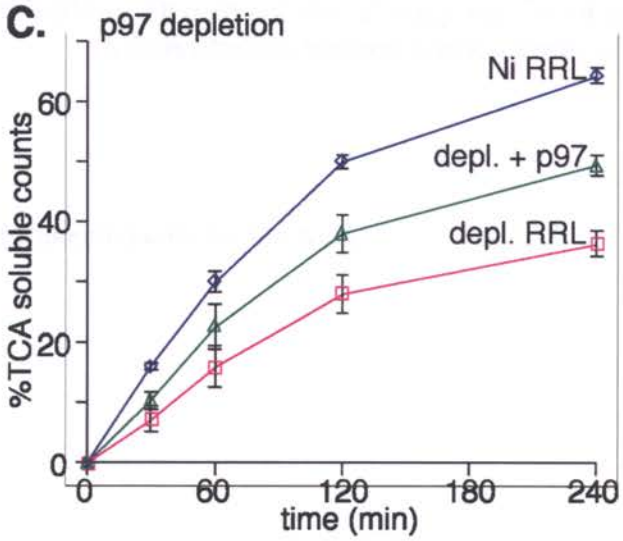
C.
p97 depletion
Ni RRL
depl. + p97
depl. RRL
%TCA soluble counts
0
20
40
60
0
60
120
180
240
time (min)

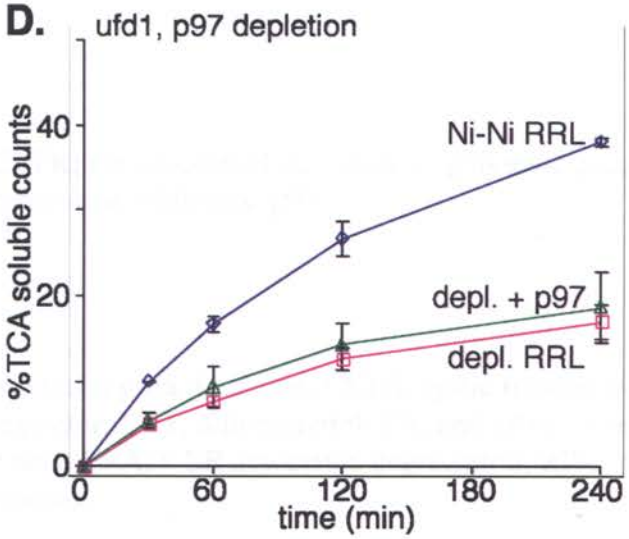
D.
ufd1, p97 depletion
Ni-Ni RRL
depl. + p97
depl. RRL
%TCA soluble counts
0
20
40
0
60
120
180
240
time (min)

CHAPTER 3

Uncoupling Proteasome Peptidase and ATPase Activities Results in Cytosolic Release of an ER Polytopic Protein

Note: published in J Cell Sci, 119: 303-313. 2006.

Jon Oberdorf*†, Eric J. Carlson†, William R. Skach

Department of Biochemistry and Molecular Biology, Oregon Health & Sciences University. Portland, OR
* Current address: Division of Hematology and Oncology, Portland Veterans Administration Medical Center, Portland, OR.

† Authors contributed equally to this work.

Key words: CFTR; ER-associated degradation; polytopic proteins; cystic fibrosis; ER dislocation, proteasome inhibitors, p97

Abbreviations:
β-lactone, *clasto*-lactacystin β-lactone; CFTR, cystic fibrosis transmembrane conductance regulator; DTT, dithiothreitol; ER, endoplasmic reticulum; TCA, trichloroacetic acid, ERAD, ER associated degradation; RRL, rabbit reticulocyte lysate; TM, transmembrane;

Summary

The 26S proteasome is the primary protease responsible for degrading misfolded membrane proteins in the endoplasmic reticulum. Here we examine the specific role of β subunit function on polypeptide cleavage and membrane release of CFTR, a prototypical ER-associated degradation substrate with 12 transmembrane segments. In the presence of ATP, cytosol and fully active proteasomes, CFTR was rapidly degraded and released into the cytosol solely in the form of trichloroacetic acid (TCA)-soluble peptide fragments. Inhibition of proteasome β subunits markedly decreased CFTR degradation but surprisingly, had relatively minor effects on membrane extraction and release. As a result, large TCA-insoluble degradation intermediates derived from multiple CFTR domains accumulated in the cytosol where they remained stably bound to inhibited proteasomes. Production of TCA-insoluble fragments varied for different proteasome inhibitors and correlated inversely with the cumulative proteolytic activities of β_1, β_2 and β_5 subunits. In contrast, ATPase inhibition decreased CFTR release but had no effect on the TCA-solubility of the released fragments. Our results indicate that the physiologic balance between membrane extraction and peptide cleavage is maintained by excess proteolytic capacity of the 20S subunit. Active site inhibitors reduce this capacity, uncouple ATPase and peptidase activities, and generate cytosolic degradation intermediates by allowing the rate of unfolding to exceed the rate of polypeptide cleavage.

Introduction

Membrane proteins in the endoplasmic reticulum (ER) that fail to acquire proper tertiary or quaternary structure are recognized by ER quality control machinery and degraded by the ubiquitin-proteasome pathway (Ellgaard and Helenius, 2001; McCracken and Brodsky, 2003; Plemper et al., 1998). This process, called ER-associated degradation, ERAD (Brodsky and McCracken, 1997; Hirsch et al., 2004; Romisch, 2005), involves covalent attachment of ubiquitin by ubiquitin conjugating (E2) and ubiquitin ligating (E3) enzymes that either reside within (e.g. Hrd1p/Der3p, Der1p, Ubc6) or are recruited to (e.g. Ubc7, CHIP) the ER membrane (Biederer et al., 1997; Hampton et al., 1996; Hiller et al., 1996; Jiang et al., 2001; Meacham et al., 2001). Ubiquitinated substrate is then degraded by the 26S proteasome, a cytosolic protease comprised of two 19S regulatory subunits and a 20S particle containing protease activity sequestered along the interior of four stacked heptameric rings (reviewed in (Voges et al., 1999)).

Because proteasomes are restricted to cytosolic and nuclear compartments, degradation of membrane proteins involves multiple steps: extraction of TM segments from the lipid bilayer, retrotranslocation of lumenal domains, unfolding and insertion of polypeptide into the proteasome, and substrate cleavage by proteolytically active 20S β subunits (Lilley and Ploegh, 2004; Mayer et al., 1998; Pilon et al., 1997; Plemper et al., 1998; Wiertz et al., 1996; Ye et al., 2004). Given the potential consequences of exposing large hydrophobic domains to the cytosolic environment, one would predict that proteolytic cleavage should be tightly coordinated with unfolding and extraction. Consistent with this, several studies have indicated that degradation is coupled to retrotranslocation at the cytosolic face of the ER membrane. For example, cytosolic and lumenal epitopes of ATP Binding Cassette (ABC) transporters, Pdr5 and CFTR, are degraded concurrently and require intact proteasomes as well as functional Sec61 translocation machinery (Plemper et al., 1998; Xiong et al., 1999). Intact proteasomes are also required for the membrane

extraction of MHC class II proteins (Tomazin et al., 1999) and a polytopic protein containing an N-terminal degradation signal (Mayer et al., 1998). In addition, we previously showed that ubiquitinated forms of CFTR remain tightly associated with the ER membrane in vitro until they are degraded by the 26S proteasome (Oberdorf et al., 2001; Xiong et al., 1999). Other studies, however, have indicated that retro-translocation may proceed independently of degradation. CFTR and other ERAD substrates accumulate as amorphous aggregates (aggresomes) in the cytosol of cells treated with proteasome inhibitors (Bebok et al., 1998; Johnston et al., 1998; Wigley et al., 1999). Similarly, in the presence of proteasome inhibitors, unstable connexins (VanSlyke and Musil, 2002), the T-cell receptor alpha subunit (Yu et al., 1997), MHC class I molecules (Wiertz et al., 1996), and other membrane proteins can be dislocated from the ER membrane and released en block into the cytosol. Thus, the temporal and mechanistic relationship between peptide cleavage and membrane extraction varies for different substrates and/or degradation conditions.

Eukaryotic proteasomes require that substrates be unfolded in order to reach the three active β1, β2 and β5 subunits within the core of the 20S particle (Voges et al., 1999). Unfolding is facilitated by a ring of AAA-ATPases located at the base of the 19S regulatory subunit that gate open and translocate polypeptide into the axial pore of cylinder (Benaroudj et al., 2003; Braun et al., 1999; Kohler et al., 2001; Lee et al., 2001; Pickart and Cohen, 2004). One appealing hypothesis has been that 19S AAA-ATPases might also provide the driving force for retro-translocation (Mayer et al., 1998; Plemper and Wolf, 1999). Indeed, the 19S subunit is sufficient to dislocate a mutant form of the soluble ERAD substrate pro-alpha factor into the cytosol (Lee et al., 2004). A second AAA-ATPase, p97(VCP/Cdc48) has also been implicated in ERAD. p97 forms a homohexameric ring that, together with adapter proteins Npl4 and Ufd1, binds ubiquitinated substrates and facilitates their presentation to the proteasome (Braun et al.,

2002; Jarosch et al., 2002; Kobayashi et al., 2002; Rabinovich et al., 2002; Ye et al., 2001; Ye et al., 2004). Precisely how these two ATPase complexes function during ERAD remains unclear, but p97 inactivation or overexpression of dominant negative p97 inhibits retrotranslocation and degradation of transmembrane substrates including CFTR (Bays and Hampton, 2002; Bays et al., 2001; Dalal et al., 2004; Gnann et al., 2004; Huyer et al., 2004; Kobayashi et al., 2002; Rabinovich et al., 2002). A significant question in membrane protein degradation therefore is how the ERAD system coordinates all of the steps required for extraction and degradation while minimizing accumulation and aggregation of hydrophobic degradation intermediates.

In the current study, we examine the role of polypeptide cleavage in membrane extraction and release of a prototypical ERAD substrate CFTR, a polytopic membrane protein with 12 transmembrane segments and three large cytosolic domains. Both in vivo and in vitro CFTR fails to efficiently mature in the ER membrane and is recognized and degraded via the ubiquitin-proteasome pathway (Jensen et al., 1995; Ward et al., 1995; Xiong et al., 1999). Using a reconstituted system that allows direct analysis of degradation products, we now show that fully functional proteasomes release CFTR into the cytosol solely in the form of TCA-soluble peptide fragments. Thus membrane extraction is normally tightly coupled to terminal cleavage events at the cytosolic face of the ER membrane. With progressive ß subunit inhibition, however, production of TCA soluble fragments decreased, and large heterogeneous TCA-insoluble fragments were released into the cytosol in a stable complex with the proteasome. These findings support a model in which excess proteolytic capacity of the 20S proteasome is required to maintain the physiologic balance between membrane extraction and substrate cleavage. By uncoupling peptidase and ATPase activities, proteasome active site inhibitors allow the rate of extraction to exceed the capacity for peptide cleavage and thus give rise to large cytosolic degradation intermediates.

Results

Proteasome β subunit inhibition releases large CFTR fragments from the ER membrane. We previously developed a cell free reticulocyte lysate-based (RRL) system that reconstitutes CFTR synthesis, core glycosylation, membrane integration and ER-associated degradation (Xiong et al., 1999). In this system, newly synthesized CFTR is selectively and specifically radiolabeled at 38 methionine residues broadly distributed throughout the molecule. This enables us to directly monitor both the rate and extent of degradation based on the generation of radiolabeled, TCA-soluble peptide fragments (Oberdorf and Skach, 2002; Xiong et al., 1999). We previously used this system to show that CFTR degradation is ATP-dependent, localized to the ER membrane and sensitive to proteasome active site (β subunit) inhibitors (Oberdorf et al., 2001; Xiong et al., 1999). Because β subunit inhibitors block degradation but do not affect proteasome ATPase activity (Hoffman and Rechsteiner, 1996), this system provides the unique opportunity to directly examine the specific role of peptidase function during the extraction and cytosolic release of a polytopic ERAD substrate.

ER microsomal membranes containing in vitro-synthesized CFTR were isolated, and degradation was carried out in fresh RRL in the presence and absence of proteasome inhibitors (Fig. 1). At progressive time intervals, membranes were pelleted, and cytosolic CFTR fragments were quantitated by scintillation counting before and after TCA precipitation. Under control conditions, CFTR was rapidly released from the ER membrane solely as small TCA-soluble fragments (Fig. 1A). Both degradation and membrane release were completely abolished by ATP depletion (Fig. 1G). In the presence of MG132, both the rate and extent of TCA-soluble fragment production was decreased by ~90% (Fig. 1B). Surprisingly, even though degradation was inhibited, CFTR continued to be released from the ER membrane at nearly 70% of the control rate

as large TCA-insoluble fragments (Fig. 1B, arrow). A cocktail of proteasome inhibitors, *clasto*lactacystin β-lactone, GPFL and leupeptin, which also inhibit all three 20S active β subunits by >95% (Oberdorf et al., 2001) resulted in a similar release of TCA-insoluble fragments (Fig. 1C). *Clasto*lactacystin β-lactone and ALLN, which primarily inhibit chymotrypsin-like activity (β5 subunit), had a smaller effect on CFTR degradation and generated fewer TCA-insoluble fragments (Fig. 1D, E). These results support previous studies showing that CFTR degradation is proteasome-mediated (Gelman et al., 2002), but can be carried out at a reduced rate by residual caspase-like (PGPH) and trypsin-like activities of β1 and β2 subunits (Oberdorf et al., 2001). In contrast to β subunit inhibitors, hemin, an inhibitor of proteasome 19S ATPases (Hoffman and Rechsteiner, 1996; Oberdorf et al., 2001), markedly decreased CFTR release from the membrane, but the small fraction of cytosolic fragments were all TCA-soluble (Fig. 1F). Thus different mechanisms of proteasome inhibition yield very different patterns of ER fragment release.

MG132 exhibits dose dependent effects on proteasome β subunit activities (Bogyo et al., 1997) that directly reflect the rate of CFTR conversion into TCA soluble fragments (Oberdorf et al., 2001). At a concentration of 10 μM, MG132 inhibits β1, β2 and β5 proteolytic activities in RRL by 87%, 66% and >99%, respectively (Table 1), which is similar to that observed for *clasto*lactacystin β-lactone (41%, 85% and >99% inhibition of ß1, ß2 and ß5, respectively). Consistent with these findings, 10 μM MG132 resulted in total CFTR release and a relative proportion of TCA-insoluble fragments that was nearly identical to that observed for *clasto*lactacystin ß-lactone (compare Figs. 2B and 1D). Higher MG132 concentrations caused a dose-dependent increase in production of cytosolic TCA-insoluble fragments (Fig. 2B-E). The cumulative activities of all three proteasome β subunits therefore play a critical role not only in the rate and extent of CFTR degradation, but also in membrane release and degradation product size.

Cytosolic degradation intermediates are heterogeneous (15-45 kDa) and derived from multiple CFTR domains. Because CFTR is the only radiolabeled substrate in cell free reactions, we were able to examine full length products and degradation intermediates directly by SDS-PAGE and autoradiography (Fig. 3). Cytosolic supernatants collected in the presence of MG132 revealed a significant accumulation of heterogeneous 15-45 kDa fragments as well as a much larger species that resembled poly-ubiquitinated CFTR (Fig. 3A, lanes 1-6) (Xiong et al., 1999). Fragments released in the presence of the proteasome inhibitor cocktail (*clasto*lactacystin β-lactone, GPFL and leupeptin) were similar to those observed for MG132 (data not shown). ALLN and *clasto*lactacystin β-lactone also generated visible cytosolic fragments 15-30 kDa but to a lesser extent than MG132 (Fig. 3A, lanes 7-18). As expected, no cytosolic fragments were visualized in control reactions because functional proteasomes generated only TCA-soluble fragments too small to be detected (Fig. 3A, lanes 19-24). Similarly, ATP depletion stabilized full length CFTR, and prevented cytosolic release. Finally, hemin resulted in CFTR accumulation as a high molecular weight ubiquitinated complex that remained quantitatively bound to ER membrane (Fig. 3A,B), consistent with previous membrane flotation experiments (Xiong et al., 1999).

To determine the origin of CFTR cytosolic fragments, we compared the fate of three endogenous epitopes located within N-terminal, C-terminal and internal (R) domains by counting aliquots of degradation reactions either prior to, or following immunoprecipitation with peptide specific antisera (Fig. 4). Because methionine residues are relatively uniformly distributed, the signal recovered by immunoprecipitation approximates the average bulk of CFTR protein attached to each epitope. Under control conditions, epitopes associated with N-, R- and C- domains were cleaved at nearly identical rates and only slightly faster than the rate of conversion into TCA soluble counts

(Fig. 4, compare panels A and B). At later time points there was a minor but consistent sparing of the N-terminal epitope. MG132 markedly slowed the generation of TCA soluble counts and correspondingly decreased the rate at which epitopes were cleaved from the remaining protein. Following ATP depletion, CFTR was quantitatively recovered with all three antisera, demonstrating that all CFTR cleavage events are strictly ATP dependent (Fig. 4D).

TCA-insoluble fragments were next generated in the presence of MG132, and cytosolic and membrane-bound CFTR were recovered by immunoprecipitation and quantitated by scintillation counting (Fig. 5). Under these conditions, 50% of CFTR remaining at the membrane was recovered with each of the three antisera, indicating that residual membrane-bound material consisted of very large fragments. However, cytosolic fragments are primarily 15-45 kDa in size (Fig. 3) and therefore most contain only a single epitope. 43% of total cytosolic counts were recovered by immunoprecipitation, and 20%, 15% and 8% of total cytosolic CFTR remained associated with N-, R- and C-domains, respectively. The CFTR N-terminus, which was most highly protected by MG132, was also the epitope recovered with the largest amount of CFTR protein in the supernatant fraction. Note that there is only one methionine residue N-terminal to the first TM segment that represents only 2.6% of total CFTR methionine content. Thus if all CFTR N-termini were simply shaved off the membrane, then the N-terminal epitope would recover <3% of total CFTR radioactivity. However, 7% of total radioactivity (20% recovery of 35% protein released into the cytosol) was recovered by N-terminus antisera when >50% of N-terminus associated radioactivity remained membrane bound. This indicates that N-terminal cytosolic fragments recovered by immunoprecipitation also contain additional TM segments that have been extracted from the membrane. This conclusion was also consistent with SDS-PAGE analysis of immunoprecipitated fragments (data not shown). Taken together, these data indicate that TCA-insoluble

cytosolic fragments generated by proteasome inhibition are derived from all regions of CFTR including transmembrane domains.

Cytosolic CFTR fragments remain sequestered by the proteasome. Given their hydrophobic nature, CFTR degradation intermediates would be highly prone to aggregation and could pose significant toxicity to cells. We therefore tested whether these fragments were released freely into the cytosol or as part of a larger complex. When supernatants were analyzed by glycerol gradient centrifugation, TCA-soluble fragments were quantitatively recovered near the top of the gradient along with a minor fraction of TCA-insoluble fragments too small to be visualized by SDS-PAGE (Fig. 6A, Fractions #1-4). However, all TCA-insoluble fragments visualized by SDS-PAGE were recovered in denser fractions (#10-13) that corresponded to a molecular mass of ~1,000-2,000 kDa (Fig. 6B). Fractions #10-13 also corresponded to the distribution of proteasomes as determined by Western blotting (data not shown). We therefore tested whether degradation intermediates remained associated with the proteasome after release from the ER membrane by co-immunoprecipitation of membrane pellets and supernatants using a well-characterized antisera that recognizes intact 20S and 26S proteasomes (α_3 20S subunit (Yang et al., 1995)). As shown in Fig. 6C, the entire spectrum of cytosolic TCA-insoluble fragments specifically co-immunoprecipitated with proteasomes, whereas little residual membrane-bound CFTR was recovered. Therefore proteasomes bind to ubiquitinated CFTR at the cytosolic face of the ER membrane where degradation is initiated (Fig. 1 and (Xiong et al., 1999)) and remain quantitatively associated with large fragments after they are released into the cytosol.

p97 is inhibited by hemin and contributes to in vitro CFTR degradation. Recent studies have indicated that in addition to the 19S subunit, the ternary complex p97-Ufd1-Npl4 facilitates ERAD in cells by presenting ubiquitinated substrates to the proteasome.

p97 is also an abundant component of RRL, comprising ~0.1% of total protein (~100 μg/ml, data not shown). Moreover, while hemin is known to inhibit the proteasome 19S subunit, its specificity for other AAA-ATPases has not been extensively studied. We therefore used a recombinant p97 and a dominant negative mutant that lacks ATPase activity (E305Q/E578Q) to determine whether p97 also contributes to CFTR degradation in RRL. Both purified proteins migrated as 600 kDa hexamers on glycerol gradients indicating that they were properly assembled (Fig. 7A). 40 μM hemin inhibited ATPase activity of purified RRL 26S proteasomes (80% inhibition) as expected (Fig. 7B). In addition, hemin also inhibited >95% of p97 ATPase activity. Mutant p97 lacked ATPase activity and further decrease by hemin could not be detected. Moreover, when dominant negative p97 (p97QQ) was added to CFTR degradation reactions, we observed a dose-dependent decrease in the production of CFTR TCA-soluble fragments such that a 10 fold molar excess reduced degradation by ~50% (Fig. 7C). Thus our results are consistent with in vivo studies (Dalal et al., 2004; Gnann et al., 2004) and show that p97 also contributes to proteasome-mediated CFTR degradation in vitro.

Discussion

Polytopic proteins pose a particular challenge for the ERAD pathway because substrates must not only be unfolded, but transmembrane domains must also be extracted from the lipid bilayer, and translocated into the 20S subunit prior to degradation. Here we show that all of these steps are normally coordinated in a processive manner at the cytosolic face of the ER membrane. In the presence of fully functional proteasomes, CFTR was released from the ER membrane solely in the form of free TCA-soluble peptide fragments. Progressive ß subunit inhibition decreased substrate cleavage but had only a modest effect on total protein released from the membrane. This resulted in excessive CFTR unfolding and the uncoordinated generation of large cytosolic TCA-insoluble fragments that were derived from multiple domains throughout the molecule. TCA-

insoluble fragments were generated most efficiently when all three active β subunits were inhibited with either MG132 or a combination of *clasto*lactacystin β-lactone, GPFL and leupeptin. However, partial suppression of proteolytic function (β5 subunit inhibition) with *clasto*lactacystin β-lactone or ALLN also gave rise to a very small fraction of degradation intermediates. Importantly, partially degraded intermediates remained quantitatively sequestered by inactivated proteasomes after their release into the cytosol. In contrast to active site inhibitors, the non-specific AAA-ATPase inhibitor hemin primarily blocked CFTR release from the membrane, but the small percentage of fragments released were entirely TCA-soluble. Taken together, these data indicate that excess proteolytic activity of the 20S subunit assures that the rate of substrate cleavage normally exceeds that of unfolding and as a result, membrane extraction is obligatorily coupled to terminal cleavage events. When protease activity is compromised, however, this balance is disrupted and substrate unfolding in the absence of cleavage gives rise to large cytosolic degradation intermediates.

In vitro CFTR degradation was ATP dependent and highly sensitive to proteasome inhibitors. This is consistent with the ATP requirement for ubiquitination, which is a prerequisite for degradation of most 26S proteasome substrates including CFTR. However, cytosolic fragments continued to be released in the presence of MG132, raising that possibility that other proteases might be involved in clipping CFTR. Indeed, several non-proteasome pathways involving signal peptide peptidase (Crawshaw et al., 2004), insulin-degrading enzyme (Schmitz et al., 2004), ER-60 (Qiu and Kohen-Avramoglu, 2004), and other lumenal and membrane bound proteases (Cabral et al., 1997; Loo and Clarke, 1998) have been implicated in the degradation of some ERAD substrates. However, non-proteasome ERAD pathways discovered to date are ATP-independent. Thus our findings that all CFTR cleavage and fragment release were completely abolished by ATP depletion (Fig. 4D) make it less likely that alternative proteases are

involved in CFTR degradation in vitro. Moreover, if ATP depletion masked these secondary protease sites by stabilizing CFTR interactions with cytosolic or lumenal chaperones, e.g. Hsp40, Hsp70 or Hsp90 (Loo and Clarke, 1998; Meacham et al., 1999; Meacham et al., 2001; Yang et al., 1993; Youker et al., 2004), then we would have expected at least some large fragments to be released when AAA-ATPases were inhibited in the presence of ATP. This we did not see, since only TCA soluble fragments were released in the presence of hemin. Finally, given our findings that degradation intermediates can be titrated by β subunit inhibition, and previous studies demonstrating that degradation is completely inhibited in the presence of both MG132 and hemin (Xiong et al., 1999), the most likely that explanation for our findings is that residual proteasome peptidase activity is responsible for the release of cytosolic TCA-insoluble CFTR fragments.

How then are TCA-insoluble fragments generated? The "limited diffusion" model predicts that the size of proteasome degradation products is governed by their ability to diffuse out of the of the 20S particle (Kisselev et al., 1999a; Kohler et al., 2001), which may involve repeated cycles of binding and release of the 19S caps (Babbitt et al., 2005). Our results suggest a novel variation in this model in which product size can also be influenced by the relative capacities of protein unfolding and peptide cleavage. Previous studies have shown that genetic inactivation of a single β subunit changes fragment composition but does not significantly affect product size (Dick et al., 1998; Kisselev et al., 1999a; Nussbaum et al., 1998). This is consistent with results that β5 subunit inhibition (*clasto*lactacystin ß-lactone and ALLN), modestly decreases the rate of CFTR degradation and has very minor effects on the fraction of TCA-insoluble fragments produced. In contrast, genetic inactivation of all β subunit activity in the prokaryotic Lon protease not only blocks degradation but also prevents polypeptide translocation through the proteasome core (Melderen and Gottesman, 1999). We propose that MG132

inhibition of eukaryotic proteasomes represents an intermediate between these two states in which all three protease activities are severely but incompletely compromised (β1, β2, and β5 subunits exhibit <2%, 6.5% and <0.1% activity, respectively, in 100 μM MG132 (Oberdorf et al., 2001)). This allows substrate to be unfolded and threaded into the 20S subunit where rare cleavage events can still be carried out by the weak residual β subunit activity.

Our findings that TCA-insoluble CFTR fragments remain associated with inhibited proteasomes also suggest that β subunit inhibitors can induce a partial block in peptide translocation similar to that observed for Lon (Groll et al., 1997; Melderen and Gottesman, 1999). As with prokaryotic ATP-dependent proteases, unfolding and membrane extraction would be expected to continue with accumulation of substrate at or near the surface of the ATPase ring (Benaroudj and Goldberg, 2000; Groll et al., 1997; Hoskins et al., 1998; Melderen and Gottesman, 1999; Navon and Goldberg, 2001; Reid et al., 2001; Singh et al., 2000). Thus fragment size is increased because reduced diffusion of the large peptide fragments through the proteasome is compensated by a severe decrease in proteolytic capacity. Based on the size of cytosolic CFTR fragments recovered (15-45 kDa), it is likely that smaller ERAD substrates could undergo complete retro-translocation by a similar mechanism. This likely explains why intact proteins are often found in cytosolic fractions in the presence of proteasome inhibitors (McCracken and Brodsky, 1996; VanSlyke and Musil, 2002; Wiertz et al., 1996; Yu et al., 1997).

Our findings provide additional evidence that AAA-ATPases participate in unfolding and/or membrane extraction of ERAD substrates (Bays et al., 2001; Braun et al., 2002; Jarosch et al., 2002; Kobayashi et al., 2002; Mayer et al., 1998; Meyer et al., 2002; Plemper and Wolf, 1999; Rabinovich et al., 2002; Ye et al., 2001; Ye et al., 2003; Ye et al., 2004). Hemin has long been known to inhibit proteasome-mediated degradation in

RRL by blocking proteasome 19S ATPase activity (Etlinger and Goldberg, 1980; Haas and Rose, 1981; Hoffman and Rechsteiner, 1996; Hough et al., 1986; Hough et al., 1987; Xiong et al., 1999). However, it does not affect β subunit activity of 20S or 26S RRL proteasomes as measured by cleavage of fluorogenic substrates (Oberdorf et al., 2001). We now show that hemin also inhibits p97. Moreover, p97 facilitates CFTR degradation in vitro, which is consistent with recent in vivo studies (Dalal et al., 2004; Gnann et al., 2004). Thus our data indicate that in the presence of active site inhibitors, CFTR unfolding and extraction continues to be carried out by 19S and p97 ATPases independently of proteolytic cleavage.

In cells that contain fully functional proteasomes, degradation of polytopic proteins is processive (Mayer et al., 1998; Plemper et al., 1998; Plemper and Wolf, 1999), and cytosolic CFTR intermediates are not generally observed (Bence et al., 2001; Ward et al., 1995). However, active-site inhibitors (e.g. MG132, ALLN and lactacystin) result in CFTR accumulation in perinuclear inclusion bodies called aggresomes (Bebok et al., 1998; Jensen et al., 1995; Johnston et al., 1998; Ward et al., 1995; Wigley et al., 1999). Such inclusions characteristically lack cellular membranes, contain aggregated immunoreactive CFTR, and are highly concentrated in ubiquitin, proteasomes and cellular chaperones. The TCA-insoluble cytosolic CFTR fragments observed in this study thus likely represent aggresome precursors. They retain multiple CFTR epitopes, resemble high molecular weight ubiquitinated species on SDS PAGE, and remain stably associated with the proteasome. TCA-insoluble fragments were generated much more efficiently by MG132 than by *clasto*lactacystin β-lactone or ALLN. This is consistent with the greater in vivo effect of MG132 on CFTR degradation (Gelman et al., 2002) and the more pronounced stress response when compared to lactacystin or ALLN (Bush et al., 1997). The observation that all three inhibitors give rise to aggresomes in vivo, however, suggests that intact cells may be more sensitive than RRL, possibly because aggregation

requires only a small fraction of degradation intermediates in the face of ongoing protein synthesis. This would likely induce secondary effects by sequestering proteasomes and potentiating a general inhibition of the proteasome pathway (Bence et al., 2001; Ma et al., 2002). We propose that commonly used β subunit inhibitors thus give rise to aggresomes by uncoupling cleavage from the ATP-dependent process of membrane extraction, thereby releasing large retro-translocated intermediates and/or intact proteins from the ER membrane.

Materials and Methods

*Clasto*lactacystin β-lactone was obtained from Cal-Biochem (San Diego, Ca.). Nucleotides and DTT were purchased from Roche Molecular Biochemicals (Indianapolis, IN). N- terminal, C-terminal and R-domain CFTR antisera are described elsewhere (Xiong et al., 1999). Proteasome C-9 antisera against the α_3 subunit was provided by Dr. Klaus Früh (Yang et al., 1995). Tran[^{35}S]-label was purchased from ICN Pharmaceuticals (Irvine CA). Purified 26S proteasomes were kindly provided by Dr. Martin Rechsteiner. Rabbit reticulocyte lysate, RRL, was prepared from freshly harvested reticulocytes by hypotonic lysis using a slightly modified method of Jackson and Hunt (Jackson and Hunt, 1983; Oberdorf and Skach, 2002). Lysate was digested at 24° C for 10 minutes with staphylococcus S7 nuclease (Roche, Indianapolis, IN), and nuclease was inactivated by addition of 2.0 mM EGTA. Hemin was added (40 μM) for translation reactions. Canine pancreas microsomal membranes were prepared as previously described (Oberdorf and Skach, 2002). GPFL peptide was kindly provided by Dr. Christopher Cardozo. Chemicals were purchased from Sigma (St. Louis, MO) unless otherwise stated.

Recombinant proteins: Plasmids pQE9 p97wt and pQE9 p97QQ (E305Q/E578Q), provided by Dr. Hemmo Meyer, were used to sub clone the P97 coding sequence into

NcoI and BamH1 sites of pET15b (EMD Biosciences, San Diego, CA) by PCR amplification using primers (sense) GTGGCCATGGGACACCATCACCATCACCATATGGCCTCTGGAGCCGAT, (antisense) TGCGGATCCTTAGCCATACAGGTCATC. p97 expression was induced for 3 hours at 37°C in *E. coli* BL21(DE3) by addition of 0.4 mM Isopropyl β-D-1-thiogalactopyranoside. Cells were pelleted and lysed (2x) by French Press (1250 psi), loaded onto a 5.0 ml Ni-NTA column (Qiagen, Valencia, CA), and washed extensively with 50 ml of 300 mM NaCl, 1mM β-mercaptoethanol, 5% glycerol, 0.4 mM PMSF, 25 mM imidazole, and 50 mM Tris-HCl (pH 7.5). His tagged p97 was eluted with a linear 25 mM-500 mM imidazole gradient. Fractions were pooled and dialyzed in 100mM NaCl, 1mM β-mercaptoethanol, and 25 mM Tris-HCl (pH 7.5), concentrated on a Centriplus YM-30 or YM-50 filter, flash frozen and stored at –80°C.

In vitro Transcription/Translation. CFTR mRNA was transcribed in vitro at 40°C for 1 hour in reactions containing 0.4 mg/ml plasmid DNA (plasmid pSPCFTR (Xiong et al., 1999), 40 mM Tris-HCl (pH 7.5), 6.0 mM $MgAc_2$, 2 mM spermidine, 0.5 mM each of ATP, CTP, UTP, 0.1 mM GTP, 0.5 mM GpppG (Amersham Pharmacia, Piscataway, NJ), 10 mM DTT, 0.2 mg/ml bovine calf tRNA, 0.75 U/ml RNAse inhibitor (Promega, Madison, WI), and 0.4 U/ml SP6 RNA polymerase (Epicentre, Madison, WI). Mock transcription was identical except that no plasmid DNA was added. Translation was performed at 25°C for 2 hours in reactions containing 20% transcript mixture, 40% nucleased rabbit reticulocyte lysate (Oberdorf and Skach, 2002), plus additional 1 mM ATP, 1 mM GTP, 12 mM creatine phosphate, 40 μM each of 19 essential amino acids, except methionine, 1 μCi/μl of Tran[^{35}S]-label, 40 μg/ml creatine kinase, 0.1 mg/ml tRNA, 0.2 U/μl RNAse inhibitor (Promega, Madison WI), 10 mM Tris-HCl (pH 7.5), 100 mM KOAc, and 2 mM $MgCl_2$. Canine pancreas microsomal membranes (Walter and Blobel, 1983) were added at the start of translation (final concentration, 6.0 OD_{280}).

50μM aurin tricarboxylic acid was added at T = 15 minutes to synchronize protein synthesis.

Proteasome peptidase activities. Crude proteasomes were prepared by diluting RRL five fold in 20mM Tris-HCl (pH 7.5), 1 mM ATP, 1 mM $MgCl_2$ and 1 mM DTT and pelleting at 290,000 X G for 2 h. Pellets were resuspended in 100 mM Tris-HCl (pH 8.0), 1 mM ATP, 1mM DTT at dilutions yielding activity equivalent to that found in RRL (Oberdorf et al., 2001). Fluorogenic substrates cbz-LLE-AMC (CalBiochem, San Diego, CA), t-boc-LRR-AMC (Sigma, St. Louis, MO), suc-LLVY-AMC (Sigma, St. Louis, MO) were used to monitor β1, β2 and β5 peptidase activities, respectively. Reactions were carried out at 37°C as described previously (Oberdorf et al., 2001) and terminated by adding one volume of 10% SDS followed by 18 volumes of 100 mM Tris-HCl (pH 9.0). AMC release was determined in opaque micro-titer plates using a BioRad FluoroMark plate reader (355Ex/460Em) after correcting for background fluorescence (T=0). Purified AMC was used to generate a standard curve, and proteasome inhibition was expressed as the percent of control activity. The length of the incubation was adjusted so that the rate of hydrolysis remained linear over the time course of the reaction.

In vitro degradation. ER membranes containing in vitro translated CFTR were collected by pelleting twice through 0.5 M sucrose in Buffer A (50 mM HEPES-KOH (pH 7.5,) 0.1M KCl, 5 mM MgCl2, and 1mM DTT) at 180,000 X g for 10 minutes as described (Oberdorf et al., 2001; Oberdorf and Skach, 2002). The membrane pellet was resuspended in Buffer A with 0.1 M sucrose and added to a degradation reaction with final concentrations of 68% reticulocyte lysate, 20% microsomal membranes, 10 mM Tris-HCl (pH 7.5), 1 mM ATP, 5 mM $MgCl_2$, 12 mM creatine phosphate, 3 mM DTT and 80 μg/ml of creatine kinase. RRL used for degradation was prepared as above except that it was not

nucleased and no exogenous hemin was added. Because degradation activities varied between similarly prepared lysates from different animals (unpublished observation), individual lysates were tested separately, and preparations that yielded the most robust CFTR degradation (e.g. typically 50-70% in 4 h) were used for ERAD experiments. The reasons this variability are unknown but may reflect slight differences in degradation machinery and/or endogenous hemin levels. We favor the latter explanation because different RRL preparations also exhibited varying levels of translation in the absence of exogenous hemin (unpublished observation). Degradation was carried out at 37°C. ATP was depleted by substituting creatine kinase with hexokinase (20 units/ml) and deoxyglucose (20mM). Where indicated, purified recombinant mutant p97 (p97QQ) was added to 0.1 mg/ml, 0.5 mg/ml, or 1 mg/ml. Degradation was quantitated by precipitating samples in 20% TCA and counting supernatants (Beckman LS6500 scintillation counter). Total [^{35}S] incorporation was determined by direct scintillation counting. For all experiments, CFTR degradation was corrected for by subtracting counts typically released from Mock translations (~22% of total), which represent a reversible association of [^{35}S] species with components of ER microsomal membranes (Oberdorf et al., 2001). TCA-soluble counts (CPM released) were expressed as a percentage of the total [^{35}S] labeled CFTR present at T=0 using the formula:

$$\%\ \text{TCA counts} = \frac{[\text{TCA-soluble CPM(CFTR)}] - [\text{TCA-soluble CPM (Mock)}]}{((\text{Total CFTR incorporated } [^{35}\text{S}] * 0.78) - (\text{TCA-soluble CPM at T=0}))}$$

Error bars represent SEM derived from at least three experiments.

Release of CFTR from the ER membrane. CFTR released from the ER membrane was determined by pelleting degradation samples through Buffer A as above and counting supernatant prior to and after TCA precipitation. The fraction of TCA soluble and insoluble CFTR released into the supernatant was calculated using the formula above.

Supernatants and total products were also analyzed directly by SDS-PAGE on 7-12% or 7% gels, respectively. Gels were treated with En^{3}Hance (NEN Life Science Products, Boston, Ma) fluorography, autoradiography and digitized using an UMax Powerlook III scanner and Adobe Photoshop software.

Glycerol gradient centrifugation. CFTR degradation was performed in the presence of 100μM MG132, and membranes were removed by dilution into 7 vol of 0.1M sucrose in Buffer A and centrifugation (180,000 X G for 10 min). Supernatant was then loaded onto a 15-40% glycerol gradient containing 100mM Tris-HCl (pH 7.5), 100 mM KCl, 5 mM $MgCl_2$ and 1mM DTT. Samples were centrifuged at 260,000 X g for 2.5 h, and fractions were collected from top to bottom and subjected to scintillation counting prior to and following precipitation in 20% TCA precipitation or analysis by SDS-PAGE.

Immunoprecipitation. For CFTR immunoprecipitation, samples were diluted into 1 ml of Buffer B (0.1 M NaCl, 10 mM EDTA, 1% Triton X-100 and 0.1 M Tris-HCl (pH 8.0)) at specified times after initiation of degradation reaction. 1μl of N-terminal , C-terminal , or R-domain antisera was added followed by 5 μl of protein A Affi-Gel beads (BioRad, Hercules, Ca). Samples were rotated overnight at 4° C, washed three times with 0.5 ml Buffer B and twice with 0.5 ml 0.1M NaCl, 0.1 M Tris, pH 8.0. Antigen was eluted by addition of 1.0% SDS, 0.1 M Tris-HCl (pH 8.0) and quantitated by scintillation counting. Counts immunoprecipitated from mock translation were equivalent to background CPM. The percent of CFTR counts that remained associated with each epitope was determined by:

$$\% \text{ CFTR bound to epitope} = \frac{(\text{CPM recovered at t=n} - \text{background}) \times 100}{(\text{CPM recovered at t=0} - \text{background})}$$

To determine the relative signal associated with each epitope released into the supernatant, degradation was carried out for 2 hr in the presence of 100 μM MG132. Membrane and supernatant fractions were separated by centrifugation and immunoprecipitated as above. Fragments recovered were quantitated by scintillation counting and expressed as the percent of total radioactivity in each fraction that remained associated with each epitope. Counts recovered by IP were corrected for IP efficiency of each antibody as determined below.

$$\% \text{ radioactivity associated with epitope} = \frac{\text{CPM IP'd from fraction t=2h / (IP efficiency)}}{\text{(total CPM in fraction t=2h)}}$$

$$\text{IP efficiency (determined independently for each antibody)} = \frac{\text{CPM IP'd t=0}}{\text{CPM t=0}}$$

Proteasomes were immunoprecipitated using C9 antisera (Yang et al., 1995) in 1% NP-40, 100 mM NaCl, 25 mM HEPES (pH7.5), 1 mM EDTA, 2 mM ATP and 5 mM $MgCl_2$. Samples were incubated overnight, washed 5x with IP buffer and beads were eluted directly with SDS-loading buffer and analyzed by SDS-PAGE and autoradiography.

ATPase assay: ATPase activities of p97 and 26 proteasomes were performed as described previously (Hoffman and Rechsteiner, 1996; Song et al., 2003). Purified recombinant p97, p97QQ (0.25 μg total) or RRL 26S proteasomes (2 μg) ATP were added to 1mM $MgCl_2$, 1mM DTT, and 20mM HEPES (pH 7.5) with or without 40 μM hemin. Reactions were incubated at 24°C for 10 min. 1mM ATP was then added and the reaction was incubated at 37°C for 30 minutes (p97 constructs) or 1 hour (26S). 200 μl of 6 mM ammonium molybdate, 0.8M HCl, 120μM malachite green and 0.06% polyvinyl alcohol was added. Reactions were further incubated 10 minutes at 24°C, and

absorbance at 630nm was measured in a 96-well plate on a Biotek plate reader. Inorganic phosphate released was calculated from a standard curve using KH_2PO_4.

Acknowledgments:

The authors thank the following individuals for generously providing the following reagents: Dr. C. Cardozo for GPFL peptide, Dr. K. Früh for C9 anti-proteasome antisera, Dr. H. Meyer and Dr. G. Warren for providing wild type and mutant p97 cDNA, and Dr. M. Rechsteiner for purified RRL proteasomes. We also thank C. Daniel and Dr. P. Sahaayaruban for technical assistance, and Drs. L. Musil and C. Enns for their critical review of the manuscript. This work was funded by grants from the Cystic Fibrosis Foundation and NIH, GM53457 (W.S.), DK51818 (W.S.) and T32 DK07674 (J.O.) and an Established Investigator Grant from the American Heart Association.

Table 1

% Residual Protease Acvity

[MG132]	β1	β2	β5
10 μM	13+/-3.1%	34+/-4.9%	0.6+/-0.5%
25 μM	5.3+/-1.6%	16.6+/-2.6%	ND
50 μM	3.3+/-2.3%	11.1+/-1.8%	ND
100 μM	1.8+/-0.5%	6.5+/-0.7%	ND

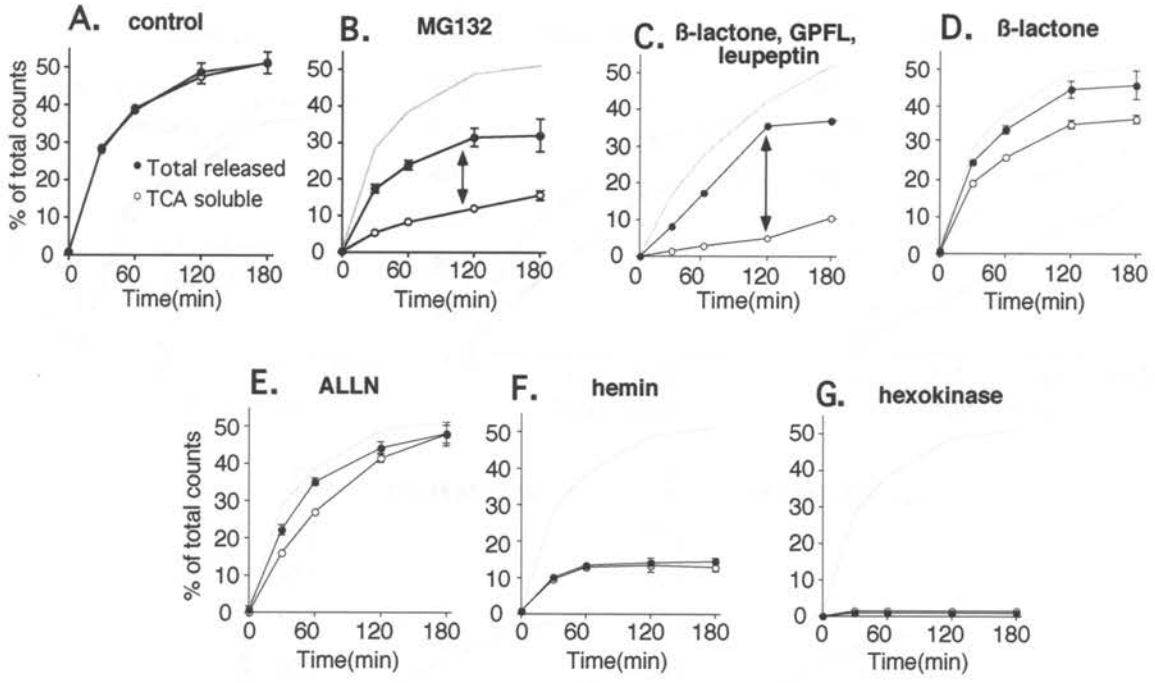

Figure 3-1. Cytosolic release of TCA-insoluble CFTR fragments. CFTR degradation was carried out (A) in the absence of inhibitors, or in the presence of (B)100μM MG132 (C), 100μM *clasto*lactacystin β-lactone plus 500μM GPFL plus 100μM leupeptin, (D)100 μM *clasto*lactacystin β-lactone, (E) 100 μM ALLN, (F) 40 μM hemin or (G) hexokinase and 2-deoxyglucose as described in Methods. Total (•) and TCA-soluble (^{o}) CFTR radioactive fragments recovered in the cytosolic fraction are expressed as the percentage of total CFTR counts present at t=0. Difference between total and TCA-soluble counts released (double arrow) indicates relative amount of CFTR released in the form of TCA-insoluble fragments. Gray line (panels B-G) shows total CFTR converted into TCA-soluble counts under control conditions.

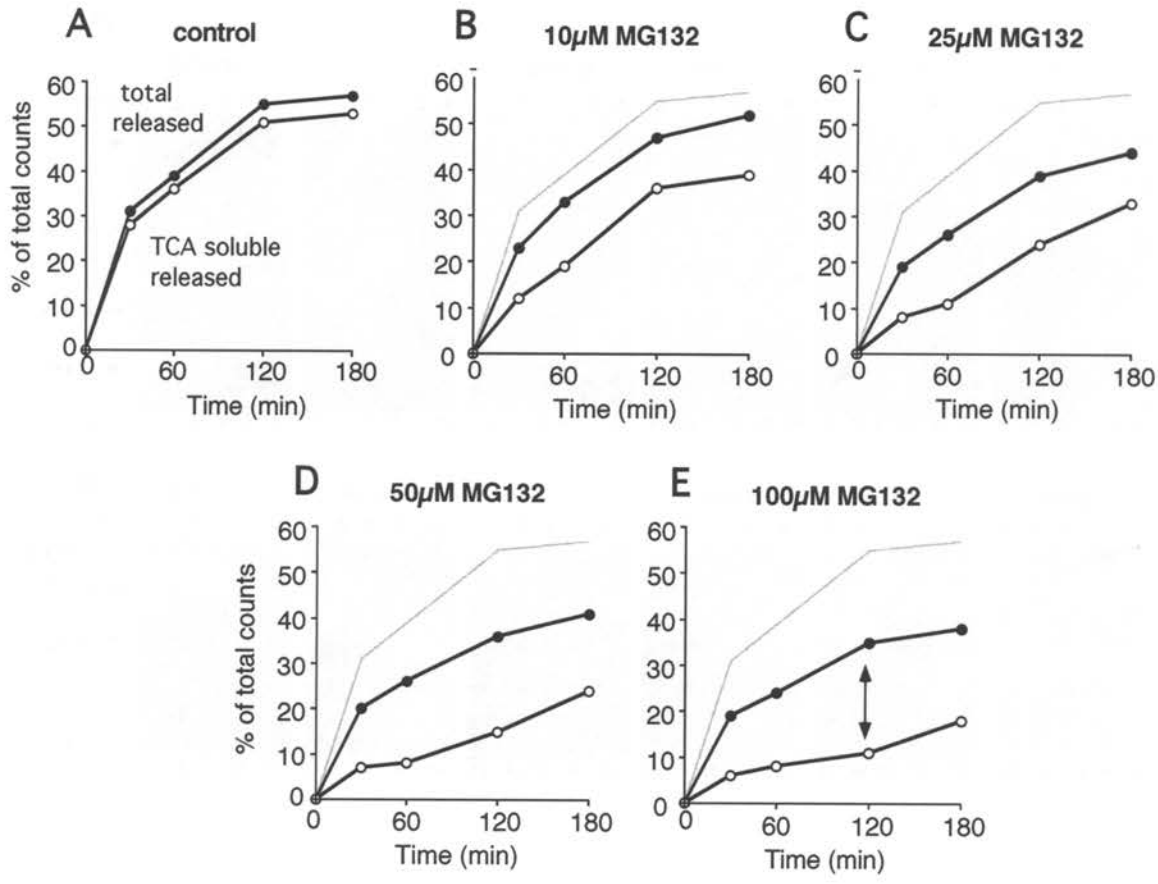

Figure 3-2. Release of TCA-insoluble fragments is proportional to β subunit inhibition. CFTR degradation was carried out at indicated concentrations of MG132. The amount of total (•) and TCA-soluble (o) fragments released from ER membrane was determined as in Fig. 1. TCA-insoluble fragments released are indicated by double arrow.

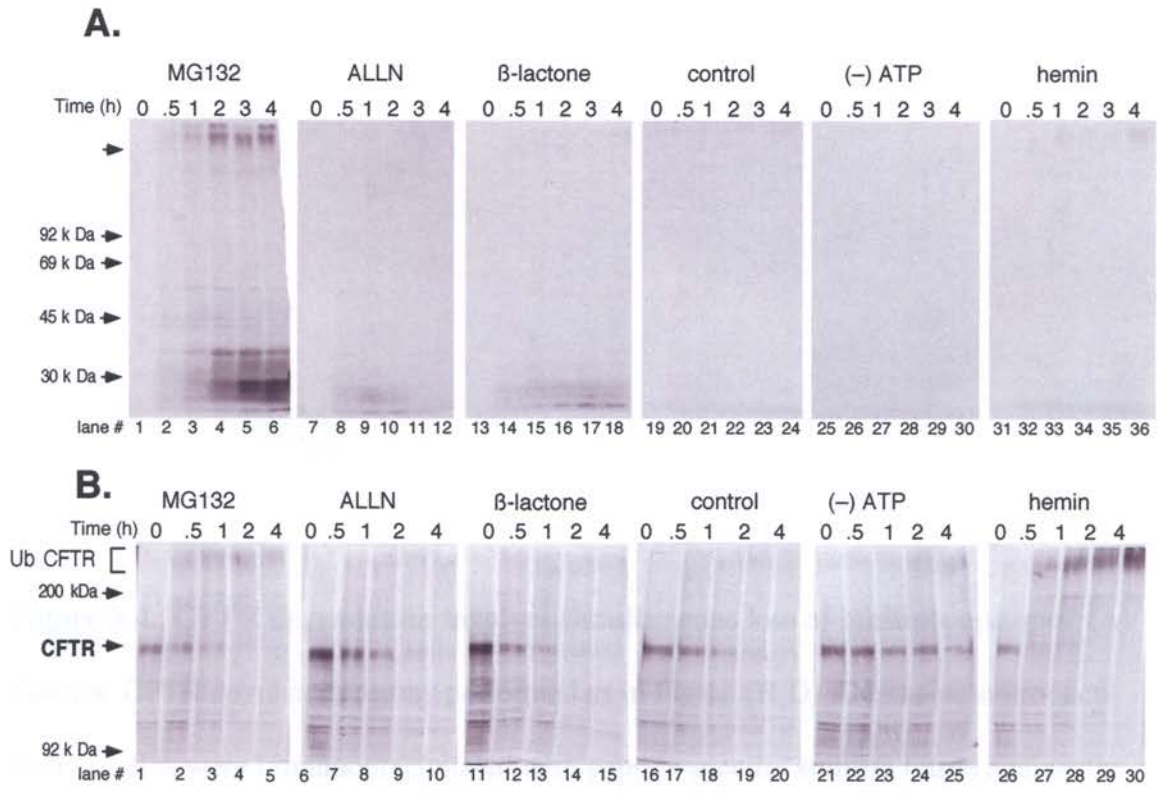

Figure 3-3. Released CFTR fragments are heterogeneous. (A) Supernatants of CFTR degradation reactions were collected at times indicated and analyzed by SDS-PAGE (7-12% gel) and autoradiography. Inhibitor concentrations were 100 μM for MG132, ALLN, *Clasto*lactacystin β-lactone (β lactone) and 40 μM for hemin. Hexokinase and 2-deoxyglusose were added to deplete ATP (–ATP). (B) Total products of the degradation reaction are shown to demonstrate the rate of disappearance of CFTR protein. High M_r material in lanes 26-30 (hemin treatment) represents ubiquitinated CFTR products (Xiong et al., 1999). Exposure of the top panel was longer (5X) than the bottom panel.

Figure 3-4. CFTR degradation involves simultaneous loss of multiple epitopes (A) Control CFTR degradation assay performed as in Fig 1. (B-D) Degradation products from panel A were immunoprecipitated with peptide specific antisera raised against the N-terminus (■), C-terminus (▼), or R-domain (▲) epitopes. Fragments recovered with each antibody were quantitated by scintillation counting and expressed as the percentage of counts recovered at T=0.

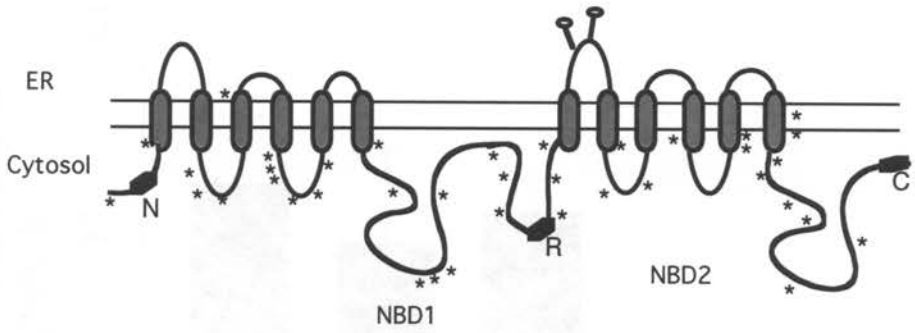
ER
Cytosol
N
C
R
NBD1
NBD2

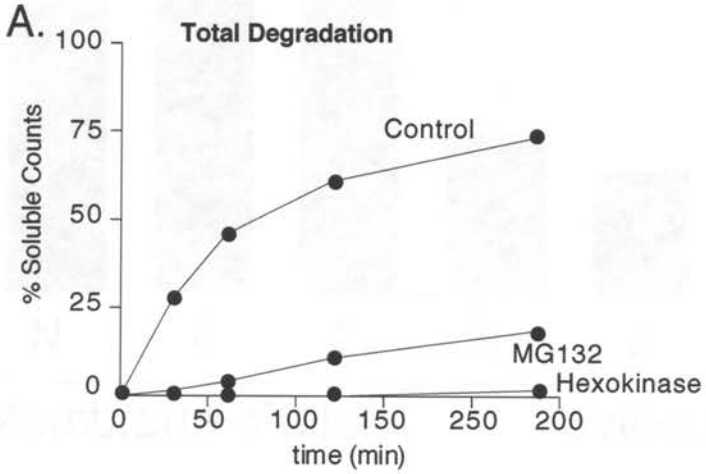
A.
Total Degradation
% Soluble Counts
100
75
50
25
0
Control
MG132
Hexokinase
0
50
100
150
250
200
time (min)

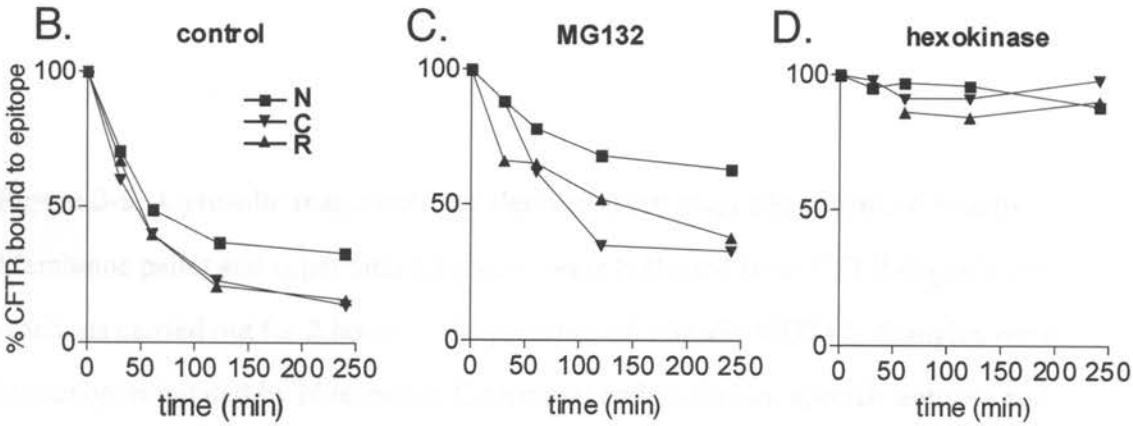
B.
control
% CFTR bound to epitope
100
50
0
N
C
R
0 50 100 150 200 250
time (min)
C.
MG132
100
50
0
0 50 100 150 200 250
time (min)
D.
hexokinase
100
50
0
0 50 100 150 200 250
time (min)

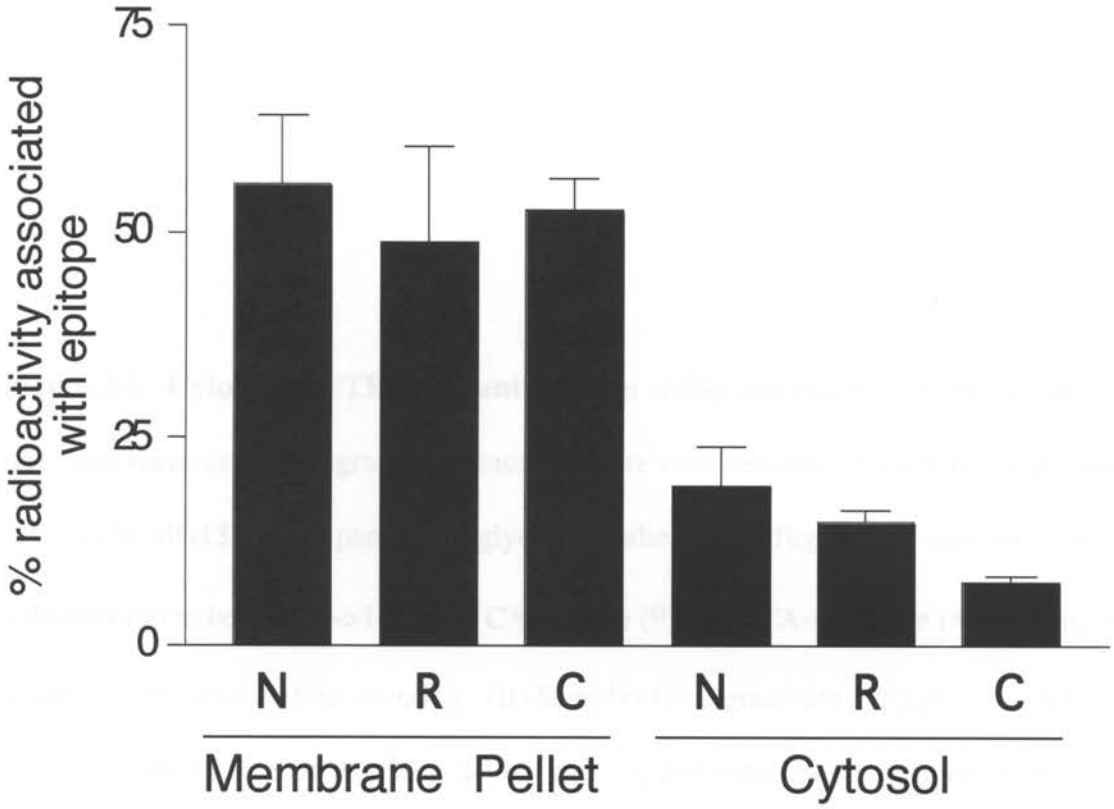

Figure 3-5. Cytosolic fragments are derived from multiple peptide domains. Membrane pellet and supernatant fractions were collected from CFTR degradation reactions carried out for 2 hours in the presence of 100 μM MG132. Samples were immunoprecipitated by N-terminal, C-terminal and R-domain specific antisera and quantitated by scintillation counting as in Fig. 5. Data are expressed as the fraction of total radioactive counts in pellet and supernatant fractions that remained associated with indicated epitopes.

Figure 3-6. Cytosolic CFTR fragments remain stably associated with proteasomes. (A) Supernatants from degradation reactions were collected after 2 hours in the presence of 100 μM MG132 and separated by glycerol gradient centrifugation. Fractions were collected top to bottom (1->14) and TCA-soluble (^{o}) and TCA-insoluble ($\bullet$) material was quantitated by scintillation counting. (B) Samples from gradients in panel (A) were analyzed directly by SDS-PAGE (12-17% gel) and autoradiography. Migration of molecular weight markers in the gradient are indicated at top of the gel. (C) Degradation was carried out as in panel (A) and membranes were pelleted through a 0.5 M sucrose cushion. Supernatant and pellet fractions were analyzed directly (lanes 1,5) or immunoprecipitated with preimmune sera (PIS) or antisera against the α_3 proteasome subunit.

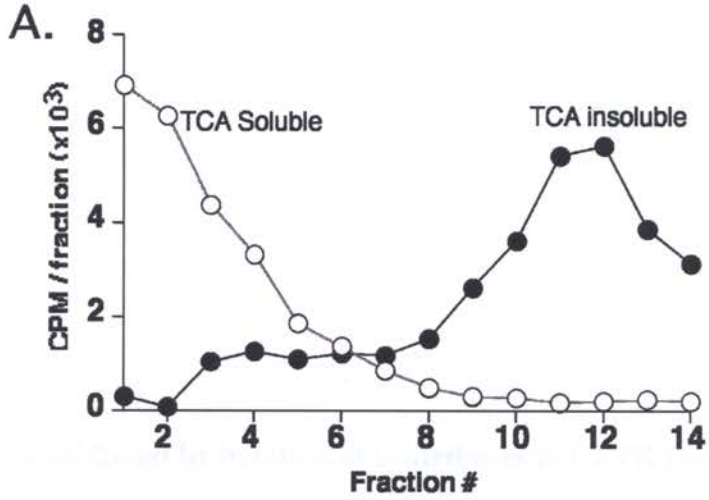
A.
CPM / fraction (x10^3)
TCA Soluble
TCA insoluble
Fraction #

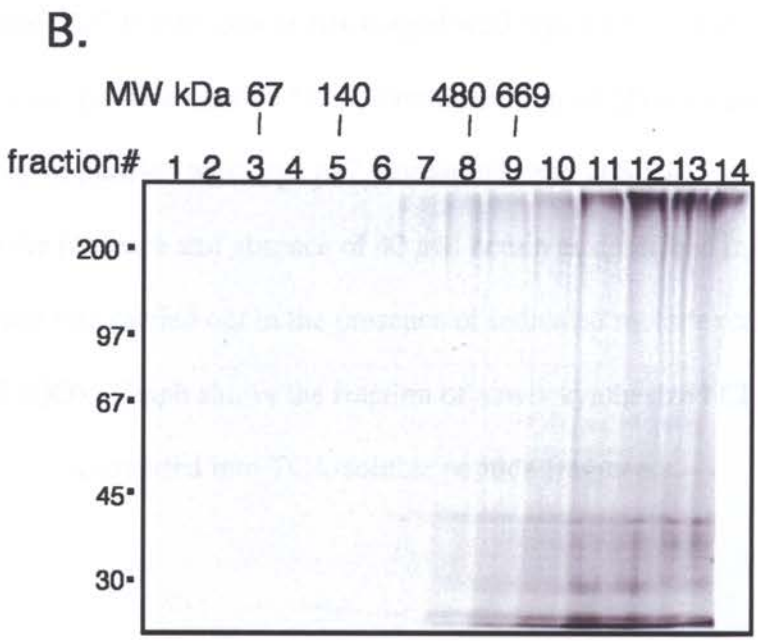
B.
MW kDa 67 140 480 669
fraction# 1 2 3 4 5 6 7 8 9 10 11 12 13 14
200
97
67
45
30

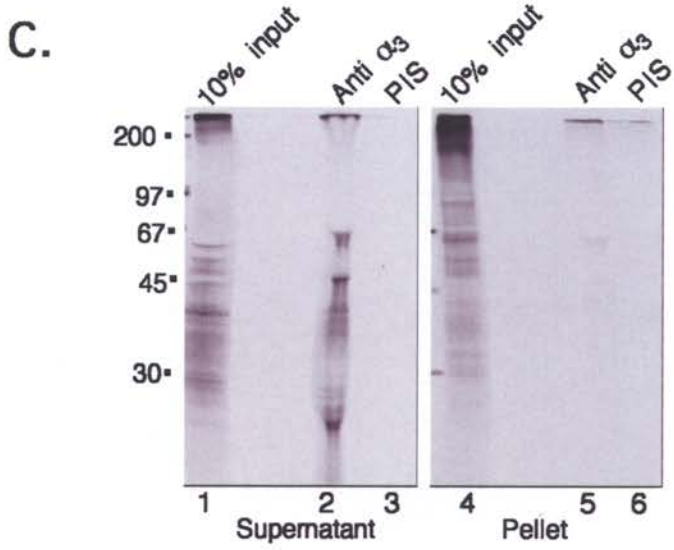
C.
10% input
Anti α3
PIS
10% input
Anti α3
PIS
200
97
67
45
30
1 2 3 4 5 6
Supernatant
Pellet

Figure 3-7. p97 is inhibited by hemin and contributes to CFTR degradation. (A) Coomassie stained SDS-PAGE gels of His-tagged wild type (WT) and dominant-negative mutant (QQ) p97 purified on a Ni NTA column and run on glycerol gradients. (B) ATPase activity of purified wild type p97, mutant p97 and 26S RRL proteasomes was determined in the presence and absence of 40 μM hemin as described in Methods. (C) CFTR degradation was carried out in the presence of indicated molar excess of dominant-negative p97 (QQ). Graph shows the fraction of newly synthesized CFTR that was converted into TCA-soluble peptide fragments.

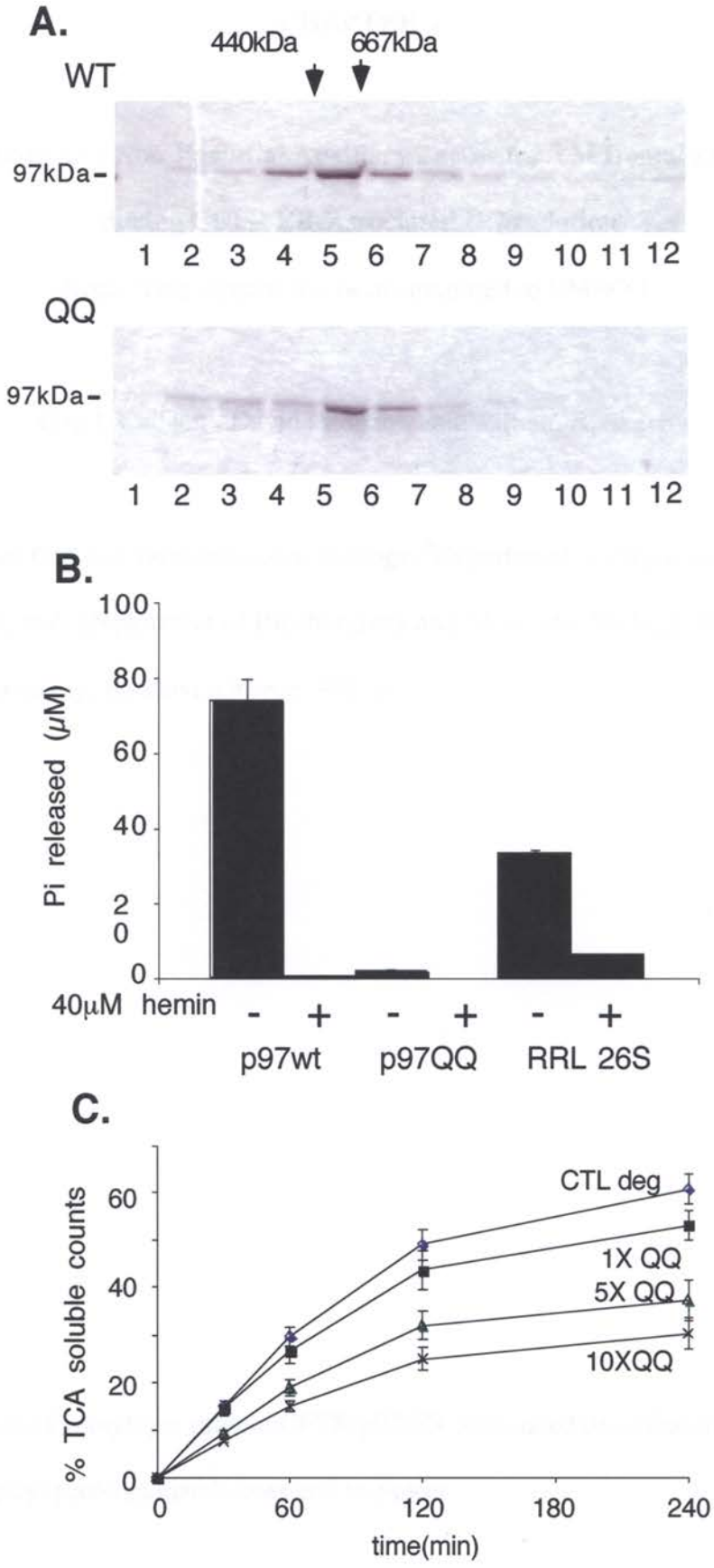
A.
440kDa
667kDa
WT
97kDa-
1 2 3 4 5 6 7 8 9 10 11 12
QQ
97kDa-
1 2 3 4 5 6 7 8 9 10 11 12
B.
Pi released (μM)
100
80
60
40
2
0
0
40μM hemin
- + - + - +
p97wt
p97QQ
RRL 26S
C.
% TCA soluble counts
60
40
20
0
CTL deg
1X QQ
5X QQ
10XQQ
0
60
120
180
240
time(min)

CHAPTER 4

p97 Functions as a Non-Essential Auxiliary Factor for TM Domain Extraction during CFTR ER-Associated Degradation

Note: This chapter has been submitted to EMBO J.

Eric J. Carlson[1], David Pitonzo[2], and William R. Skach[3]

[1]Department of Cell and Developmental Biology, [2]Department of Physiology and Pharmacology, and [3]Department of Biochemistry and Molecular Biology, Oregon Health & Science University, Portland, Oregon 97239

Key Words: ERAD/polytopic protein/CFTR/p97/ER-associated degradation

Subject Category: proteins/membranes and transport

Abstract

The AAA-ATPase p97 has been implicated in the degradation of misfolded and unassembled proteins in the endoplasmic reticulum (ERAD). To better understand its role in this process, we used a reconstituted cell-free system to define the precise contribution of p97 in degrading immature forms of the polytopic, multi-domain protein CFTR. Although p97 augmented both the rate and the extent of CFTR degradation, it was not obligatorily required for ERAD. Only a 50% decrease in degradation was observed in the complete absence of p97. Moreover, p97 specifically stimulated the degradation of CFTR transmembrane (TM) domains but had no effect on isolated cytosolic domains. Consistent with this, p97-mediated extraction of intact TM domains was independent of proteolytic cleavage and influenced by TM segment hydrophobicity, indicating that the relative contribution of p97 is partially determined by substrate stability. Thus we propose that p97 functions in ERAD as a nonessential but important ancillary component to the proteasome where it facilitates substrate presentation and increases the degradation rate and efficiency of stable (TM) domains.

Introduction

A fundamental obstacle in membrane protein degradation is the presentation of substrate to cytosolic and/or extracytosolic proteases. In this regard, two AAA-ATPases (ATPases Associated with various cellular Activities) (Ogura and Wilkinson, 2001) have been proposed to facilitate retrotranslocation and membrane extraction of misfolded and unassembled proteins in the endoplasmic reticulum (ER) (Mayer et al., 1998; McCracken and Brodsky, 2003; Pickart and Cohen, 2004; Plemper et al., 1998; Ye et al., 2001). One ATPase is comprised of a ring of six subunits located at the base of the 19S proteasome regulatory complex (RC) (Glickman et al., 1998). The second is the homohexameric protein p97 (VCP/cdc48) that functions together with cofactors Ufd1 and Npl4 (Bays and Hampton, 2002). Both ATPases associate with the 20S proteasome, bind directly to polyubiquitinated proteins and facilitate degradation of both ER and cytosolic substrates (Bays and Hampton, 2002; Dai et al., 1998; Pickart and Cohen, 2004). The base of the 19S RC has been reported to interact directly with the Sec61 translocation machinery (Kalies et al., 2005). In contrast, p97 binds the ER via one or more large complexes that include several ubiquitin ligases (gp78, Doa10 and/or Hrd1), VIMP1, the tetraspan protein Derlin-1, and Ubx2 (Lilley and Ploegh, 2004; Neuber et al., 2005; Schuberth and Buchberger, 2005; Ye et al., 2004; Zhong et al., 2004).

Despite genetic, biochemical and functional evidence implicating the 19S RC and p97 in ER-associated degradation (ERAD), their precise role remains unknown and somewhat controversial. Of the 18 proteins in the 19S RC, few have known functions. However, AAA-ATPases (Rpt1-6) collectively open the gate into the 20S core (Kohler et

al., 2001), exhibit chaperone-like activity (Braun et al., 1999; Liu et al., 2002) and facilitate assembly and disassembly of the 26S proteasome during the degradation cycle (Babbitt et al., 2005). Based on structural and functional homology to archaebacterial ATP-dependent proteases PAN (Navon and Goldberg, 2001) and ClpX (Ortega et al., 2000), the eukaryotic 19S RC is thought to unfold and actively translocate substrates into the 20S catalytic chamber. Thus an appealing, although largely untested possibility is that 19S unfolding activity might play a direct role in dislocating ERAD substrates from the ER lumen and/or bilayer. Consistent with this notion, functional proteasomes are required for the tight coupling of membrane extraction and proteolytic cleavage during degradation of ER membrane proteins (Mayer et al., 1998; Xiong et al., 1999). In addition, purified 19S RC is sufficient for ATP-dependent dislocation of the luminal substrate, pro-alpha factor (Lee et al., 2004).

On the other hand, accumulating evidence has suggested that p97 rather than the 19S regulatory subunit is primarily responsible for ER dislocation. Like the 19S RC, p97 together with its cofactors, Ufd1 and Npl4, exhibits unfolding/segregating activity and plays an important role in presenting substrates to the proteasome (Richly et al., 2005; Verma et al., 2004). Indeed, inactivation of p97, ufd1, or npl4 blocks the degradation of ubiquitinated membrane and luminal ERAD substrates including the ABC transporters PDR5, Ste6 and CFTR (Gnann et al., 2004; Huyer et al., 2004), HmgCoA reductase (Bays et al., 2001; Rabinovich et al., 2002), ER-localized transcription factors, Spt23 and Mga2 (Hitchcock et al., 2001; Rape et al., 2001), and CPY* (Elkabetz et al., 2004; Jarosch et al., 2002). p97 inhibition or addition of dominant negative p97 also decreases

accumulation of cytosolic intermediates generated in the presence of proteasome inhibitors, reduces US11-dependent retrotranslocation and degradation of MHC I (Ye et al., 2001) and stabilizes a mutant form of CFTR (ΔF508) (Dalal et al., 2004). Thus, understanding the precise role of p97 has broad and significant implications for the function and regulation of cellular degradation pathways

Despite the growing perception that p97 is an essential component of the ERAD machinery, interference with p97 function typically decreases but does not completely abolish degradation of ERAD substrates. This has been a particularly challenging issue to address in vivo because p97/cdc48 null mutants are lethal in yeast (Giaever, 2002), and conditional mutants arrest during cell division (Moir et al., 1982). Likewise, p97 (VCP) siRNA blocks cell cycle progression in HeLa cells with arrest in prometaphase/metaphase and induces apoptosis (Wojcik et al., 2004). To define the precise role of p97, we therefore used an *in vitro* system that efficiently reconstitutes the ERAD pathway (Gusarova et al., 2001; Qu et al., 1996) and examined the stability of a prototype substrate, the cystic fibrosis transmembrane conductance regulator (CFTR). CFTR is an epithelial, ATP-gated chloride channel that exhibits a typical eukaryotic domain architecture of the ATP Binding Cassette (ABC) transporter superfamily (Figure 1). It contains 2 transmembrane (TM) domains with six TM segments each, two large cytosolic nucleotide binding domains (NBDs) and a cytosolic regulatory (R) domain (Riordan et al., 1989). In most cell types studied to date, approximately 60-80% of wild type CFTR and nearly 100% of common mutant variants are rapidly degraded via ERAD (Cheng et al., 1990; Jensen et al., 1995; Meacham et al., 2001; Ward et al., 1995).

Importantly, this phenotype is recapitulated *in vitro*, where newly synthesized, membrane integrated CFTR is efficiently degraded into TCA soluble fragments in an ATP- and proteasome-dependent manner (Oberdorf et al., 2001; Oberdorf et al., 2006; Xiong et al., 1999).

In the current study, we show that while p97 specifically augments CFTR degradation, it is not obligatory for ERAD. Rather, both the rate and efficiency of CFTR degradation were decreased by only 50% in the absence of p97. Interestingly, p97 had no stimulatory effect on the degradation of isolated cytosolic domains but specifically increased both the extraction efficiency and degradation rate of CFTR TM domains. Moreover, p97-mediated domain extraction occurred independently of proteolytic cleavage and was specifically influenced by TM segment hydrophobicity, suggesting that the requirement for p97 is determined at least in part by substrate domain stability. Together, these data demonstrate that p97 plays a non-essential but important ancillary role in ERAD by increasing the degradation rate (and efficiency) of selected and possibly more thermodynamically stable protein domains.

Results

Reconstitution of *in vitro* CFTR degradation

CFTR was expressed *in vitro* in the presence of [^{35}S]methionine and ER microsomal membranes to generate a ~150-160 kDa core-glycosylated protein that was cotranslationally integrated into the ER membrane (Figure 1B,C). Microsomes were then collected and added to fresh rabbit reticulocyte lysate (RRL) lacking exogenous hemin,

and degradation was monitored by substrate conversion into trichloroacetic acid (TCA) soluble peptides (Figure 1D). After a brief five minute lag, the rate of TCA-soluble fragment production was linear for 30-60 min (Figure 1D, inset). Thus there is little delay in degradation due to substrate ubiquitination, a finding consistent with transient accumulation of polyubiquitinated CFTR observed in earlier studies (Xiong et al., 1999). At later time points a gradual decrease in degradation was observed, primarily due to run-down of RRL degradation activity (Figure 1E). Under these conditions, ~65% of CFTR was completely converted into TCA-soluble fragments (Figure 1D). Moreover, CFTR degradation is entirely ATP-dependent and sensitive to a variety of proteasome inhibitors (Oberdorf et al., 2001; Xiong et al., 1999). Because proteasome-mediated CFTR degradation is a multi-step process, the overall degradation rate depends on ubiquitination, dislocation, translocation into the catalytic core, and lastly, peptide cleavage. However, we previously showed that for fully functional proteasomes, the capacity for peptide cleavage exceeds the rate of CFTR unfolding and extraction (Oberdorf et al., 2006). Thus, the initial rate of TCA-soluble fragment production (expressed as the percent of CFTR converted into TCA-soluble fragments per minute, Figure 1E) provides an approximate measure of the rate limiting steps of CFTR degradation that include membrane extraction, unfolding and delivery of substrate to the 20S catalytic core.

p97 facilitates CFTR degradation *in vitro*

To determine the precise contribution of p97 to CFTR degradation, RRL was depleted of p97 and its cofactors by affinity chromatography using two Ni-immobilized

recombinant His-tagged proteins (Figure 2A). The first was a nonhydrolyzable ubiquitin fusion protein that contained the E2 enzyme ubcH5a fused to the C-terminus of ubiquitin^{G76V} (referred to as uu5). The second protein was p47, an independent p97 binding protein implicated in membrane fusion (Kondo et al., 1997). Adsorption of RRL to uu5 coated beads removed ~50% of p97 as determined by immunoblotting (Figure 2B, lane 1-4), and no further reduction was observed upon serial adsorption (data not shown). Quantitation was based on standard curves of purified, recombinant p97 (Supplemental Figure 1). Interestingly, uu5 adsorption depleted ufd1 to below the limits of detection (Figure 2B, lane 4), consistent with reports that ubiquitin fusion proteins bind p97 via the specific adapters ufd1/npl4 (Johnson et al., 1995). In contrast, a single adsorption step using p47 coated beads depleted ~ 99% of p97 from RRL but had no effect on ufd1 levels (Figure 2B, lane 6), whereas sequential adsorption with uu5 followed by p47 depleted both ufd1 and p97 (Figure 2B, lane 5). This process therefore generates RRLs lacking p97, ufd1, and both p97 and ufd1.

We next carried out CFTR synthesis and degradation entirely in a p97-depleted system. CFTR was translated in p97-depleted RRL, which was supplemented with p97-stripped microsomal membranes (>98% depleted, Figure 2B). Although adsorption by Ni-NTA beads slightly decreased the initial degradation rate (0.53% +/- 0.02/min vs. 0.64% +/- 0.03/min) due to dilution of RRL (Figure 1E versus 2D), p97 depletion had no specific effect on CFTR translation, glycosylation, or membrane integration (data not shown). In contrast, p97 depletion resulted in a ~50% reduction in both the initial rate and overall extent of CFTR degradation that was partially restored by the addition of

purified recombinant His-p97 (Figure 2C&D). Depletion of both p97 and ufd1 resulted in a similar (50%) decrease in the rate of CFTR degradation, but in this case degradation activity was not restored upon addition of wild type p97 (Figure 2E&F). These results provide biochemical evidence that p97 directly contributes to the degradation of membrane-bound CFTR and that its function in ERAD requires the adaptor protein ufd1. However, CFTR continues to be degraded albeit at a reduced rate even after highly effective p97 (and ufd1) depletion. This indicates either that CFTR degradation can occur independently of p97 or that small amounts of residual p97 might account for the remaining degradation activity.

p97 is not an essential ERAD component

To rule out the possibility that trace amounts of p97 might be sufficient for CFTR degradation, RRL was incubated with increasing amounts of p47-saturated Ni beads, and the inhibition of degradation was examined as a function of p97 depletion (Figure 3A). These results revealed that only ~20% of endogenous p97 was needed to sustain near normal CFTR degradation activity (Figure 3A). This was not surprising given that the *in vitro*-translated CFTR present in microsomal membranes is several orders of magnitude less than endogenous RRL p97 (data not shown). We then subjected RRL to two serial depletions with p47, which together with microsomal stripping, removed > 99% of total p97 from the reaction. Consistent with results of Figure 2, this decreased the rate of CFTR degradation by 48 +/-2.3% (Figure 3B). Small amounts of undepleted RRL (0.25%, 1%, 2%, and 4% of total volume) were then added back to titrate the effects of very low p97 levels. When the amount of residual p97 was titrated between 1% and 5%, a

roughly linear relationship was obtained between the initial degradation rate and the p97 concentration. Linear regression analysis (R^2=0.91) indicated that at 100% p97 depletion the rate of CFTR degradation would be decreased by only 51% (Figure 3B). These results provide strong evidence that CFTR degradation can be carried in the complete absence of p97, and that the major effect of p97 is to increase the degradation rate by approximately 2-fold.

p97 selectively stimulates degradation of CFTR TM domains.

p97 exhibits the unique ability to discriminate among polyubiquitinated substrates and selectively present individual components of multi-protein complexes to the proteasome (Dai et al., 1998; Hitchcock et al., 2001; Rape et al., 2001). However, it is unknown whether p97 exerts different effects on different domains within the same protein. CFTR provides an ideal ERAD substrate to examine this question because it contains multiple well-defined domains that reside either in the cytosol or within the ER membrane (Figure 1). We therefore examined the requirement for p97 on the degradation of isolated CFTR cytosolic and TM domains. His-tagged constructs encoding cytosolic NBD1 (residues V358-S588) or NBD1-R (residues V358-D835) domains were translated in p97-depleted RRL, isolated by Ni-affinity purification, and added directly to degradation reactions. As shown in Figure 4, both constructs were rapidly converted into TCA soluble fragments in an ATP-dependent manner. The degradation rate of NBD1 was ~4 fold faster than that of full length CFTR, and nearly 90% of the polypeptide was converted into TCA-soluble fragments within two hours (Figure 4A, B). Remarkably, p97 depletion had no effect on NBD1 degradation and only a minor effect on NBD1-R

turnover (15% decrease in initial rate). Thus, degradation of CFTR cytosolic domains was nearly entirely independent of p97. Similar results were also observed for two other soluble proteasome substrates, lysozyme and casein (data not shown).

We next examined degradation requirements for CFTR TMD1 (residues M1-V393), which contains the first 6 TM segments and connecting loops that vary in length from 2-66 residues (Figure 5A). *In vitro* translated TMD1 was quantitatively resistant to carbonate extraction, indicating that the protein was fully integrated into the ER membrane (Figure 5A). Because twelve of the thirteen TMD1 methionines (92%) are located within 30 residues of the membrane, and the linear distance from the 19S ATPase ring to proteolytic sites in the 20S core is ~11nm (Baumeister et al., 1998), only the N-terminal methionine should be accessible to proteolytic cleavage in the intact domain (Lee et al., 2001). As expected, TMD1 was also subject to ERAD as demonstrated by ATP-dependent conversion into TCA soluble fragments and MG132 sensitivity (Figure 5B). Approximately 45% of TMD1 methionines were converted into TCA soluble fragments, confirming that TMD1 was extracted from the ER membrane during degradation. The initial rate of degradation (0.44+/-0.04%/min) was somewhat slower than for full-length CFTR (Figure 5C). In addition, p97 depletion resulted in a ~50% reduction in both the rate and extent of TMD1 degradation which was almost entirely restored by addition of recombinant p97 (Figure 5B&C). These data indicate that CFTR TMD1 is degraded 2-5 fold slower than isolated cytosolic NBD1 and NBD1-R domains in intact RRL and 3-9 fold slower in p97-depleted RRL. Thus p97 selectively enhances the rate of TMD1 degradation over that of CFTR cytosolic domains.

p97 contribution is dependent on TM domain hydrophobicity

The inverse correlation between degradation rate and p97 dependence suggested that p97 might selectively facilitate the unfolding of more thermodynamically stable (and hence more slowly degraded) peptide regions. If this were true, then TMs that were less stable in the lipid bilayer might also show less p97 dependence. We therefore examined a shorter construct containing the CFTR N-terminus and first two TM segments (Figure 6A). This construct (TM1-2) efficiently acquires its correct two-spanning topology *in vitro* and contains 5 methionines, 4 of which are located within 18 residues of the membrane. Like TMD1, *in vitro* synthesized TM1-2 was membrane-integrated (Figure 6B) and was degraded by the proteasome only slightly faster (0.73+/-0.08%/min) than full length CFTR (Figure 6C,D). In contrast to TMD1, however, the rate of TM1-2 degradation was only modestly affected (~20% reduction) by p97 depletion.

CFTR TM1-2 is somewhat unusual in that both TMs contain potentially charged residues (Riordan et al., 1989), namely E92 and K95 reside near the center of TM1 (Figure 6A), and R134 resides near the C-terminus of TM2. E92 and K95 were therefore replaced with alanine residues to generate a more stable transmembrane structure (predicted free energy of transfer (ΔG) for TM1 decreases from -5.1 kcal/mol to -10.1 kcal/mol (octanol-water partitioning, whole residue hydrophobicity scale (White and Wimley, 1998)). The TM1-2 E92A/K95A mutations had a striking effect, decreasing the initial degradation rate by ~2.5-fold (0.28%+/-.03/min) in the presence of p97 (Figure 6E&F), and further decreasing the degradation rate by an additional 2.3-fold following

p97 depletion (0.12% +/- 0.01/min). Degradation was substantially restored by the addition of recombinant p97.

p97 specifically augments TM domain extraction independently of proteolytic cleavage.

Finally, to determine whether p97 facilitates extraction of CFTR TM domains directly and independently of proteasome-mediated peptide cleavage, TMD1 degradation products were separated into membrane-bound and cytosolic fractions prior to analysis. Consistent with previous studies (Oberdorf et al., 2006), all cytosolic fragments were TCA soluble under control conditions (Figure 7A). In the presence of MG132, however, very few TCA-soluble fragments were generated, but CFTR continued to be released into the cytosol as large TCA insoluble polypeptides (Figure 7A, vertical arrow). SDS-PAGE and autoradiography revealed that these cytosolic fragments were predominantly comprised of full length TMD1, which had been integrated into the ER membrane during translation (Figure 5A), but then extracted en block during the degradation reaction (Figure 7C, lanes1-5). p97 depletion decreased the rate of fragment release as expected but had no effect on the TCA solubility of cytosolic fragments (Figure 7B). When degradation was inhibited by MG132, p97 depletion again decreased the rate of TMD1 release from the ER membrane by ~3 fold (Figure 7D,E). Under these conditions, release of TCA-insoluble cytosolic fragments was also decreased (Figure 7B) as was the cytosolic accumulation of full-length TMD1 (Figure 7C, lanes 1-5 versus lanes 6-10). As expected, no large cytosolic fragments were visualized in ATP-depleted RRL or in the absence of MG132 (Figure 7C, lanes 11-20). These results demonstrate that p97 can

facilitate extraction of intact CFTR TMs, and that the stimulatory effect of p97 on CFTR degradation occurs independently and upstream of proteolytic cleavage.

Discussion

Two AAA-ATPase complexes, p97-ufd1-Npl4 and the proteasome 19S RC, are currently implicated in the dislocation and degradation of misfolded proteins from ER membrane. Using an *in vitro* system that reconstitutes the ERAD pathway, we now quantitate the relative contribution of p97 in facilitating degradation of a prototypical ERAD substrate, CFTR. In the complete absence of p97, the rate of CFTR degradation was decreased by only ~50% as determined by proteasome-dependent conversion of substrate into TCA soluble fragments. Detailed depletion and add-back experiments confirmed that residual traces of p97 did not account for the substantial degradation activity observed after depletion. Thus while p97 clearly facilitates the degradation of ERAD substrates, it is not obligatorily required for either extraction, unfolding or proteolysis of a large, membrane integrated polytopic membrane protein.

Remarkably, the stimulatory effect of p97 on CFTR degradation was restricted to TM domains, whereas degradation of cytosolic domains was nearly entirely p97 independent. The relative contribution of p97 was also markedly influenced by changes in the hydrophobicity of individual TM segments. These findings raise the possibility that p97 primarily increases the degradation efficiency of specific domains that are more stable and/or slowly degraded. Indeed, we found a strong inverse correlation between the baseline degradation rate of different CFTR domains and the stimulatory contribution of

p97 (Figure 8). Although additional studies are clearly needed before this effect can be generalized, our analysis suggests p97 does not exert stimulatory effects until the degradation rate falls below a critical threshold (<0.5%/min in our study). p97 also directly stimulated the extraction and membrane release of intact TM domains independently of proteolytic cleavage. Thus, p97 functions as a non-essential, yet important ancillary component of the ERAD pathway that stimulates presentation of thermodynamically stable substrates or domains to the 26S proteasome.

Cryo EM studies have suggested that unfolding by AAA-ATPases occurs via conformational changes caused by ATP binding/hydrolysis (Ogura and Wilkinson, 2001). For example, unfolding by the prokaryotic PAN AAA-ATPase takes place on the surface of the hexameric ring and leads directly to peptide translocation through the central pore (Navon and Goldberg, 2001). In the case of the 26S proteasome, substrate must also be translocated through both 19S AAA-ATPase and the axial pore of the 20S cylinder. Although it is unlikely that translocation occurs through the pore of p97 (DeLaBarre and Brunger, 2003), there may be an analagous unfolding on the surface of the hexamer. However, our findings clearly demonstrate that such an interaction with p97 is not necessarily obligatory even for substrates where p97 can and normally does facilitate degradation. This raises a significant mechanistic question. How and when is p97 recruited to substrate? Two scenarios seem to be most likely. One possibility is that the proteasome provides a baseline unfolding activity that processively degrades substrate until it encounters a stable region that it is unable to unfold (Lee et al., 2001). This stalled complex could then recruit p97 to assist in extraction/unfolding and thus stimulate the

degradation rate. In a second, and perhaps more plausible model, both the 26S proteasome and p97 could processively scan and unfold substrates together. However, p97 would not contribute substantially to the rate of unfolding until a specific region of protein was encountered in which its ATPase activity would increase the basal rate provided by the proteasome. In support of the former possibility, purified 26S proteasomes are clearly capable of degrading substrates *in vitro* in the absence of p97 (Lee et al., 2004). However, the proteasome and p97 can also interact directly during substrate presentation (Dai et al., 1998).

A third plausible explanation for our findings is that substrate presentation to the proteasome occurs via multiple pathways (Verma et al., 2004). These involve a growing repertoire of proteasome interacting proteins (PIPs) that include p97, rad23, and hPLIC/dsk2 as well as co-chaperones such as BAG-1 (Hartmann-Petersen and Gordon, 2004). Thus it is possible that CFTR could use parallel means for recruitment, ubiquitination and presentation to the 19S RC. Consistent with this we recently reported that during proteasome-mediated degradation, CFTR N-terminal, C-terminal and R-domain epitopes were lost at similar rates, suggesting degradation could be initiated at multiple sites within the polypeptide (Oberdorf et al., 2006). Moreover, CFTR ubiquitination and degradation can be initiated by a cytosolic complex involving the U-box protein CHIP, Hsc70 and ubcH5 (Meacham et al., 2001) as well as membrane bound E2/E3 proteins Hrd1/Hrd3, Doa10 and Ubc6 (Gnann et al., 2004). Thus different recognition machinery may operate on different CFTR domains depending on their cellular compartment and the nature of the folding defect. This model is further supported

by recent studies indicating that a large protein complex at the ER membrane involving Der1, Rma1 and Ubc6 is specifically involved in recognizing destabilizing mutations within TMD1 (D. Cyr, Personal Communication) whereas the CHIP-Hsc70-UbcH5 complex primarily recognizes cytosolic (NBD) folding defects (Younger et al., 2004). Intriguingly, the Hrd1/3 and Doa10 pathways in yeast, and the Rma1 pathway in mammalian cells, all converge at p97/cdc48. If p97 functions to present substrates to the proteasome as predicted, this may also explain why CFTR TMDs preferentially display augmented degradation in the presence of p97. Recently, it was reported that the yeast protein ubx2 is a central component of this complex and through its UBA and UBL domains links substrates with E3 ligases, Der-1 and p97 (Neuber et al., 2005; Schuberth and Buchberger, 2005). It will therefore be most interesting to determine whether Ubx2 and additional components are also required for p97 augmentation of TMD degradation.

To our knowledge this is the first study demonstrating that p97 contributes differentially to the degradation of different domains derived from the same protein. While recruitment of degradation machinery likely plays a role in this process, it is also important to consider that the inefficient maturation of CFTR observed in most cell types is caused by failure to acquire proper tertiary and/or quaternary structure. Although the timing of NBD folding during synthesis is somewhat controversial (Du et al., 2005; Kleizen et al., 2005), NBDs are thought to fold particularly inefficiently, and this kinetic defect is amplified by deletion of a phenylalanine at residue 508 in NBD1, a commonly inherited mutation found in nearly 90% of CF patients (Du et al., 2005; Qu et al., 1997; Thibodeau et al., 2005). Thus the relatively unfolded state of isolated NBD1 (and NBD-

R) in RRL likely contributes to the rapid baseline degradation rate observed and the lack of requirement for p97. By contrast, CFTR TM helices buried in the lipid bilayer are degraded much more slowly and demonstrate a clear augmentation by p97. These findings parallel observations for the cytosolic substrate, titin, which can also exhibit two degradation rates, a slow rate that requires domain unfolding and fast rate when the substrate is presented in a pre-denatured state (Kenniston et al., 2003). Each pathway is characterized by marked differences in energy consumption, four ATP/aa for the folded substrate versus 1 ATP/aa for denatured substrate. This difference results from the inefficient, iterative engagement of folded substrates with the AAA-ATPase ClpXP, which is cooperatively promoted during denaturation at the surface of the ring (Kenniston et al., 2003). Moreover, this process provides a mechanism for partitioning stable from misfolded or denatured substrates based on their affinity for the AAA-ATPase (Kenniston et al., 2005). By analogy the eukaryotic 19S RC is predicted to have a similar cooperative unfolding behavior such that unfolded or partially unfolded substrates would energetically less costly and more efficiently degraded.

Importantly, the unfolding process is highly cooperative and influenced by local structure (helices and surface loops) at the site of initial unfolding (Lee et al., 2001). In the case of membrane proteins, extraction of TMDs likely represents a significant energy barrier, particularly where short lumenal loops (e.g. CFTR TM3-4, TM5-6) necessitate pair-wise extraction of TM segments (Muller et al., 2002). Indeed, TMD1-6 was degraded at a much slower rate than cytosolic domains, suggesting that membrane extraction may be generally a rate-limiting step in polytopic protein degradation. In the

TM1-2 construct, polar/charged residues likely provide a locally unstable environment in the lipid bilayer for which the 19S ATPases provide sufficient force for extraction. Interestingly, replacing TM1 charged residues with alanine resulted in the most stable of the constructs examined and slowed degradation by nearly 5 fold (in the absence of p97) when compared to wild type TM1-2 and nearly 20 fold when compared to the isolated NBD1. p97 likely plays a key role in stimulating TM1-2 E92A/K95A degradation by providing a second step for substrate partitioning, thus generating a locally unfolded domain which preferentially engages the AAA-ATPase ring of the 19S RC. The net result of two serial partitioning steps would be to dramatically increase the efficiency of engagement by both AAA-ATPases and the ultimate delivery of substrate into the proteasome catalytic core.

Materials and methods

Constructs: Plasmid cloning details are described in Supplemental Online-information.

Recombinant proteins: Recombinant protein expression was induced in transformed BL21(DE3) cultures using 0.4mM isopropyl β-D-1-thiogalactopyranoside (IPTG; Fisher Scientific, Pittsburgh, PA) as previously described (Carlson et al., 2005). Cell lysates were loaded onto a 5 ml Ni-NTA column (Qiagen, Inc., Valencia, CA), washed with 50 ml 300mM NaCl, 1mM βME, 5% glycerol, 0.4mM PMSF, 25mM imidazole, and 50mM Tris-HCl, pH 7.5, and eluted with a 25mM-500mM linear gradient of imidazole. Fractions were pooled, dialyzed against 100mM NaCl, 1mM βME, and 25mM Tris-HCl, pH 7.5 (Buffer A), then concentrated, and stored at –80^{o}C. Aliquots were thawed once

and discarded.

Affinity Depletion of RRL and CRM: Rabbit reticulocyte lysate (RRL) and canine pancreatic rough microsomes (CRMs) were affinity depleted as described (Carlson et al., 2005). Briefly, Ni-NTA beads containing near saturating amounts His-tagged recombinant proteins were added to RRL at a ratio of 5:1 (RRL:Ni-NTA) and incubated at least 4 hr at 4°C with continuous mixing. Supernatants were removed and frozen in liquid nitrogen. Mock depletions were performed using equal volumes of uncoupled Ni-NTA beads. CRMs were depleted of p97 by 50-fold dilution in 0.25M sucrose in Buffer B (1mM DTT, and 50 mM triethanolamine-acetate, pH 7.5) at 24°C for 15 min. Membranes were pelleted at 180,000 x g for 20 min, and resuspended in their original volume of Buffer B. Following depletion, RRL or CRMs were separated by SDS-PAGE, transferred to nitrocellulose or PVDF, and blotted with mouse α–p97 (1:500; BD Transduction Laboratories, San Jose, CA) or mouse α-ufd1 (1:1,000; BD Transduction Laboratories) followed by α-mouse- HRP secondary Ab (1:20,000. Biorad, Hercules, CA). The blots were imaged on Kodak film using Pierce west pico supersignal substrate according to the manufacturer's directions (Pierce Biotechnology, Inc., Rockford, IL). For quantitation (see supplemental Figure1) α-mouse-AP secondary antibody (1:2,500; Promega, Madison, WI) was used in conjunction with ECF substrate (Amersham Biosciences, Piscataway, NJ), and blots were imaged using a Biorad FX phosphoimager (Biorad, Hercules, CA) followed by analysis with QuantityOne software.

In vitro transcription/translation: mRNA was transcribed with SP6 RNA polymerase for 1 hour at 40°C and translated in a transcription-linked reaction for 1-2 hr at 24°C as described in detail elsewhere (Carlson et al., 2005). RNAse-free H_2O was substituted for DNA in mock transcription reactions. Endogenous RRL and CRM mRNAs were digested prior to translation (Carlson et al., 2005). Canine pancreatic rough microsomal membranes (A_{280}= 4) were added at the start of all translations, except the cytosolic NBD and NBD-R constructs. Aurin tricarboxylic acid (25 - 50μM) was added after 15-20 minutes to synchronize translation. Following translation, CRM containing *in vitro*-synthesized protein were isolated by centrifugation, 180,000 x g for 10 min, through a cushion containing 0.5M sucrose in Buffer C (100mM KCl, 5mM $MgCl_2$, 1mM DTT, 50mM HEPES, pH 7.5) and resuspended in 1/2 original volume in 0.1M sucrose in Buffer C. Prior to pelleting, TM1-2 E92A/K95A was released from ribosomes by addition of 1mM puromycin. Soluble NBD and NBD-R proteins were isolated by diluting translation reactions with 3 volumes of Buffer A and mixing with 10 μl Ni-NTA at 4°C for 30 minutes. Beads were then washed in 10 x 1ml 10mM imidazole in Buffer A, and proteins were eluted with 250mM imidazole in Buffer A.

Degradation Assay: Isolated CRMs from translation reactions were added to RRL supplemented with 1mM ATP, 12mM creatine phosphate, 5mM $MgCl_2$, 3mM DTT, 10mM Tris-Cl, pH 7.5 and 4μg creatine kinase/50μl reaction (Carlson et al., 2005)and incubated at 37°C. 100μM MG132 or 20mM 2-deoxyglucose and 20U hexokinase was added to the reaction mixture as indicated to inhibit proteasomes or deplete ATP, respectively. Recombinant p97 (200ng/μl RRL) (Oberdorf et al., 2006) was also added to

p97-depleted RRL where indicated. Samples were removed at indicated times (T_n), precipitated in 20% TCA and centrifuged at 16,000 x g for 10 min. TCA supernatants (TCA Sol) were then counted in ScintiSafe (Fisher Chemicals) using a Beckmann LS6500 scintillation counter. Total [^{35}S] present in each sample was determined by directly counting an aliquot of the degradation reaction. Mock reactions were used as a control to correct for small amounts of nonspecific, ATP-independent association of [^{35}S] with the membranes (Carlson et al., 2005). The percent of protein degraded at each time point was determined using the following formula:

$$\% \text{ of total counts} = \{(CFTR(T_n\text{-}T_0) - Mock(T_n\text{-}T_0))/(CFTR(\text{total} - \text{TCA sol } T_0) - Mock(\text{total} - \text{TCA sol } T_0))\}*100$$

Where T_n = TCA soluble counts at T=n and T_0 = TCA soluble counts at T=0 for indicated CFTR and Mock translation reactions. All values are reported as mean of 3 or more experiments+/- SEM.

Membrane Release Assay: The release assay is similar to the degradation assay except that at each time point microsomes from degradation reactions were first pelleted at 180,000 x g for 10 min through 0.5M sucrose in Buffer B. The cytosolic supernatant was then either counted directly to measure total CFTR released from the membrane, precipitated in 20% TCA to determine TCA soluble counts released, or analyzed by SDS-PAGE and autoradiography. The percent membrane-bound CFTR substrate released into the supernatant and %TCA soluble counts released at each time point were calculated by the same formula as used for the degradation assay.

Carbonate extraction: CRMs containing translation products were added to 1 ml 0.25M sucrose, 1μg BSA, and 0.1M Tris-Cl, pH 7.5 or 1 ml 0.1M Na_2CO_3, pH 11.5, 1μg BSA and incubated on ice for 30 min, followed by centrifugation at 180,000 x g for 30 min. Pellets were solubilized in 30 μl SDS-PAGE loading buffer. Supernatants were precipitated in 20% TCA, and the resulting pellets were solubilized in 30 μl SDS-PAGE loading buffer. Samples were analyzed by SDS-PAGE and EN^{3}HANCE (Perkin Elmer, Boston, MA) fluorography and imaged on Kodak film.

Acknowledgements

We thank Dr. H. Meyer for the gifts of p47 and p97 cDNAs, Dr. M. Hochstrasser for human ubiquitin cDNA, and Dr. P. Howley for ubcH5a cDNA. Also, we thank Drs. C. Enns, K. Frueh, L. Musil, and S. Lutsenko for helpful comments on the manuscript.

Figure 4-1. CFTR is degraded into TCA soluble peptides. Schematic representation of CFTR showing relative location of methionine residues and topology of transmembrane domains (TMDs), nucleotide binding domains (NBDs), and regulatory (R) domain. Approximate location of residues V358, S589 and D835 are also indicated. (B) CFTR translated in the presence (lane 2) of CRMs yields the expected full length ~150-160 kD glycosylated protein. (C) Carbonate extraction of CFTR (lanes 1-4) and control transmembrane TM and secretory (sec) proteins (lanes 5-8) (Skach and Lingappa, 1993). (D) *In vitro* CFTR degradation showing the % of intact, [^{35}S] methionine-labeled protein that is converted into radiolabeled TCA soluble fragments at each time point. Inset shows brief delay and then linear degradation during the first 30 min. (E) RRL was preincubated at 37 °C for indicated times prior to addition of CRM containing radiolabeled CFTR. Values indicate the rate of CFTR degradation (% CFTR converted to TCA soluble fragments/min) during the first 30 min. All values are reported as mean of 3 or more experiments +/- SEM.

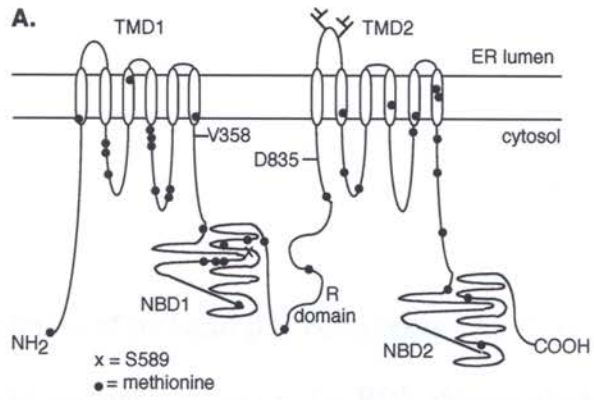
A.
TMD1
TMD2
ER lumen
cytosol
V358
D835
NBD1
R
domain
NBD2
NH2
COOH
x = S589
● = methionine

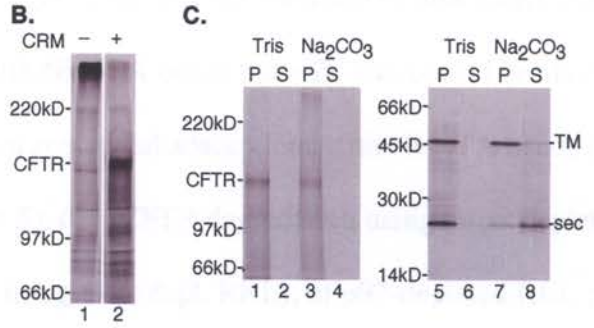
B.
CRM – +
220kD
CFTR
97kD
66kD
1 2
C.
Tris Na2CO3 Tris Na2CO3
P S P S P S P S
220kD
CFTR
97kD
66kD
1 2 3 4
66kD
45kD
30kD
14kD
TM
sec
5 6 7 8

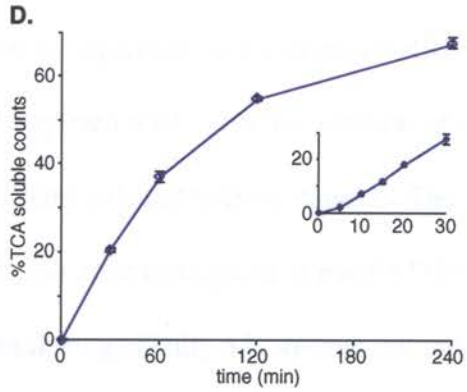
D.
%TCA soluble counts
0
20
40
60
0 60 120 180 240
time (min)
0
20
0 10 20 30

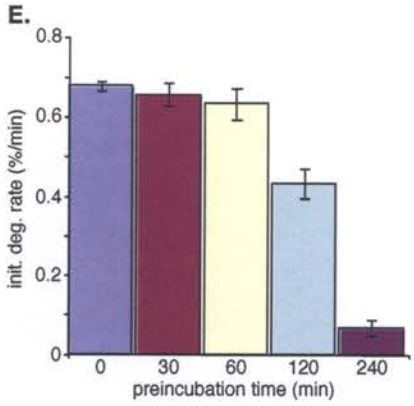
E.
init. deg. rate (%/min)
0
0.2
0.4
0.6
0.8
0 30 60 120 240
preincubation time (min)

Figure 4-2. RRL depletion of p97 and p97 complexes. (**A**) Coomassie stained gel of recombinant His-tagged proteins used as bait for RRL affinity depletion. (**B**) Immunoblots for either p97 (top) or ufd1 (bottom) of intact RRL (lane 1), RRL following a single adsorption with Ni-NTA beads (lane 2), uu5 coated beads (lane 4) or p47 coated beads (lane 6), and two sequential adsorptions with Ni-NTA beads (lane 3) or uu5 followed by p47 (lane 5). (**C**) CFTR degradation using mock depleted RRL (Ni RRL), RRL depleted of p97 using p47 (depl. RRL), or p97-depleted RRL plus recombinant p97 (depl.+p97). (**D**) Initial degradation rates were calculated from panel C as in Figure 1A. (**E**) CFTR degradation in sequential mock-depleted RRL (Ni-Ni), ufd1 and p97-depleted RRL (depl. RRL) and depleted RRL with the addition of recombinant p97 (depl.+p97). (**F**) Initial degradation rates calculated from panel E. The slight decrease in the initial rates of CFTR degradation after adsorption in panels D&E was caused by dilution of RRL by the beads used during affinity adsorption. All values are reported as mean of 3 or more experiments +/- SEM.

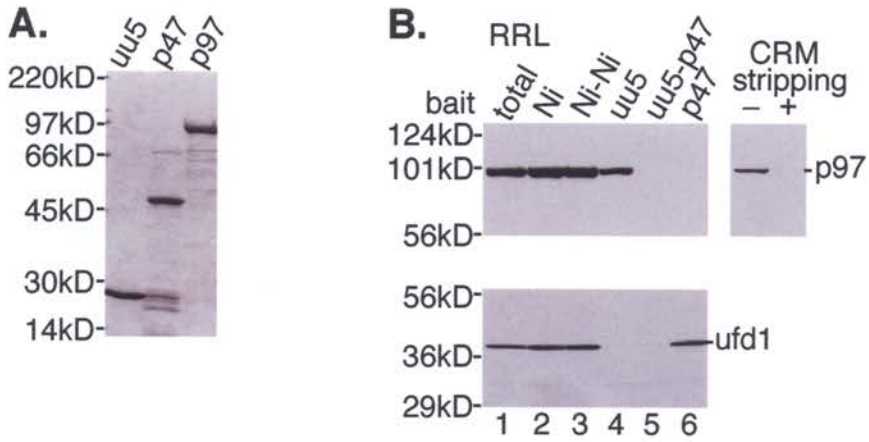
A.
uu5
p47
p97
220kD
97kD
66kD
45kD
30kD
14kD
B.
RRL
bait
total
Ni
Ni-Ni
uu5
uu5-p47
p47
CRM stripping
– +
124kD
101kD
56kD
p97
56kD
36kD
29kD
ufd1
1 2 3 4 5 6

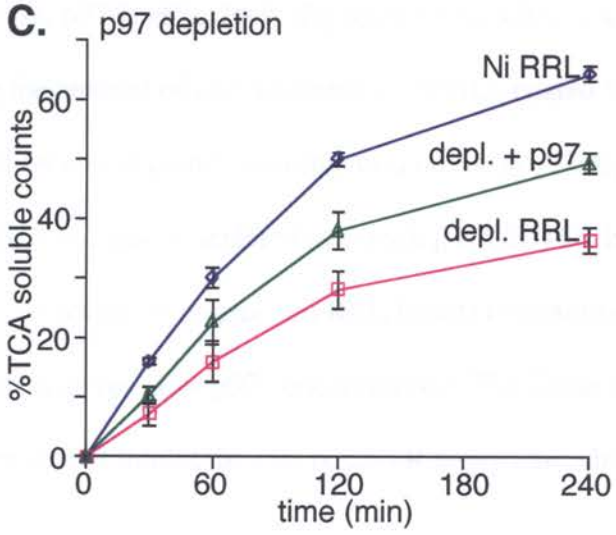
C.
p97 depletion
Ni RRL
depl. + p97
depl. RRL
%TCA soluble counts
0
20
40
60
0
60
120
180
240
time (min)

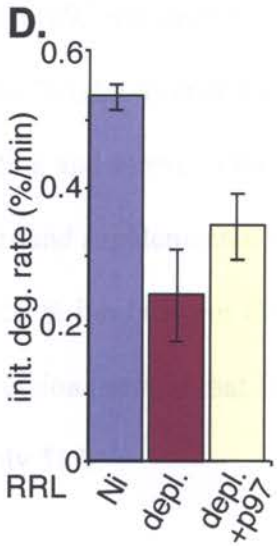
D.
0.6
0.4
0.2
0
init. deg. rate (%/min)
RRL
Ni
depl.
depl. +p97

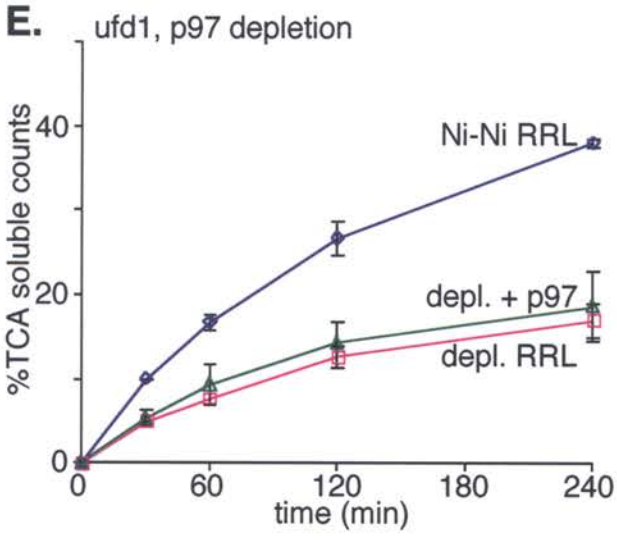
E.
ufd1, p97 depletion
Ni-Ni RRL
depl. + p97
depl. RRL
%TCA soluble counts
0
20
40
0
60
120
180
240
time (min)

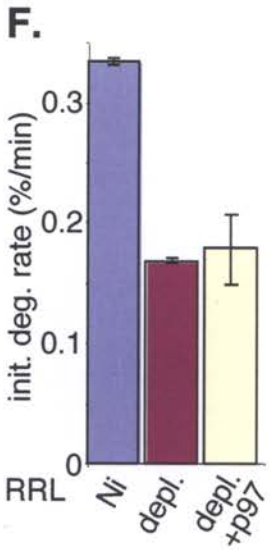
F.
0.3
0.2
0.1
0
init. deg. rate (%/min)
RRL
Ni
depl.
depl. +p97

Figure 4-3. p97 is effectively depleted from RRL. **(A)** RRL p97 was depleted by varying the amount of p47-saturated Ni-NTRA coated beads. % inhibition of the CFTR degradation rate is plotted as a function of the % p97 depletion and shown in the inset. **(B)** RRL was serially depleted (x2) with p47 Ni-NTA beads and supplemented with the indicated amounts of undepleted RRL (inset) to quantitate the % inhibition of CFTR degradation at very low p97 concentrations. The linear regression predicts that 100% p97 depletion would inhibit the rate of CFTR degradation by only 51%.

A.

%p97 depl.	%inh.(+/-sem)
0	0+/-0
20	2+/-2.7
32	4+/-3.6
77	12+/-2.8
97	36+/-2.1
99	48+/-2.3

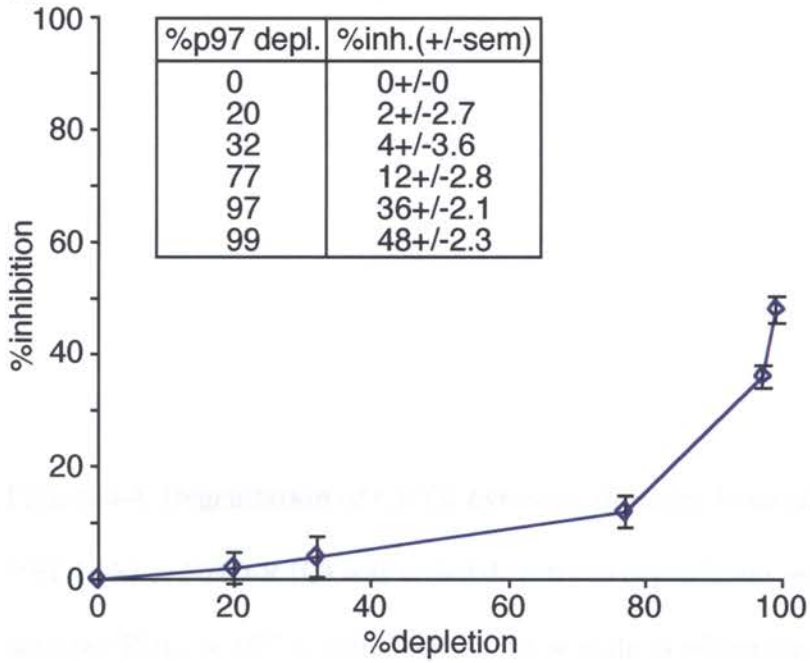

B.

%undepl. RRL added back	%p97 depl.	%inh.(+/-sem)
0	99	48+/-2.3
0.25%	99	47+/-3.7
1%	98	46+/-5.7
2%	97	37+/-2.3
4%	94	34+/-2.4

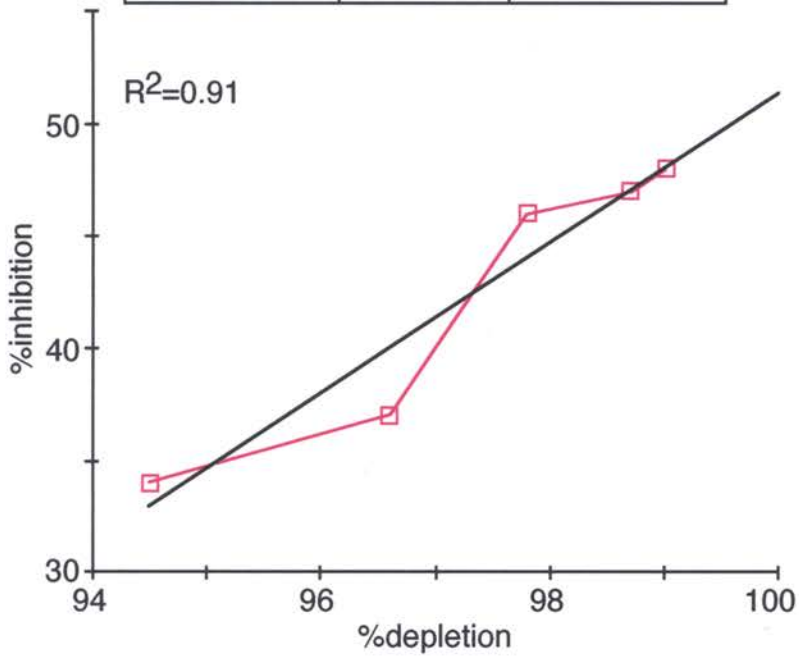

Figure 4-4. Degradation of CFTR cytosolic domains is unaffected by p97. Purified NBD1 (**A**) or NBD-R (**C**) was added directly to degradation reactions containing mock-depleted RRL, or p97-depleted RRL with or without added recombinant p97. **(B&D)** Initial degradation rates were calculated from panels A and C. Location of residues in CFTR polypeptide is indicated in Figure 1A.

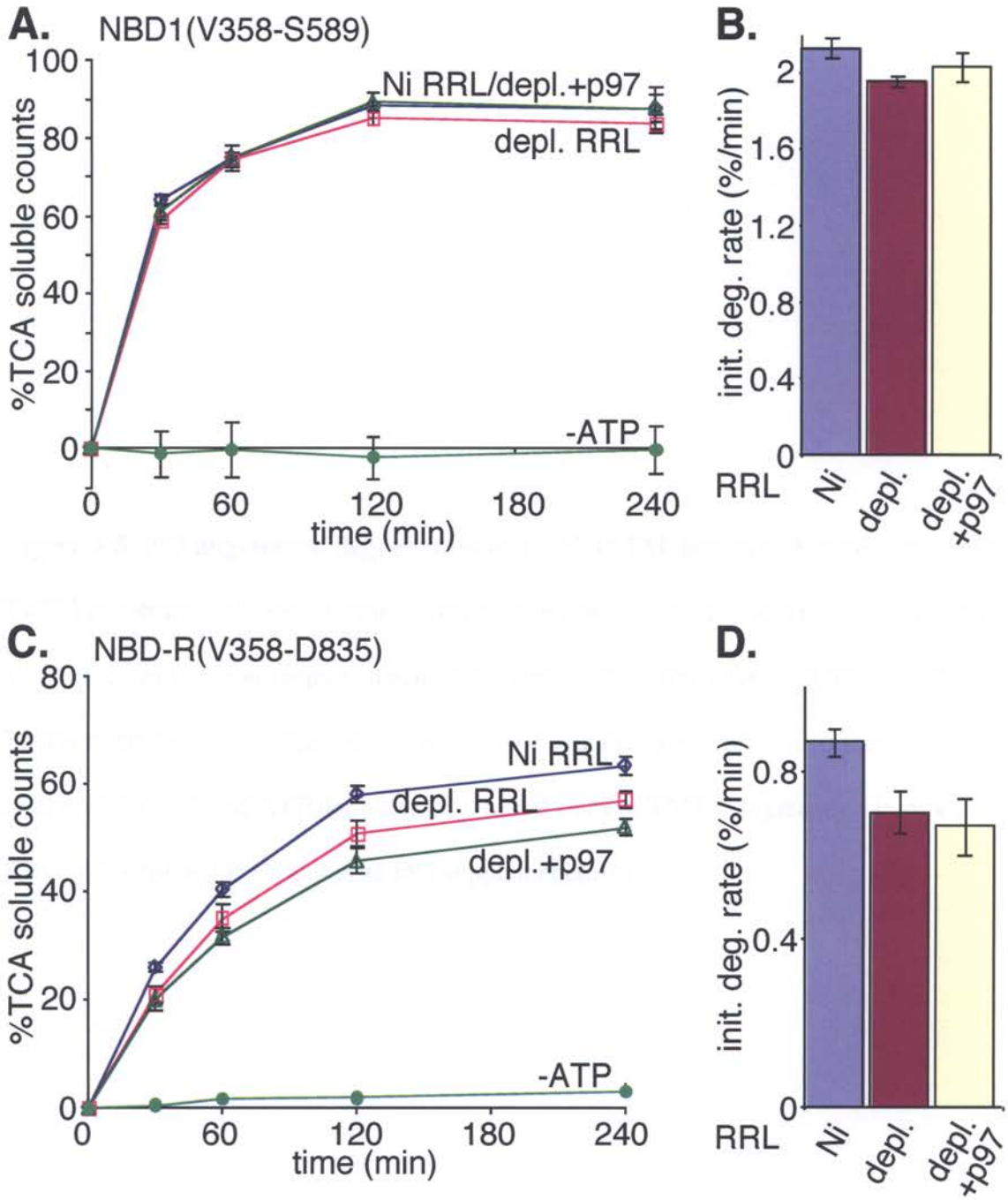
A.
NBD1(V358-S589)
%TCA soluble counts
100
80
60
40
20
0
Ni RRL/depl.+p97
depl. RRL
-ATP
0
60
120
180
240
time (min)
B.
init. deg. rate (%/min)
2
1.6
1.2
0.8
0.4
0
RRL
Ni
depl.
depl. +p97
C.
NBD-R(V358-D835)
%TCA soluble counts
80
60
40
20
0
Ni RRL
depl. RRL
depl.+p97
-ATP
0
60
120
180
240
time (min)
D.
init. deg. rate (%/min)
0.8
0.4
0
RRL
Ni
depl.
depl. +p97

Figure 4-5. P97 augmented degradation of a CFTR TM domain. (**A**) Schematic of the TMD1 construct, indicating location methionines and the number of amino acid residues in cytosolic or lumenal loops. Carbonate extraction of *in vitro*-expressed TMD1. (**B**) TMD1 degradation was assayed in the presence and absence of p97. Also shown are effects of MG132 and ATP depletion (**C**) Initial rates of TM1-6 degradation in mock RRL, p97-depleted RRL and after p97 supplementation.

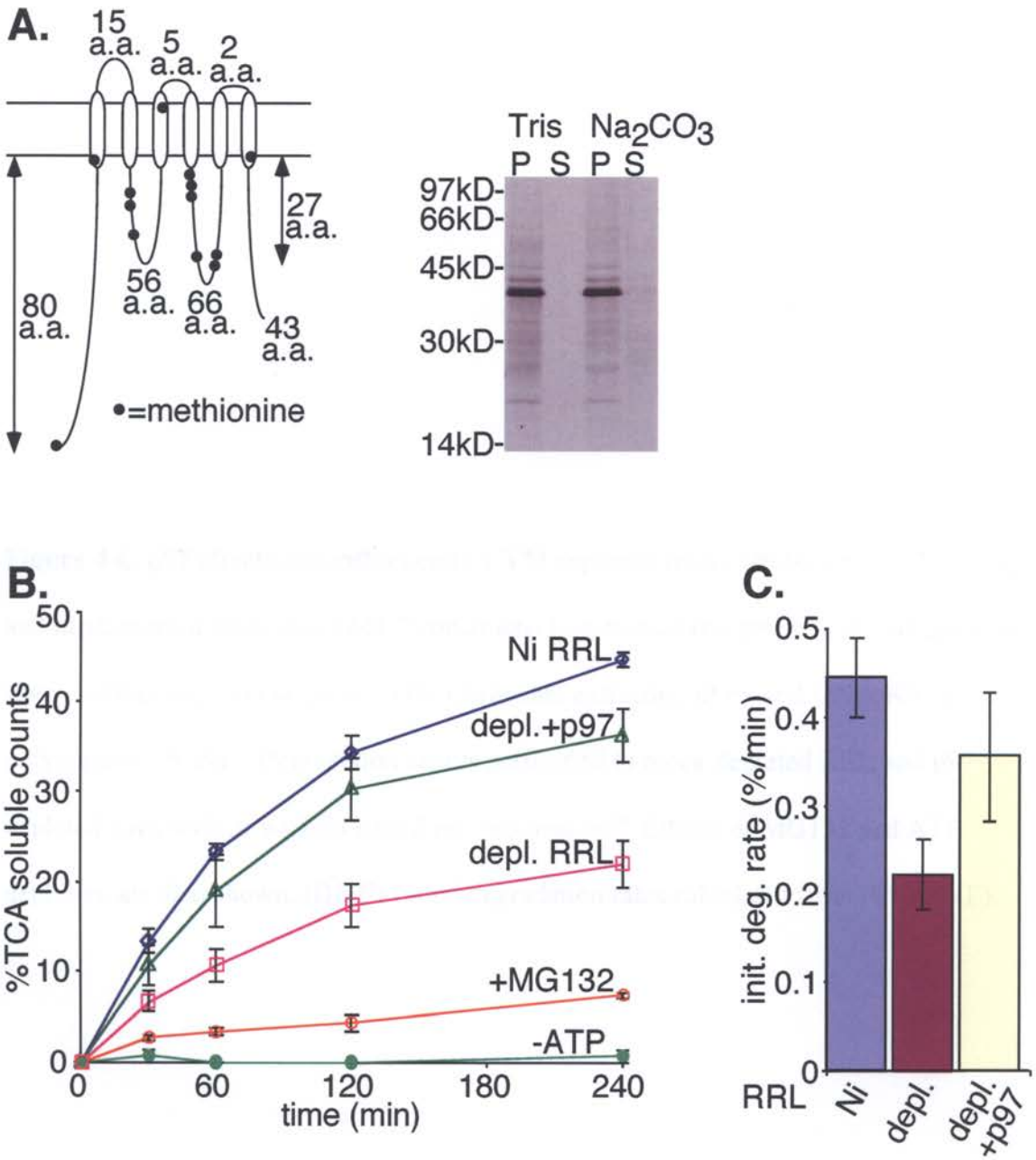
A.
15 a.a.
5 a.a.
2 a.a.
27 a.a.
80 a.a.
56 a.a.
66 a.a.
43 a.a.
•=methionine
Tris
Na2CO3
P S P S
97kD-
66kD-
45kD-
30kD-
14kD-
B.
%TCA soluble counts
time (min)
Ni RRL
depl.+p97
depl. RRL
+MG132
-ATP
C.
init. deg. rate (%/min)
RRL
Ni
depl.
depl. +p97

Figure 4-6. p97 effects are influenced by TM segment hydrophobicity. (**A**) Topology and methionine distribution TM1-2 constructs. Location of residues Glu92 and Lys95 are shown within the TM1 sequence. (**B**) Carbonate extraction of wt and E92A/K95A polypeptides. (**C&E**) Degradation assays performed in mock depleted RRL and p97 depleted RRL with or without added recombinant p97. Effects of MG132 and ATP depletion are also shown. (**D&F**) Initial degradation rates calculated from (C) and (E).

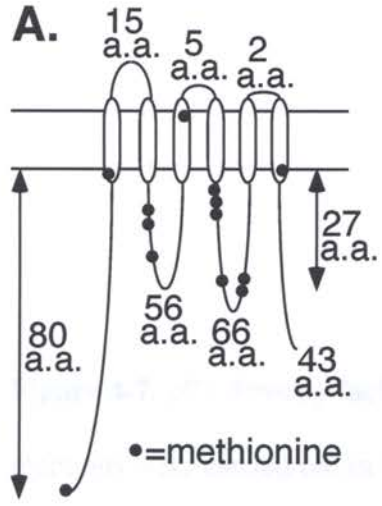
A.
15 a.a.
5 a.a.
2 a.a.
27 a.a.
80 a.a.
56 a.a.
66 a.a.
43 a.a.
•=methionine

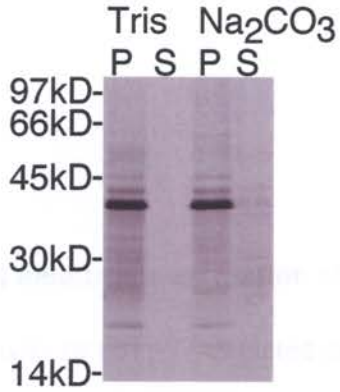
Tris
Na2CO3
P S P S
97kD-
66kD-
45kD-
30kD-
14kD-

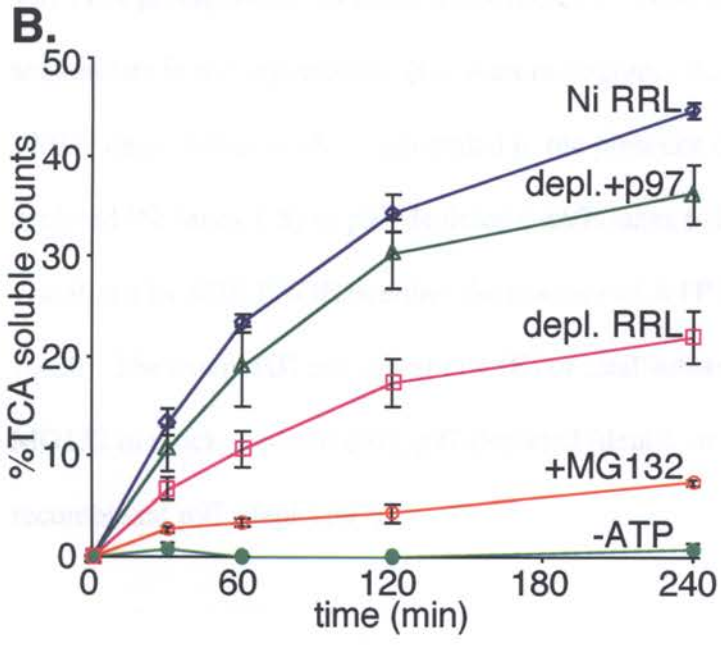
B.
%TCA soluble counts
time (min)
Ni RRL
depl.+p97
depl. RRL
+MG132
-ATP
0
10
20
30
40
50
0
60
120
180
240

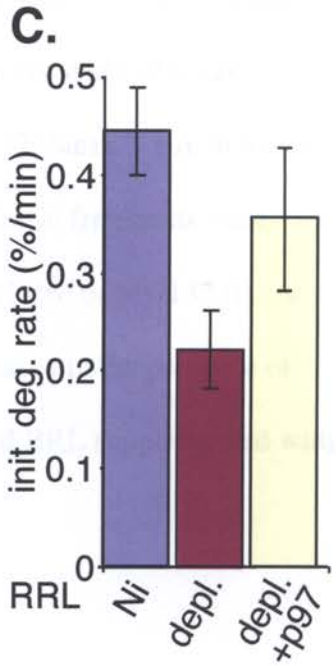
C.
init. deg. rate (%/min)
0
0.1
0.2
0.3
0.4
0.5
RRL
Ni
depl.
depl. +p97

Figure 4-7. p97 directly facilitates membrane extraction of TMs. TMD1 degradation reactions were carried out in (**A**) mock- or (**B**) p97-depleted depleted RRL and supernatants were analyzed for CFTR fragments prior to (total released) or after (TCA sol) TCA precipitation. Vertical arrow indicates TCA insoluble peptide fragments that accumulate in the supernatant. (**C**) Autoradiograms showing dislocated full length TMD1 degradation products generated in the presence of MG132 (lanes 1-10), in Mock-depleted (Ni lanes 1-5) or p97-depleted (–p97, lanes 6-10) RRL. No fragments were visualized by SDS-PAGE in either the absence of ATP (lanes 11-16) or MG132 (lanes 16-20). The extent (**D**) and initial rate (**E**) of total substrate released in the presence of MG132 in mock depleted (Ni), p97-depleted (depl.), or depleted RRL supplemented with recombinant p97 (depl.+p97).

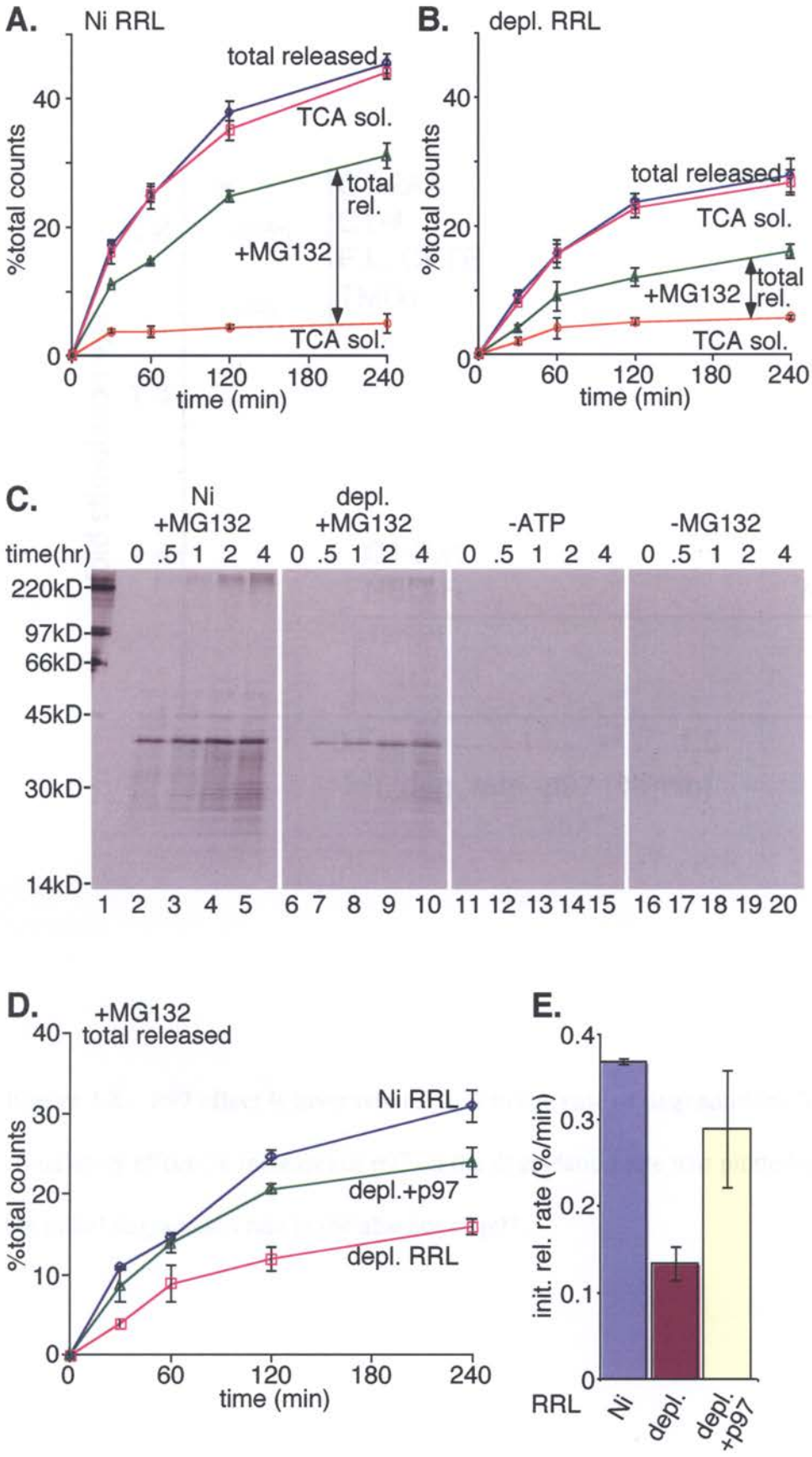
A.
Ni RRL
total released
TCA sol.
total rel.
+MG132
TCA sol.
%total counts
time (min)
B.
depl. RRL
total released
TCA sol.
+MG132
total rel.
TCA sol.
%total counts
time (min)
C.
Ni +MG132
depl. +MG132
-ATP
-MG132
time(hr)
0 .5 1 2 4 0 .5 1 2 4 0 .5 1 2 4 0 .5 1 2 4
220kD
97kD
66kD
45kD
30kD
14kD
1 2 3 4 5 6 7 8 9 10 11 12 13 14 15 16 17 18 19 20
D.
+MG132
total released
Ni RRL
depl.+p97
depl. RRL
%total counts
time (min)
E.
init. rel. rate (%/min)
RRL
Ni
depl.
depl. +p97

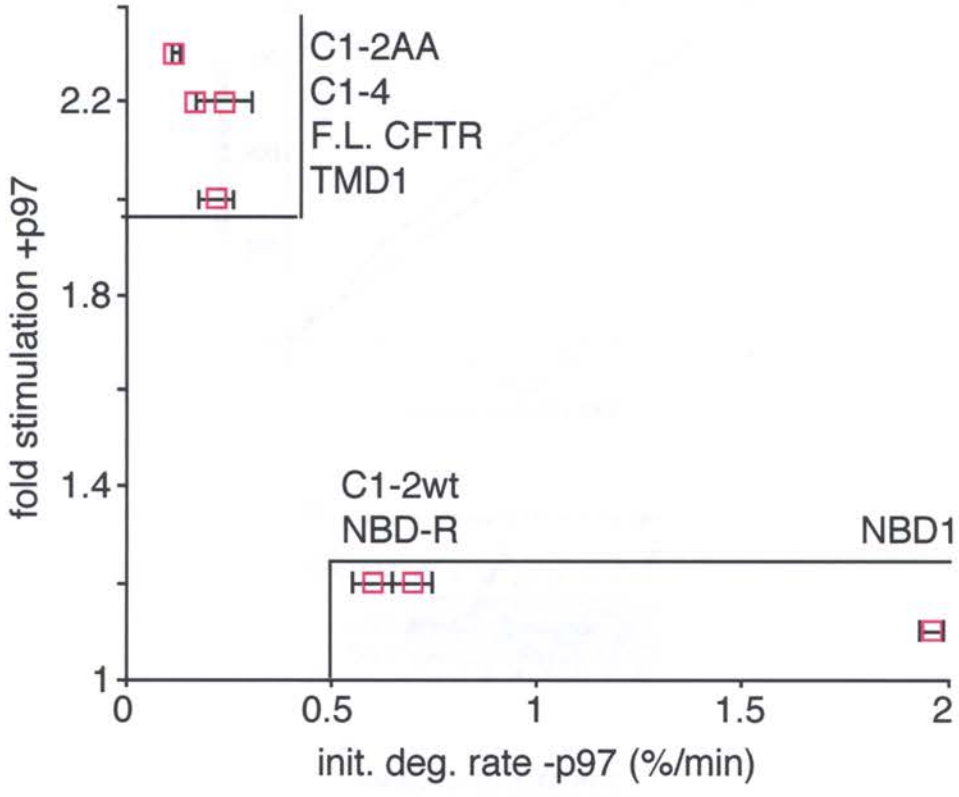

Figure 4-8. P97 effect is inversely related to the rate of degradation. The stimulatory effect (% increase) of p97 on the degradation rate was plotted as a function of the initial degradation rate in the absence of p97.

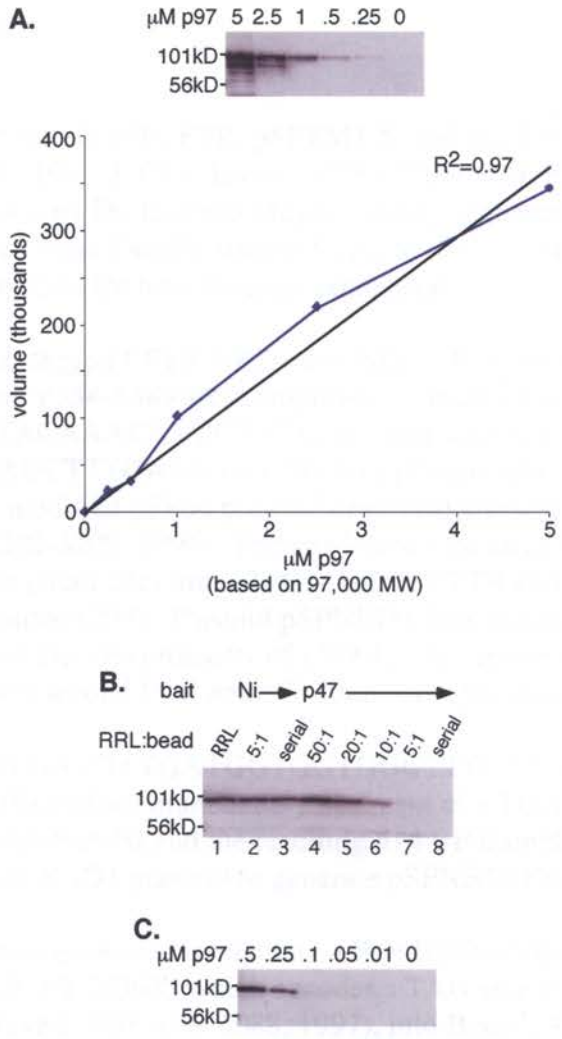

Supplemental Figure 4-1

Standard curve for p97 Quantitation. (A) Specified amounts of purified, recombinant His_6-tagged p97 were subjected to SDS-PAGE, transferred to nitrocellulose or PVDF, and immunoblotted using mAb anti-p97 (1:500; BD Transduction Laboratories) and 2° anti-mouse-AP (1:2500; Promega) with ECF substrate (Amersham Biosciences). The blot was scanned on a Biorad FX phosphoimager and fluoescent signals were visualized and quantitated using QuanityOne software. Plot shows a representative standard curve of integrated fluorescent signal as a function of p97 concentration (based on p97 monomer). **(B)** RRL was incubated for 4 hr at 4°with the indicated ratio (RRL:beads) using Ni-NTA beads (lanes 2-3) or His-tagged p47-saturated Ni-NTA beads (lanes 4-8). In lanes 3 and 8, two serial incubations were performed using 1/5 bead volume each. Depleted RRL was then subjected to immunoblotting as in panels A and B and quantitated against a standard curve of recombinant p97. To ensure that values would fall on the standard curve, RRL in lanes 1-3 were diluted 1/2. For each RRL depletion, p97 standards and depleted RRLs were run on the same gel and transferrred to the same membrane to ensure similar conditions for immunoblotting. **(C)** Decreasing amounts of recombinant p97 were immunoblotted as in panel A but with a longer incubation in ECF substrate (~10 min vs. ~4min) to determine the limits of detection and compare signals obtained at very low p97 concentrations.

Supplemental Information.

Plasmid Constructs. Plasmids pSPCFTR, pSPTM1-6, and pSPTM1-2, and are described elsewhere (Xiong. et al., 1997. J. Clin. Invest. 100: 1079-1088). PTrc-p47, and pQE-p97 were generously provided by Dr. Hemmo Meyer. Coding sequences for p97 and p47 were subcloned into Nco1 and BamH1 sites in frame to the His-6 tag of pET15b (EMD Biosciences, San Diego, CA) for heterologous expression.

Plasmids encoding His6-tagged CFTR NBD1 and NBD1-R domains were constructed as follows. CFTR residues V358-S589 were amplified by PCR using sense (TTTCCCTCCATGGTACAAACATGGTATGAC) and antisense (AGTTTCTGCAGCTAGCTTTCAAATATTTCTT) primers and ligated into NcoI/BamHI sites of a modified pSP64 plasmid described elsewhere (Skach, et al., Cancer Research, 54:3202-3209, 1994). Primers introduced an in-frame ATG translational start codon (NcoI site) immediately before CFTR codon V358 and a TAG stop codon at CFTR residue C590. Plasmid pSPNBD1 thus contains the coding sequence of NBD1 downstream of the SP6 promoter of pSP64. This construct pSPNBD1was then used as the template for a second PCR amplification using the same sense primer and an antisense primer (GAAGGATCCTCAGTGATGATGATGGTGGTGGCTTTCAAATATTTCTTT) encoding six in-frame His codons immediately upstream of a TGA stop codon. The PCR product was digested with BamHI and the resulting 414 BP BamHI fragment was ligated into BamHI-digested pSPNBD1 plasmid to generate pSPNBD1His_6.

Plasmid pSPNBD1-R was generated by ligating a BamHI/PvuII fragment (PvuII site is in pSP64 vector) from pSPCFTR836X, which encodes a TAG stop codon at residue D836 (Xiong, et al., J. Clin. Invest. 100:1079-1088, 1997), into BamHI/PvuII digested pSPNBD1. The resulting plasmid, encoding CFTR residues V358 to D835, was then used as a PCR template with sense (TTTCCCTCCATGGTACAAACATGGTATGAC) and antisense (AGACAGCTGTTAATGATGGTGGTGATGATGATCAAAAAGGCACTCCTT) primers. The antisense primer encodes $(His)_6$Val, immediately upstream of the stop codon followed by an engineered PvuII site. This fragment was digested with BamHI and PvuII and inserted into BamHI/PvuII digested pSPNBD-R, yielding NBD-R with a C-terminal His_6-tag.

Plasmid $pETUb^{G76V}$ was made by amplifying the human ubiquitin cDNA coding sequence (gift of Dr. M. Hochstrasser) with sense primer (AAGACTTCATGATGCAGATCTTCGTCAAC) and antisense primer (AACCAGCCATGGCCACACCTCTTAGTCTTAAGAC), digesting with NcoI and BspHI, and ligating into an NcoI digested pET15b vector. The antisense primer also introduced a G to V mutation at Ubiquitin codon 76. Plasmid pETUb-ubcH5a was then made by amplifying ubcH5a (gift of Dr. Peter Howley) with sense primer (TGACCCATGGCGCTGAAGAGGATT) and antisense primer (TCCGGCGGATCCTTAGTGATGATGATGATGATGCATTGCATATTTCTGAGT),

digesting with NcoI and BamHI and ligating between the NcoI and BamHI sites of pET15ub^{G76V}. The resulting in pET15Ub-ubcH5a encodes a non-cleavable ubiquitin fusion protein with a C-terminal His_6 tag.

TM1-2 (E92A/K95A) was amplified from plasmid pSPCFTR E92A/K95A (Lu et al., 1998) with sense primer (AGGATCTGGCTAGCGATCACC) and antisense primer (GTTCAGGTTTCACGTCACCTTGTTGGAAAGGAGACT), and the resulting DNA fragment was used directly in transcription reactions.

SUMMARY

Over the course of these studies we developed a highly versatile cell free system to dissect the biochemical requirements and physiological relationship between membrane extraction, unfolding, peptide cleavage, and degradation of a prototypical ERAD substrate, CFTR. This work demonstrated that all three peptidase activities of the proteasome contribute substantially to CFTR degradation. Additionally, the ATPase and proteolytic activities of the proteasome were uncoupled by β-subunit inhibition to allow the extraction of membrane proteins in the absence of degradation. The extraction of TMDs is specifically facilitated by the ERAD accessory factor, p97. Moreover, released polypeptides were found to be associated with the proteasome, and there may be a substrate size preference for different proteasome species suggesting the possibility that cap exchange occurs as degradation goes to completion (TCA soluble fragments) (Figure S-1).

P97, while contributing to CFTR ERAD, was found to function primarily in increasing the rate of extraction of TMDs from the membrane, and this interaction was influenced by the hydrophobicity of transmembrane segments. Most importantly, affinity depletion revealed that p97, while contributing to degradation, was not essential, as degradation continued at a reduced rate in its absence. Thus, at least for CFTR, p97 appears to function as an accessory factor to the proteasome by facilitating membrane extraction and substrate presentation.

CFTR is a glycoprotein with 12 TMs and three large cytosolic loops. This complex architecture is characterized by a kinetic folding defect that results in ERAD for both wild type and mutant proteins (Du et al., 2005; Kleizen et al., 2005; Qu et al., 1997;

Thibodeau et al., 2005). Four E3 ligases have been identified that recognize different features of CFTR. CHIP/Hsp70/ubcH5 form a ligase complex that likely interacts with cytosolic NBDs (Meacham et al., 2001; Younger et al., 2004). SCF^{fbx2} is a lectin E3 that targets dislocated glycoproteins , Doa10/MARCH VI is an ER-localized ligase (Bartee et al., 2004; Gnann et al., 2004), and Rma1 is a tail-anchored protein that forms a ligase complex with Derlin-1 at the ER membrane and recognizes CFTR with mutations in TM1(Cyr, D.M., personal communication). These findings are consistent with the degradation of the different constructs used in our studies. Additionally, these ligases may target CFTR to the proteasome via different pathways. Hsp70 interacts with the UBL protein Bag-1 (Luders et al., 2000) and dsk2/hPLIC (Kaye et al., 2000) which likely bind proteasome regulatory subunits Rpn1 and 2 (Elasser et al., 2002; Saeki et al., 2002), whereas Rma1 and Doa10 appear to converge at p97 and thus may share a common pathway for proteasome presentation.

An intriguing finding from our work is that p97 has little effect on the degradation of CFTR cytosolic domains, but causes a pronounced enhancement of TMD degradation. However, TM domains with charged residues are affected by p97 to a variable degree. The most stable construct tested contained only two TMs in which endogenous charged residues in TM1were mutated to alanine. In contrast, its wild type counterpart was readily degraded and largely unaffected by p97. This suggests that the contribution of p97 may be influenced by the relative stability of protein folding, in this case the stability of TMs within the lipid bilayer. Such an explanation is consistent with the dependence of other membrane proteins such as MHCI (Ye et al., 2001), PDR5 (Gnann et al., 2004), and HmgCoA (Bays et al., 2001; Rabinovich et al., 2002) on p97 for extraction from the

membrane. Our results thus suggest a model in which p97 together with the proteasome provide two complementary unfoldases that partition misfolded membrane proteins into a productive degradation cycle. Inefficient, iterative engagement of folded substrates during denaturation at the surface of the rings provides a mechanism for partitioning stable from misfolded or denatured substrates based on their affinity for the AAA-ATPase, ClpXP (Kenniston et al., 2005). By analogy, cooperative unfolding by eukaryotic p97 and the 19S RC are predicted to increase productive engagements to more efficiently extract and unfold energetically costly degradation substrates such as membrane proteins.

Future Studies

Role of PA28 in ERAD: One of our most recent findings is that CFTR fragments released into the cytosol are associated with four distinct proteasome populations: 19S double-capped, PA28 single- and double-capped, and hybrid 19S/PA28 capped (Figure S-1). Moreover, different sized fragments were associated with specific proteasome species, implying that different caps are exchanged as degradation proceeds. In this model degradation of ubiquitinated substrates is initiated by 26S proteasomes and 19S cap are gradually replaced by PA28 due to deubiquitination and as substrate size decreases. PA28 depletion would allow this question to be directly addressed by providing a system with only 19S capped proteasomes for degradation. A decrease in the rate or extent in the production of TCA soluble peptides would indicate if and when cap exchange occurs and the relative importance of this process to degradation .

Role of Hsp70: Other proteins, such as Hsp70, could be specifically targeted for depletion, and effects on both maturation and degradation could be assessed. Two

peptides that specifically bind different regions of Hsp70 have been described (Thulasiraman et al., 2002) and may prove to be useful baits in depleting RRL of Hsp70. Given the importance of Hsp70 in both the maturation and degradation (Zhang et al., 2001), these roles could be dissected. In maturation, Hsp70/Hsp40 binds CFTR NBDs (Meacham et al., 1999) and without Hsp70 present aggregation may occur. However, Hsp70 is also a component of the CHIP E3 ligase complex which targets CFTR for degradation (Meacham et al., 2001), and stabililization of CFTR would be anticipated, particularly if combined with proteolyzed membranes. This approach could be useful for addressing the important question of when chaperones switch their substrates from the maturation pathway into the degradation pathway.

Identification of membrane-bound ligases: ER membranes selectively depleted of E2/E3 complexes also provide valuable tools to further dissect functions of distinct ERAD components. In conjunction with affinity depletion and expression of various CFTR domains, the regions of CFTR recognized by the known ligases can now be studied in detail. For example, TMD1 would be expected to be stabilized in proteolyzed membranes, as both Rma1 (Cyr, D.M., personal communication) and MARCHVI (Bartee et al., 2004) are membrane-localized and would likely be cleaved. Rma1 recognizes defects in TMDs, whereas the function of MARCHVI is entirely unknown. C-terminal domains, whether cytosolic or transmembrane, may also be differentially affected. An alternate possibility enabled by these studies is to examine biogenesis events, such as reinitiation of translocation following the translation of large cytosolic loops.

Figure S-1. (**A**) Autoradiogram showing SDS-PAGE gel showing translation products (t) for *in vitro* translated CFTR (lane 1) and cytosolic degradation intermediates released into the supernatant (s) in the presence of MG132 (lane 2). Input for lane 2 = 6x lane 1 for clarity. (**B**) BN-PAGE analysis of cytosolic fragments of [^{35}S]-CFTR (lanes 1,2) and [^{14}C]-lysozyme (lanes 3,4) after degradation in RRL in the presence of MG132. Migration of proteasomes was determined by silver or Coomassie staining (lanes 1,3, respectively) and gels were then subjected to autoradiography (lanes 2,4). CFTR fragments remained specifically bound to four distinct proteasome species, whereas lysozyme was bound to both proteasomes and the TRiC complex. (**C**) BN-PAGE gel strip containing cytosolic CFTR fragments was separated by 2-D SDS-PAGE and analyzed by autoradiography (top) and silver staining (bottom). *Adapted from Shibatani, T. et al, Global organization and function of cytosolic proteasome pools analyzed by 2-dimensional blue native-PAGE, submitted to Mol. Biol. Cell.*

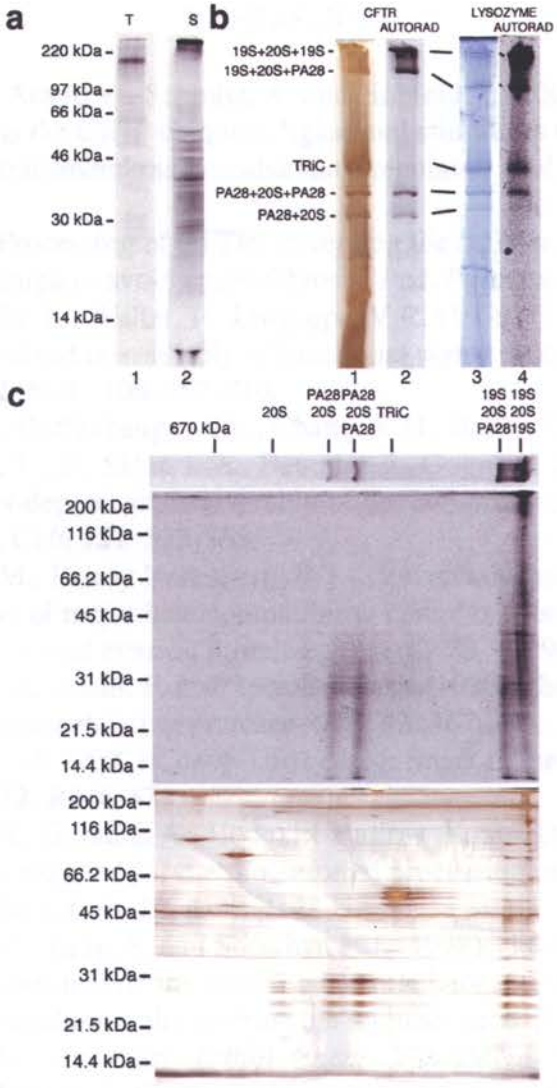
a
T
S
220 kDa
97 kDa
66 kDa
46 kDa
30 kDa
14 kDa
1
2
b
CFTR AUTORAD
LYSOZYME AUTORAD
19S+20S+19S
19S+20S+PA28
TRiC
PA28+20S+PA28
PA28+20S
1
2
3
4
c
670 kDa
20S
PA28 20S
PA28 20S PA28
TRiC
19S 20S PA28
19S 20S 19S
200 kDa
116 kDa
66.2 kDa
45 kDa
31 kDa
21.5 kDa
14.4 kDa
200 kDa
116 kDa
66.2 kDa
45 kDa
31 kDa
21.5 kDa
14.4 kDa

REFERENCES

Alberti, S., Bohse, K., Arndt, V., Schmitz, A. and Hohfeld, J. (2004) The cochaperone HspBP1 inhibits the CHIP ubiquitin ligase and stimulates the maturation of the cystic fibrosis transmembrane conductance regulator. *Mol. Biol. Cell*, **15**, 4003-4010.

Amaral, M.D. (2005) Processing of CFTR: traversing the cellular maze-how much CFTR needs to go through to avoid cystic fibrosis. *Ped. Pulmonol.*, **39**, 479-491.

Andrews, D.W., Lauffer, L., Walter, P., Lingappa, V.R. (1989) Evidence for a two-step mechanism involved in assembly of functional signal recognition particle receptor. *J. Cell Biol.*, **108**, 797-810.

Babbitt, S.E., Kiss, A., Deffenbaugh, A.E., Chang, Y.H., Bailly, E., Erdjument-Bromage, H., Tempst, P., T., B., Sklar, L.A., Baumler, J., Gogol, E. and Skowyra, D. (2005) ATP hydrolysis-dependent disassembly of the 26S proteasome is part of the catalytic cycle. *Cell*, **121**, 553-565.

Bartee, E., Mansouri, M., Hovey Nerenberg, B.T., Gouveia, K. and Fruh, K. (2004) Downregulation of major histocompatibility complex class I by human ubiquitin ligases related to viral evasion proteins. *J. Virol.*, **78**, 1109-1120.

Baumeister, W., Walz, J., Zuehl, F. and Seemueller, E. (1998) The proteasome: paradigm of a self-compartmentalizing protease. *Cell*, **92**, 367-380.

Bays, N. and Hampton, R. (2002) Cdc48-Ufd1-Npl4: Stuck in the middle with Ub. *Current Biol.*, **12**, R366-371.

Bays, N., Wilhovsky, S., Goradia, A., Hodgkill-Harlow, K. and Hampton, R. (2001) HRD4/NPL4 is required for the proteasomal processing of ubiquitinated ER proteins. *Mol. Biol. Cell*, **12**, 4114-4128.

Bebok, Z., Mazzochi, C., King, S. and Sorscher, E.J. (1998) The mechanism underlying cystic fibrosis transmembrane conductance regulator transport from the endoplasmic reticulum to the proteasome includes sec61β and a cytosolic, deglycosylated intermediary. *J. Biol. Chem.*, **273**, 29873-29878.

Benaroudj, N. and Goldberg, A. (2000) PAN, the proteasome -activating nucleotidase from archaebacteria, is a protein-unfolding molecular chaperone. *Nature Cell Biol.*, **2**, 833-839.

Benaroudj, N., Zwickl, P., Seegmueller, E., Baumeister, W. and Goldberg, A. (2003) ATP hydrolysis by the proteasome regulatory complex PAN serves multiple functions in protein degradation. *Mol. Cell*, **11**, 69-78.

Bence, N., Sampat, R. and Kopito, R. (2001) Impairment of the ubiquitin-proteasome system by protein aggregation. *Science*, **292**, 1552-1555.

Biederer, T., Volkwein, C. and Sommer, T. (1997) Role of Cue1P in ubiquitination and degradation at the ER surface. *Science*, **278**, 1806-1809.

Bilan, F., Thoreau, V., Nacfer, M., Derand, R., Norez, C., Cantreau, A., Garcia, M., Becq, F. and Kitzis, A. (2004) Syntaxin 8 impairs trafficking of cystic fibrosis transmembrane conductance regulator (CFTR) and inhibits its channel activity. *J. Cell Sci.*, **117**, 1923-1935.

Bogyo, M., McMaster, J., Gaczynska, M., Tortorella, D., Goldberg, A. and Ploegh, H. (1997) Covalent modification of the active site threonine of proteasomal beta

subunits and the *Escherichia coli* homolog HsIV by a new class of inhibitors. *Proc. Natl. Acad. Sci. USA*, **94**, 6629-6634.

Borden, K. (2000) RING domains: master builders of molecular scaffolds? *J. Mol. Biol.*, **295**, 1103-1112.

Braun, B., Glickman, M., Kraft, R., Dahlmann, B., Kloetzel, P.-M., Finley, D. and Schmidt, M. (1999) The base of the proteasome regulatory particle exhibits chaperone-like activity. *Nature Cell Biol.*, **1**, 221-226.

Braun, S., Matuschewski, K., Rape, M., Thoms, S. and Jentsch, S. (2002) Role of the ubiquitin-selective CDC48(UFD1/NPL4)chaperone (segregase) in ERAD of OLE1 and other substrates. *EMBO J*, **21**, 615-621.

Brodsky, J. and McCracken, A. (1997) ER-associated and proteasome-mediated protein degradation: how two topologically restricted events came together. *Trends Cell Biol.*, **7**, 151-155.

Brodsky, J.L., Hamamoto, S., Feldheim, D. and Schekman, R. (1993) Reconstitution of protein translocation from solubilized yeast membranes reveals topologically distinct roles for BiP and cytosolic Hsc70. *J. Cell Biol.*, **120**, 95-102.

Buchberger, A. (2002) From UBA to UBX: new words in the ubiquitin vocabulary. *Trends Cell Biol.*, **12**, 216-221.

Bush, K., Goldberg, A. and Nigam, S. (1997) Proteasome inhibition leads to a heat-shock response, induction of endoplasmic reticulum chaperones and thermotolerance. *J. Biol. Chem.*, **272**, 9086-9092.

Cabral, C., Goldberg, A.L. and Nigam, S. (1997) Processing by endoplasmic reticulum mannosidase partitions a secretion-impaired glycoprotein into two distinct pathways. *J. Biol. Chem.*, **275**, 25015-25022.

Carlson, E., Bays, N., David, L. and Skach, W. (2005) *Reticulocyte lysate as a model system to study endoplasmic reticulum membrane protein degradation.* Humana Press, Inc., Totowa, NJ.

CFF. (2004) Cystic Fibrosis Foundation National Patient Registry Annual Data Report 2003. *Bethesda, MD.*

Chan, S. and Smith, D.F. (1998) Hop as an adaptor in the heat shock protein (Hsp70) and hsp90 chaperone machinery. *J. Biol. Chem.*, **273**, 35194-35200.

Chappe, V., Irvine, T., Liao, J., Evagelidis, A. and Hanrahan, J.W. (2005) Phosphorylation of CFTR by PKA promotes binding of the regulatory domain. *EMBO J.*, **24**, 2730-2740.

Cheng, S.H., Gregory, R.J., Marshall, J., Paul, S., Souza, D.W., White, G.A., O'Riordan, C.R. and Smith, A.E. (1990) Defective intracellular transport and processing of CFTR is the molecular basis of most cystic fibrosis. *Cell*, **63**, 827-834.

Chillon, M., Casals, T. and Mercier, B. (1995) Mutations in the cystic fibrosis gene in patients with congenital absence of the vas deferens. *N. Engl. J. Med.*, **332**, 1475-1480.

Choi, J.Y., Muallem, D., Kiselyov, K., Lee, M.G., Thomas, P.J. and Muallem, S. (2001) Aberrant CFTR-dependent HCO_3-transport in mutations associated with cystic fibrosis. *Nature*, **410**, 94-97.

Ciechanover, A. (1994) The ubiquitin-proteasome pathway. *Cell*, **79**, 13-21.

Crawshaw, S., Martoglio, B., Meacock, S. and High, S. (2004) A misassembled transmembrane domain of a polytopic protein associates with signal peptide peptidase. *Biochem. J*, **384**, 9-17.

Dai, R.M., Chen, E., Longo, D.L., Gorbea, C.M. and Li, C.H. (1998) Involvement of valosin-containing protein, an ATPase co-purified with IκBα and 26S proteasome , in ubiquitin-proteasome-mediated degradation of IκBα. *J. Biol. Chem.*, **273**, 3562-3573.

Dalal, S., Rosser, M.F., Cyr, D.M. and Hanson, P.I. (2004) Distinct roles for the AAA-ATPases NSF and p97 in the secretory pathway. *Mol. Biol. Cell*, **15**, 637-648.

DeLaBarre, B. and Brunger, A.T. (2003) Complete structure of p97/valosin-containing protein reveals communication between nucleotide domains. *Nat. Struct. Biol.*, **10**, 856-863.

Deshaies, R.J. (1999) SCF and cullin/RING H2-based ubiquitin ligases. *Annu. Rev. Cell Dev Biol.*, **15**, 435-467.

Dick, T., Nussbaum, A., Deeg, M., Heinemeyer, W., Groll, M., Schirle, M., Keilholz, W., Stevanovic, S., Wolf, D., Huber, R., Rammensee, H. and Schild, h. (1998) Contributions of proteasomal beta-subunits to the cleavage of peptide substrates analyzed with yeast mutants. *J. Biol. Chem.*, **273**, 25637-25646.

Du, K., Sharma, M. and Lukacs, G.L. (2005) The ΔF508 cystic fibrosis mutation impairs domain-domain interactions and arrests post-translational folding of CFTR. *Nat. Struct. Mol. Biol.*, **12**, 17-25.

Dubiel, W., Pratt, G., Ferrell, K. and Rechsteiner, M. (1992) Purification of an 11S regulator of the multicatalytic protease. *J. Biol. Chem.*, **267**, 22369-22377.

Egerton, M. and Samelson, L.E. (1994) Biochemical characterization of valosin-containing protein, a protein tyrosine kinase substrate in hematopoietic cells. *J. Biol. Chem.*, **269**, 11345-11341.

Elasser, S., Gali, R.R., Schwickart, M., Larsen, C.N., Leggett, D.S. and Muller, B. (2002) Proteasome subunit Rpn1 binds ubiquitin-like protein domains. *Nat. Cell Biol.*, **4**, 725-730.

Elkabetz, Y., Shapira, I., Rabinovich, E. and Bar-Nun, S. (2004) Distinct steps in dislocation of luminal endoplasmic reticulum-associated substrates. *J. Biol. Chem.*, **279**, 3980-3989.

Ellgaard, L. and Helenius, A. (2001) ER quality control: toward an understanding at the molecular level. *Curr. Opin. Cell Biol.*, **13**, 431-437.

Emmerich, N., Nussbaum, A., Stevanovic, S., Priemer, M., Toes, R., Rammensee, H.-G. and Schild, H. (2000) The human 26S and 20S proteasomes generate overlapping but different sets of peptide fragments from a model protein substrate. *J. Biol. Chem.*, **275**, 21140-21148.

Etlinger, J. and Goldberg, A. (1980) Control of protein degradation in reticulocytes and reticulocyte extracts by hemin. *J. Biol. Chem.*, **255**, 4563-4568.

Ferrell, K., Wilkinson, C., Dubiel, W. and Gordon, C. (2000) Regulatory subunit interactions of the 26S proteasome, a complex problem. *TIBS*, **25**, 83-88.

Frydman, J. and Hohfeld, J. (1997) Chaperones get in touch: The Hip-Hop connection. *Trends Biol. Sci.*, **22**, 87-92.

Gadsby, D.C. and Nairn, A.C. (1999) Control of CFTR channel gating by phosphorylation and nucleotide hydrolysis. *Physiol. Rev.*, **79**, S77-107.

Gelman, M., Kannegaard, E. and Kopito, R. (2002) A principal role for the proteasome in ER-associated degradation of misfolded intracellular CFTR. *J. Biol. Chem.*, **In Press**.

Giaever, G., et al. (2002) Functional profiling of the Saccharomyces cerevisiae genome. *Nature*, **418**, 387-391.

Gibson, R.L., Burns, J.L. and Ramsey, B.W. (2003) Pathophysiology and management of pulmonary infections in cystic fibrosis. *Am. J. Respir. Crit. Care Med.*, **168**, 918-951.

Gilmore, R., Blobel, G., Walter, P. (1982) Protein translocation across the endoplasmic reticulum. I Detection in the microsomal membrane of a receptor for the signal recognition particle. *J. Cell Biol.*, **95**, 463-469.

Glickman, M.H. and Ciechanover, A. (2002) The ubiquitin-proteasome proteolytic pathway: destruction for the sake of construction. *Physiol. Rev.*, **82**, 373-428.

Glickman, M.H., Rubin, D.M., Fried, V.A. and Finley, D. (1998) The regulatory particle of the *Saccharomyces cerevisiae* proteasome. *Mol. Cell Biol.*, **18**, 3149-3162.

Gnann, A., Riordan, J.R. and Wolf, D.H. (2004) Cystic fibrosis transmembrane conductance regulator degradation depends on the lectins Htm1p/EDEM and the cdc48 protein complex in yeast. *Mol. Biol. Cell*, **15**, 4125-4135.

Groll, M., Ditzel, L., Lowe, J., Stock, D., Bochtler, M., Bartunik, H. and Huber, R. (1997) Structure of the 20S proteasome from yeast at 2.4 Å resolution. *Nature*, **386**, 463-471.

Gusarova, V., Caplan, A.J., Brodsky, J.L. and Fisher, E.A. (2001) Apoprotein B degradation is promoted by the molecular chaperones hsp90 and hsp70. *J. Biol. Chem*, **276**, 24891-24900.

Haas, A. and Rose, I. (1981) Hemin inhibits ATP-dependent ubiquitin-dependent proteolysis: role of hemin in regulating ubiquitin conjugate degradation. *Proc. Natl. Acad. Sci. USA*, **78**, 6845-6848.

Hall, R.A., Ostedgaard, L.S., Premont, R.T., Blitzer, J.T., Rahman, N., Welsh, M.J. and Lefkowicz, R.J. (1998) A C-terminal motif found in the beta2-adrenergic receptor, P2Y1 receptor and cystic fibrosis transmembrane conductance regulator determines binding to the Na^+/H^+exchanger regulatory factor family. *Proc. Natl. Acad. Sci., USA*, **95**, 8496-8501.

Hampton, R., Gardner, R. and Rine, J. (1996) Role of 26S proteasome and HRD genes in the degradation of 3-hydroxy-3-methylglutaryl-CoA reductase, an integral endoplasmic reticulum membrane protein. *Mol. Biol. Cell*, **7**, 2029-2044.

Hartmann-Petersen, R. and Gordon, C. (2004) Integral UBL domain proteins: a family of proteasome interacting proteins. *Sem. Cell Dev. Biol.*, **15**, 247-259.

Hatakeyama, S., Yada, M., Matsumoto, M., Ishida, N. and Nakyama, K.I. (2001) U box proteins as a new family of ubiquitin-protein ligases. *J. Biol. Chem.*, **276**, 33111-33120.

Hershko, A. and Ciechanover, A. (1998) The ubiquitin system. *Annu. Rev. Biochem.*, **67**, 425-479.

Hiller, M., Finger, A., Schweiger, M. and Wolf, D. (1996) ER degradation of a misfolded luminal protein by the cytosolic ubiquitin-proteasome pathway. *Science*, **273**, 1725-1728.

Hirsch, C., Jarosch, E., Sommer, T. and Wolf, D.H. (2004) Endoplasmic reticulum-associated protein degradation--one model fits all? *Biochim. Biophys. Acta*, **1695**, 208-216.

Hitchcock, A.L., Krebber, H., Frietze, S., Lin, A., Latterich, M. and Silver, P.A. (2001) The conserved npl4 protein complex mediates proteasome-dependent membrane-bound transcription factor activation. *Mol. Biol. Cell*, **12**, 3226-3241.

Hoffman, L. and Rechsteiner, M. (1996) Nucleotidase activities of the 26 S proteasome and its regulatory complex. *J. Biol. Chem.*, **271**, 32538-32545.

Hohfeld, J., Minami, Y. and Hartl, F. (1995) Hip, a novel cochaperone involved in the eukaryotic Hsc70/Hsp40 reaction cycle. *Cell*, **83**, 589-598.

Hoskins, J., Pak, M., Maurizi, M. and Wickner, S. (1998) The role of the ClpA chaperone in proteolysis by ClpAP. *Proc. Natl. Acad. Sci. USA*, **95**, 12135-12140.

Hough, R., Pratt, G. and Rechsteiner, M. (1986) Ubiquitin-lysozyme conjugates. *J. Biol. Chem.*, **261**, 2400-2408.

Hough, R., Pratt, G. and Rechsteiner, M. (1987) Purification of two high molecular weight proteases from rabbit reticulocyte lysate. *J. Biol. Chem.*, **262**, 8303-8313.

Huang, L., Kinnucan, E., Wang, G., Beaudenon, S., Howley, P.M., Huilbregtse, J.M. and Pavletich, N.P. (1999) Structure of an E6AP-ubcH7 complex: insights into ubiquitination by the E2-E3 enzyme cascade. *Science*, **286**, 1321-1326.

Huyer, G., Piluek, W.F., Fansler, Z., Kreft, S.G., Hochstrasser, M., Brodsky, J.L. and Michaelis, S. (2004) Distinct machinery is required in *Saccharomyces cerevisiae* for the endoplasmic reticulum-associated degradation of a multispanning membrane protein and a soluble luminal substrate. *J. Biol. Chem.*, **279**, 38369-38378.

Jackson, R. and Hunt, T. (1983) Preparation and use of nuclease-treated rabbit reticulocyte lysates for the translation of eukaryotic messenger RNA. *Methods in Enzymology*, **96**, 50-74.

Jarosch, E., Taxis, C., Volkwein, C., Bordallo, J., Finley, D., Wolf, D. and Sommer, T. (2002) Protein dislocation from the ER requires polyubiquitination and the AAA-ATPase Cdc48. *Nature Cell Biol.*, **4**, 134-139.

Jensen, T., Loo, M., Pind, S., Williams, D., Goldberg, A. and Riordan, J. (1995) Multiple proteolytic systems, including the proteasome, contribute to CFTR processing. *Cell*, **83**, 129-136.

Jiang, J., Ballinger, C., Wu, Y., Dai, Q., Cyr, D., Hohfeld, J. and Patterson, C. (2001) CHIP is a U-box-dependent E3 ubiquitin ligase: Identification of Hsc70 as a target for ubiquitylation. *J. Biol. Chem.*, **276**, 42938-42934.

Johnson, E.S., Ma, P.C., Ota, I.M. and Varshavsky, A. (1995) A proteolytic pathway that recognizes ubiquitin as a degradation signal. *J. Biol. Chem.*, **270**, 17442-17456.

Johnston, J., Ward, C. and Kopito, R. (1998) Aggresomes: A cellular response to misfolded proteins. *J. Cell. Biol.*, **143**, 1883-1898.

Kaderbhai, M., Harding, V., Karim, A., Austen, B. and Kaderbhai, N. (1995) Sheep pancreatic microsomes as an alternative to the dog source for studying protein translocation. *Biochem. J.*, **15**, 57-61.

Kalies, K.-U., Allan, S., Sergeyenko, T., Kroger, H. and Romisch, K. (2005) The protein translocation channel binds proteasomes to the endoplasmic reticulum. *EMBO J.*, **24**, 2284-2293.

Kaupp, U.B. and Seifert, R. (2002) Cyclic nucleotide-gated channels. *Physiol. Rev.*, **82**, 769-824.

Kaye, F.J., Modi, S., Ivanovska, I., Koonin, E.V., Thress, K. and Kubo, A. (2000) A family of ubiquitin-like proteins binds the ATPase domain of Hsp70-like Stch. *FEBS Lett*, **467**, 348-355.

Kenniston, J.A., Baker, T.A., Fernandez, J.M. and Sauer, R.T. (2003) Linkage between ATP consumption and mechanical unfolding during the protein processing reactions of an AAA^+ degradation machine. *Cell*, **114**, 511-520.

Kenniston, J.A., Baker, T.A. and Sauer, R.T. (2005) Partitioning between unfolding and release of native domains during ClpXP degradation determines substrate selectivity and partial processing. *Proc. Natl. Acad. Sci., USA*, **102**, 1390-1395.

Kisselev, A., Akopian, A., Woo, K. and Goldberg, A. (1999a) The sizes of peptides generated from protein by mammalian 26 and 20 S proteasomes. *J. Biol. Chem*, **274**, 3363-3371.

Kisselev, A.F., Akopian, T.N., Castillo, V. and Goldberg, A.L. (1999b) Proteasome active sites allosterically regulate each other, suggesting a cyclical bite-chew mechanism for protein breakdown. *Mol. Cell*, **4**, 395-402.

Kleizen, B., van Vlijmen, T., de Jonge, H. and Braakman, I. (2005) Folding of CFTR is predominately cotranslational. *Mol. Cell*, **20**, 277-287.

Knowles, M.R. and Boucher, R.C. (2002) Mucus clearance as a primary innate defense mechanism for mammalian airways. *J. Clin. Invest.*, **109**, 571-577.

Kobayashi, T., Tanaka, K., Inoue, K. and Kakizuka, A. (2002) Functional ATPase activity of p97/valosin-containing protein (VCP) is required for the quality control of endoplasmic reticulum in neuronally differentiated PC12 cells. *J. Biol. Chem.*, **277**, 47358-47365.

Kobilka, B. (1990) The role of cytosolic and membrane factors in processing of the human beta-2 adrenergic receptor following translocation and glycosylation in a cell free system. *J. Biol. Chem.*, **265**, 7610-7618.

Kohler, A., Cascio, P., Leggett, D.S., Woo, K.M., Goldberg, A.L. and Finley, D. (2001) The axial channel of the proteasome core particle is gated by the Rpt2 ATPase and controls both substrate entry and product release. *Mol. Cell*, **7**, 1143-1152.

Kondo, H., Rabouille, C., Newman, R., Levine, T.P., Pappin, D., Freemont, P. and Warren, G. (1997) p47 is a cofactor for p97-mediated membrane fusion. *Nature*, **388**, 75-78.

Lam, Y.A., Lawson, T.G., Velayutham, M., Zweier, J.L. and Pickart, C.M. (2002) A proteasomal ATPase subunit recognizes the polyubiquitin signal. *Nature*, **416**, 763-767.

Lee, C., Schwartz, M., Prakash, S., Iwakura, M. and Matouschek, A. (2001) ATP-dependent proteases degrade their substrates by processively unraveling them from the degradation signal. *Mol. Cell*, **7**, 627-637.

Lee, R.J., Liu, C., Harty, C., McCracken, A.A., Latterich, M., Romisch, K., DeMartino, G.N., Thomas, P.J. and Brodsky, J.L. (2004) Uncoupling retro-translocation and degradation in the ER-associated degradation of a soluble protein. *EMBO J.*, **23**, 2206-2215.

Lewis, H.A., Buchanan, S.G., Burley, S.K., Conners, K., Dickey, M., Dorwart, M., Fowler, R., Gao, X., Guggino, W.B., Hendrickson, W.A., Hunt, J.F., Kearins,

M.C., Lorimer, D., Maloney, P.C., Post, K.W., Rajashankar, K.R., Rutter, M.E., Sauder, J.M., Shriver, S., Thibodeau, P.H., Thomas, P.J., Zhang, M., Zhao, X. and Emtage, S. (2004) Structure of nucleotide-binding domain 1 of the cystic fibrosis transmembrane conductance regulator. *EMBO J.*, **23**, 282-293.

Lilley, B.N. and Ploegh, H.L. (2004) A membrane protein required for dislocation of misfolded proteins from the ER. *Nature*, **429**, 834-840.

Liu, C., Millen, L., Roman, T.B., Xiong, H., Gilbert, H., Noiva, R., DeMartino, G.N. and Thomas, P.J. (2002) Conformational remodeling of proteasome substrates by PA700, the 19S regulatory complex of the 26S proteasome. *J. Biol. Chem.*, **277**, 26815-26820.

Locher, K., Lee, A. and Rees, D. (2002) The E. coli BtuCD structure: A framework for ABC transporter architecture and mechanism. *Science*, **296**, 1091-1098.

Loo, M., Jensen, T., Cui, L., Hou, Y., Chang, X. and Riordan, J. (1998) Perturbation of Hsp90 interaction with nascent CFTR prevents its maturation and accelerates its degradation by the proteasome. *EMBO J.*, **17**, 6879-6887.

Loo, T. and Clarke, D. (1998) Quality control by proteases in the endoplasmic reticulum. Removal of a protease-sensitive site enhances expression of human P-glycoprotein. *J. Biol. Chem.*, **273**, 32373-32376.

Lowe, C.U., May, C.D. and Reed, S.C. (1949) Fibrosis of the pancreas in infants and children: a statistical study of clinical and hereditary features. *AM. J. Dis. Child*, **78**, 349-374.

Lu, Y., Turnbull, I., Bragin, A., Carveth, K., Verkman, A. and Skach, W. (2000) Reorientation of Aquaporin-1 topology during maturation in the endoplasmic reticulum. *Mol. Biol. Cell*, **11**, 2973-2985.

Lu, Y., Xiong, X., Helm, A., Kimani, K., Bragin, A. and Skach, W. (1998) Co- and Posttranslational mechanisms direct CFTR N-terminus transmembrane assembly. *J. Biol. Chem.*, **273**, 568-576.

Luders, J., Demand, J. and Hohfeld, J. (2000) The ubiquitin-related BAG-1 provides a link between the molecular chaperones Hsc70/Hsp70 and the proteasome. *J. Biol. Chem.*, **275**, 4613-4617.

Ma, J., Wollmann, R. and Lindquist, S. (2002) Neurotoxicity and neurodegeneration when PrP accumulates in the cytosol. *Science*, **298**, 1781-1785.

Matsui, H., Grubb, B.R., Tarran, R., Randell, S.H., Gatzy, J.T., Davis, C.W. and Boucher, R.C. (1998) Evidence for periciliary liquid layer depletion, not abnormal ion composition, in the pathogenesis of cystic fibrosis airways disease. *Cell*, **95**, 1005-1015.

Mayer, T., Braun, T. and Jentsch, S. (1998) Role of the proteasome in membrane extraction of a short-lived ER-transmembrane protein. *EMBO J*, **17**, 3251-3257.

McCracken, A. and Brodsky, J. (1996) Assembly of ER-associated protein degradation *in vitro*: dependence on cytosol, calnexin and ATP. *J. Cell Biol.*, **132**, 291-298.

McCracken, A. and Brodsky, J. (2003) Evolving questions and paradigm shifts in endoplasmic-reticulum-associated degradation (ERAD). *BioEssays*, **25**, 868-877.

Meacham, G., Lu, Z., King, S., Sorscher, E., Tousson, A. and Cyr, D. (1999) The Hdj-2/Hsc70 chaperone pair facilitates early steps in CFTR biogenesis. *EMBO J.*, **18**, 1492-1505.

Meacham, G., Patterson, C., Zhang, W., Younger, J. and Cyr, D. (2001) The Hsc70 co-chaperone CHIP targets immature CFTR for proteasomal degradation. *Nat. Cell Biol.*, **3**, 100-105.

Melderen, L. and Gottesman, S. (1999) Substrate sequestration by a proteolytically inactive Lon mutant. *Proc. Natl. Acad. Sci. USA*, **96**, 6064-6071.

Melton, D.A., Krieg, P.A., Bebagliati, M.R., Maniatis, T., Zinn, K. and Green, M.R. (1984) Efficient in vitro synthesis of biologically active RNA and RNA hybridization probes from plasmids containing a bacterial SP6 promoter. *Nucl. Acids Res.*, **12**, 7035-7056.

Meyer, H., Wang, Y. and Warren, G. (2002) Direct binding of ubiquitin conjugates by the mammalian P97 adaptor complexes, P47 and Ufd1-Npl4. *EMBO J*, **21**, 5645-5652.

Minami, Y., Hohfeld, J., Ohtsuka, K. and Hartl, F.U. (1996) Regulation of the heat shock protein 70 reaction cycle by the mammalian DnaJ homolog, Hsp40. *J. Biol. Chem.*, **271**, 19617-19624.

Moir, D., Stewart, S.E., Osmond, B.C. and Botstein, D. (1982) Cold-sensitive cell-division-cycle mutants of yeast: isolation, properties, and pseudoreversion studies. *Genetics*, **100**, 547-563.

Moyer, B.D., Denton, J., Karlson, K.H., Reynolds, D., Wang, S., Mickle, J.E., Milewski, M., Cutting, G.R., Guggino, W.B., Li, M. and Stanton, B.A. (1999) A PDZ-interacting domain in CFTR is an apical membrane polarization signal. *J. Clin. Invest.*, **104**, 1353-1361.

Muller, D.J., Kessler, M., Oesterhelt, F., Moller, C., Oesterhelt, D. and Gaub, H. (2002) Stability of bacteriorhodopsin α-helices and loops by single-molecule force spectroscopy. *Biophys. J*, **83**, 3578-3588.

Naren, A.P., Nelson, D.J., Xie, W., Jovov, B., Pevsner, J., Bennett, M.K., Benos, D.J., Quick, M.W. and Kirk, K.L. (1997) Regulation of CFTR chloride channels by syntaxin and Munc18 isoforms. *Nature*, **390**, 302-305.

Navon, A. and Goldberg, A. (2001) Proteins are unfolded on the surface of the ATPase ring before transport into the proteasome. *Mol. Cell*, **1339-1349**.

Neuber, O., Jarosch, E., Volkwein, C., Walter, J. and Sommer, T. (2005) Ubx2 links the Cdc48 complex to ER-associated protein degradation. *Nat. Cell Biol.*

Nishikawa, S., Brodsky, J. and Nakatsukasa, K. (2005) Roles of molecular chaperones on endoplasmic reticulum (ER) quality control and ER-associated degradation (ERAD). *J. Biochem.*, **17**, 203-212.

Nussbaum, A., Dick, T., Keilholz, W., Schirle, M., Stevanovic, S., Dietz, K., Heinemeyer, W., Groll, M., Wolf, D., Huber, R., Rammensee, H. and Schild, H. (1998) Cleavage motifs of the yeast 20S proteasome beta subunits deduced from digests of enolase 1. *Proc. Nat. Acad. Sci. USA*, **95**, 12504-12509.

Oberdorf, J., Carlson, E. and Skach, W. (2001) Redundancy of proteasome ß subunit function during endoplasmic reticulum associated degradation. *Biochem.*, **40**, 13397-13305.

Oberdorf, J., Carlson, E. and Skach, W. (2006) Uncoupling proteasome peptidase and ATPase activities results in cytosolic release of an ER polytopic protein. *J. Cell Sci.*, **119**, 303-313.

Oberdorf, J. and Skach, W. (2002) *In vitro reconstitution of CFTR biogenesis and degradation.* Humana Press Inc., Totowa, NJ.

Ogura, T. and Wilkinson, A.J. (2001) AAA^+ superfamily ATPases: common structure-diverse function. *Genes to Cells*, **6**, 575-597.

Ortega, J., Singh, S.K., Ishikawa, T., Maurizi, M.R. and Steven, A.C. (2000) Visualization of substrate binding and translocation by the ATP-dependent protease, ClpX. *Mol. Cell*, **6**, 1515-1521.

Ostedgaard, L.S., Baldursson, O. and Welsh, M.J. (2001) Regulation of the cystic fibrosis transmembrane conductance regulator Cl^- channel by its R domain. *J. Biol. Chem.*, **276**, 7689-7692.

Packschies, L., Theysser, H., Buchberger, A., Bukau, B., Goody, R.S. and Reinstein, J. (1997) GrpE accelerates nucleotide exchange of the molecular chaperone DnaK with an associative displacement mechanism. *Biochemistry*, **36**, 3417-3422.

Pickart, C.M. and Cohen, R.E. (2004) Proteasomes and their kin: proteases in the machine age. *Nat. Rev. Mol. Cell Biol.*, **5**, 177-187.

Pilon, M., Schekman, R. and Römisch, K. (1997) Sec61p mediates export of a misfolded secretory protein from the endoplasmic reticulum to the cytosol for degradation. *EMBO J.*, **16**, 4540-4548.

Pind, S., Riordan, J. and Williams, D. (1994) Participation of the endoplasmic reticulum chaperone calnexin (p88, IP90) in the biogenesis of the cystic fibrosis transmembrane conductance regulator. *J. Biol. Chem.*, **269**, 12784-12788.

Plemper, R., Egner, R., Kuchler, K. and Wolf, D. (1998) Endoplasmic reticulum degradation of a mutated ATP-binding cassette transporter Pdr5 proceeds in a concerted action of Sec61 and the proteasome. *J. Biol. Chem*, **273**, 32848-32856.

Plemper, R. and Wolf, D. (1999) Retrograde protein translocation: ERADication of secretory proteins in health and disease. *Trends Biol. Sci.*, **24**, 266-270.

Prakash, S., Tian, L., Ratliff, K.S., Lehotzky, R.E. and Matouschek, A. (2004) An unstructured initiation site is required for efficient proteasome-mediated degradation. *Nat. Struct. Mol. Biol.*, **11**, 830-837.

Qiu, W. and Kohen-Avramoglu, R. (2004) Overexpression of the endoplasmic reticulum protein ER-60 down regulates ApoB100 secretion by inducing its intracellular degradation via a nonproteasomal pathway: evidence for an ER-60-mediated and pCMB-sensitive intracellular degradative pathway. *Biochemistry*, **43**, 4819-4831.

Qu, B., Strickland, E.H. and Thomas, P.J. (1997) Localization and suppression of a kinetic defect in Cystic Fibrosis Transmembrane Conductance Regulator folding. *J. Biol. Chem.*, **272**, 15739-15744.

Qu, D., Teckman, J., Omura, S. and Perlmutter, D. (1996) Degradation of a mutant secretory protein, alpha1-antitrypsin Z, in the endoplasmic reticulum requires proteasome activity. *J. Biol. Chem*, **271**, 22971-22975.

Quinton, P.M. (1983) Chloride impermeability in cystic fibrosis. *Nature*, **301**, 421-422.

Quinton, P.M. (1986) Missing Cl^- conductance in cystic fibrosis. *Am. J. Physiol.*, **251**, C649-C652.

Quinton, P.M. (1999) Physiological basis of cystic fibrosis: a historical perspective. *Physiol. Rev.*, **79**, S3-S22.

Rabinovich, E., Kerem, A., Frölich, K.-U., Diamant, N. and Bar-Nun, S. (2002) AAA-ATPase p97/Cdc48p, a cytosolic chaperone required for endoplasmic reticulum-associated protein degradation. *Mol. Cell Biol.*, **22**, 626-634.

Rape, M., Hoppe, T., Gorr, I., Kalocay, M., Richly, H. and Jentsch, S. (2001) Mobilization of processed, membrane -tethered SPT23 transcription factor by CDC48(Ufd1/Npl4), a ubiquitin-selective chaperone. *Cell*, **107**, 667-677.

Rechsteiner, M. and Hill, C.P. (2005) Mobilizing the proteolytic machine: cell biological roles of proteasome activators and inhibitors. *Trends Cell Biol.*, **15**, 27-33.

Reid, B., Fenton, W., Horwich, A. and Weber-Ban, E. (2001) ClpA mediates directional translocation of substrate proteins into the ClpP protease. *Proc. Natl. Acad. Sci. USA*, **98**, 3768-3722.

Richly, H., Rape, M., Braun, S., Rumpf, S., Hoege, C. and Jentsch, S. (2005) A series of ubiquitin binding factors connects cdc48/p97 to substrate multiubiquitination and proteasomal targeting. *Cell*, **120**, 73-84.

Riordan, J.R. (2005) Assembly of functional CFTR chloride channels. *Annu. Rev. Physiol.*, **67**, 701-718.

Riordan, J.R., Rommens, J.M., Kerem, B.-S., Alon, N., Rozmahel, R., Grzelczak, Z., Zielenski, J., Lok, S., Collins, F.S. and Tsui, L.-C. (1989) Identification of the cystic fibrosis gene: cloning and characterization of complementary DNA. *Science*, **245**, 1066-1072.

Romisch, K. (2005) Endoplasmic Reticulum-Associated Degradation. *Annu. Rev. Cell Dev Biol.*, **21**.

Rommens, J., Iannuzzi, M., Kerem, B.-S., Drumm, M., Melmer, G., Dean, M., Rozmahel, R., Cole, J., Kennedy, D., Hidaka, N., Zsiga, M., Buchwald, M., Riordan, J., Tsui, L.-C. and Collins, F. (1989) Identification of the cystic fibrosis gene: chromosomal walking and jumping. *Science*, **245**, 1059-1065.

Rowe, S.M., Miller, S. and Sorscher, E.J. (2005) Mechanisms of disease: Cystic fibrosis. *N. Engl. J. Med.*, **352**, 1992-2001.

Saeki, Y., Sone, T., Toh-e, A. and Yokosawa, H. (2002) Identification of ubiquitin-like protein-binding subunits of the 26S proteasome. *Biochem. Biophys. Res. Commun.*, **296**, 813-819.

Sato, S., Ward, C. and Kopito, R. (1998) Cotranslational ubiquitination of cystic fibrosis transmembrane conductance regulator *in vitro*. *J. Biol. Chem.*, **273**, 7189-7192.

Schmitz, A., Schneider, A., Kummer, M. and Herzog, V. (2004) Endoplasmic reticulum-localized amyloid β-peptide is degraded in the cytosol by two distinct pathways. *Traffic*, **5**, 89-101.

Schuberth, C. and Buchberger, A. (2005) Membrane-bound Ubx2 recruits Cdc48 to ubiquitin ligases and their substrates to ensure efficient ER-associated degradation. *Nat. Cell Biol.*

Schwarz, S.E., Rosa, J.L. and Scheffner, M. (1998) Characterization of human HECT domain family members and their interaction with ubcH5 and ubcH7. *J. Biol. Chem.*, **273**, 12148-12154.

Sheppard, D.N. and Welsh, M.J. (1999) Structure and function of the CFTR chloride channel. *Physiol. Rev.*, **79**, S23-45.

Short, D.B., Trotter, K.W., Reczek, D., Kreda, S.M., Bretscheer, A., Boucher, R.C., Stutts, M.J. and Milgram, S.L. (1998) An apical PDZ protein anchors the cystic

fibrosis transmembrane conductance regulator to the cytoskeleton. *J. Biol. Chem.*, **273**, 19797-19801.

Singh, S., Grimaud, R., Hoskins, J., Wickner, S. and Maurizi, M. (2000) Unfolding and internalization of proteins by the ATP-dependent proteases ClpXP and ClpAP. *Proc. Natl. Acad. Sci. USA*, **97**, 8898-8903.

Skach, W. and Lingappa, V. (1993) Amino terminus assembly of human P-glycoprotein at the endoplasmic reticulum is directed by cooperative actions of two internal sequences. *J. Biol. Chem.*, **268**, 23552-23561.

Song, C., Wang, Q. and Li, C.H. (2003) ATPase activity of p97-VCP: D2 mediates the major enzyme activity and D1 contributes to the heat-induced activity. *J. Biol. Chem.*, **278**, 3648-3655.

Steward, M.C., Ishiguro, H. and Case, R.M. (2005) Mechanisms of bicarbonate secretion in the pancreatic duct. *Annu. Rev. Physiol.*, **67**, 377-409.

Stutts, M.J., Canessa, C., Olsen, J., Hamrick, M., Cohn, J., Rossier, B. and Boucher, R. (1995) CFTR as a cAMP-dependent regulator of sodium channels. *Science*, **269**, 847-850.

Tarran, R., Button, B. and Boucher, R.C. (2005a) Regulation of normal and cystic fibrosis airway surface liquid volume by phasic shear stress. *Annu. Rev. Physiol.*, **68**, 23.21-23.19.

Tarran, R., Button, B., Picher, M., Paradiso, A.M., Ribeiro, C.M., Lazarowski, E.R., Zhang, L., Collins, P.L., Pickles, R.J., Fredberg, J.J. and Boucher, R.C. (2005b) Normal and cystic fibrosis airway surface liquid homeostasis: the effects of phasic shear stress and viral infections. *J. Biol. Chem.*, **280**, 35751-35759.

Thibodeau, P.H., Brautigam, C.A., Machius, M. and Thomas, P.J. (2005) Side chain and backbone contributions of Phe508 to CFTR folding. *Nat. Struct. Mol. Biol.*, **12**, 10-16.

Thrower, J.S., Hoffman, L., Rechsteiner, M. and Pickart, C.M. (2000) Recognition of the polyubiquitin proteolytic signal. *EMBO J.*, **19**, 94-102.

Thulasiraman, V., Yun, B.-G., Uma, S., Gu, Y., Scroggins, B.T. and Matts, R.L. (2002) Differential inhibition of Hsc70 activities by two Hsc70-binding peptides. *Biochemistry*, **41**, 3742-3753.

Tomazin, R., Boname, J., Hegde, N., Lewinsohn, D., Altschuler, Y., Jones, T., Cresswell, P., Nelson, J., Riddell, S. and Johnson, D. (1999) Cytomegalovirus US2 destroys two components of the MHC class II pathway, preventing recognition by CD4+ T cells. *Nature Med.*, **5**, 1039.

VanSlyke, J. and Musil, L. (2002) Dislocation and degradation from the ER are regulated by cytosolic stress. *J. Cell Biol.*, **157**, 381-394.

Varga, K., Jurkuvenaite, A., Wakefield, J., Hong, J.S., Guimbellot, J.S., Venglarik, C.J., Niraj, A., Mazun, M., Sorscher, E.J., Collawn, J.F. and Bebok, Z. (2004) Efficient intracellular processing of endogenous cystic fibrosis transmembrane conductance regulator in epithelial cell lines. *J. Biol. Chem.*, **279**, 22578-22584.

Verma, R., Aravind, L., Oania, R., McDonald, W.H., Yates, J.R.R., Koonin, E.V. and Deshaies, R.J. (2002) Role of Rpn11 metalloprotease in deubiquitination and degradation by the 26S proteasome. *Science*, **298**, 608-611.

Verma, R., Chen, S., Feldman, R., Schieltz, D., Yates, J.R.r., Dohmen, R.J. and Deshaies, R.J. (2000) Proteasomal proteomics: identification of nucleotide-sensitive

proteasome-interacting proteins by mass spectrometric analysis of affinity-purified proteasomes. *Mol. Biol. Cell*, **11**, 3425-3439.

Verma, R., Oania, R., Graumann, J. and Deshaies, R.J. (2004) Multiubiquitin chain receptors define a layer of substrate selectivity in the ubiquitin-proteasome system. *Cell*, **118**, 99-110.

Voges, C., Zwickl, P. and Baumeister, W. (1999) The 26S proteasome: a molecular machine designed for controlled proteolysis. *Annu. Rev. Biochem.*, **68**, 1015-1068.

Walter, J., Urban, J., Volkwein, C. and Sommer, T. (2001) Sec61p-independent degradation of the tail-anchored ER membrane protein Ubc6p. *EMBO J.*, **20**, 3124-3131.

Walter, P. and Blobel, G. (1981) Translocation of proteins across the endoplasmic reticulum II. Signal recognition protein (SRP) mediates the selective binding to microsomal membranes of *in-vitro* assembled polysomes synthesizing secretory protein. *J. Cell Biol.*, **91**, 551-556.

Walter, P. and Blobel, G. (1983) *Preparation of microsomal membranes for cotranslational protein translocation.* Academic Press, Inc, New York.

Walter, P., Jackson, R.C., Marcus, M.M., Lingappa, V.R. and Blobel, G. (1979) Tryptic dissection and reconstitution of translocation activity for nascent presecretory proteins across microsomal membranes. *Proc. Natl. Acad. Sci. USA*, **76**, 1795-1799.

Wang, X., Matteson, J., An, Y., Moyer, B., Yoo, J.S., Bannykh, S., Wilson, I.A., Riordan, J.R. and Balch, W.E. (2004) COPII-dependent export of cystic fibrosis transmembrane conductance regulator from the ER uses a di-acidic exit code. *J. Cell Biol.*, **167**, 65-74.

Ward, C., Omura, C. and Kopito, R. (1995) Degradation of CFTR by the ubiquitin-proteasome pathway. *Cell*, **83**, 121-128.

Wegele, H., Muller, L. and Buchner, J. (2004) Hsp70 and Hsp90- a relay team for protein folding. *Rev. Physiol. Biochem. Pharm.*, **151**, 1-44.

Welsh, M.J., Ramsey, B.W., Accurso, F. and Cutting, G.R. (2001) Cystic Fibrosis. In Scriver, C.L., Sly, W.S. and Valle, D. (eds.), *The Molecular and Metabolic Basis of Inherited Disease*. McGraw-Hill, New York, pp. 5121-5188.

White, S.H. and Wimley, W.C. (1998) Hydrophobic interactions of peptides with membrane interfaces. *Biochim. Biophys, acta*, **1376**, 3399-3352.

Wiertz, E., Tortorella, D., Bogyo, M., Yu, J., Mothes, W., Jones, T., Rapoport, T. and Ploegh, H. (1996) Sec61-mediated transfer of a membrane protein from the endoplasmic reticulum to the proteasome for destruction. *Nature*, **384**, 432-438.

Wigley, W., Fabunmi, R., Lee, M., Marino, C., Muallem, S., DeMartino, G. and Thomas, P. (1999) Dynamic association of proteasomal machinery with the centrosome. *J. Cell. Biol.*, **145**, 481-490.

Wilhovsky, S., Gardner, R. and Hampton, R. (2000) *HRD* gene dependence of endoplasmic reticulum-associated degradation. *Mol. Biol. Cell*, **11**, 1697-1708.

Wilkinson, C.R., Ferrell, K., Penney, M., Wallace, M., Dubiel, W. and Gordon, C. (2000) Analysis of a gene encoding Rpn10 of the fission yeast proteasome reveals that the polyubiquitin-binding site of this subunit is essential when Rpn1/Mts3 is compromised. *J. Biol. Chem.*, **275**, 15182-15192.

Wilson, R., Allen, A.J., Oliver, J., Brookman, J.L., High, S. and Bulleid, N.J. (1995) The translocation, folding, assembly, and redox-dependent degradation of secretory and membrane proteins in semi-permeabilized cells. *Biochem. J.*, **307**, 679-687.

Wojcik, C., Yano, M. and Demartino, G.N. (2004) RNA interference of valosin-containing protein (VCP/p97) reveals multiple cellular roles linked to ubiquitin/proteasome-dependent proteolysis. *J. Cell Sci.*, **117**, 281-292.

Xiong, X., Bragin, A., Widdicombe, J., Cohn, J. and Skach, W. (1997) Structural cues involved in ER degradation of G85E and G91R mutant CFTR. *J. Clin. Invest.*, **100**, 1079-1088.

Xiong, X., Chong, E. and Skach, W. (1999) Evidence that endoplasmic reticulum (ER)-associated degradation of cystic fibrosis transmembrane conductance regulator is linked to retrograde translocation from the ER membrane. *J. Biol. Chem*, **274**, 2616-2624.

Yan, J.X., Wait, R., Berkelman, T., Harry, R.A., Westbrook, J.A., Wheeler, C.H. and Dunn, M.J. (2000) A modified silver staining protocol for visualization of proteins compatible with matrix-assisted laser desorption/ionization and electrospray ionization- mass spectrometry. *Electrophoresis*, **21**, 3666-3672.

Yang, Y., Fruh, K., Ahn, K. and Peterson, P. (1995) *In vivo* assembly of the proteasomal complexes, implications for antigen processing. *J. Biol. Chem.*, **270**, 27687-27694.

Yang, Y., Janach, S., Cohn, J. and Wilson, J. (1993) The common variant of cystic fibrosis transmembrane conductance regulator is recognized by hsp70 and degraded in a pre-Golgi nonlysosomal compartment. *Proc. Natl. Acad. Sci. USA*, **90**, 9480-9484.

Ye, Y., Meyer, H. and Rapoport, T. (2001) The AAA-ATPase Cdc48/p97 and its partners transport proteins from the ER into the cytosol. *Nature*, **414**, 652-656.

Ye, Y., Meyer, H. and Rapoport, T. (2003) Function of the p97-Ufd1-Npl4 complex in retrotranslocation from the ER to the cytosol: dual recognition of nonubiquitinated polypeptide segments and polyubiquitin chains. *J. Cell Biol.*, **162**, 71-74.

Ye, Y., Shibata, Y., Yun, C., Ron, D. and Rapoport, T.A. (2004) A membrane protein complex mediates retro-translocation from the ER lumen into the cytosol. *Nature*, **429**, 841-847.

Yoshida, Y., Chiba, T., Tokunaga, F., Kawasaki, H., Iwai, K., Suzuki, T., Ito, Y., Matsuoka, K., Yoshida, M., Tanaka, K. and Tai, T. (2002) E3 ubiquitin ligase that recognizes sugar chains. *Nature*, **418**, 438-442.

Youker, R., Walsh, P., Beilarz, T., Lithgow, T. and Brodsky, J. (2004) Distinct roles for the Hsp40 and Hsp90 molecular chaperones during cystic fibrosis transmembrane conductance regulator degradation in yeast. *Mol. Biol. Cell*, **15**, 4787-4797.

Younger, J.M., Ren, H.-Y., Chen, L., Fan, C.-Y., Fields, A., Patterson, C. and Cyr, D.M. (2004) A foldable CFTR ΔF508 biogenic intermediate accumulates upon inhibition of the Hsc70-CHIP E3 ubiquitin ligase. *J. Cell Biol.*, **167**, 1075-1085.

Yu, H., Kaung, S., Kobayashi, S. and Kopito, R. (1997) Cytosolic degradation of T-cell Receptor alpha chains by the proteasome. *J. Biol. Chem.*, **272**, 20800-20804.

Zhang, H., Peters, K.W., Sun, F., Marino, C.R., Lang, J., Burgoyne, R.D. and Frizzell, R.A. (2002) Cysteine string protein interacts with and modulates the maturation

of the cystic fibrosis transmembrane conductance regulator. *J. Biol. Chem.*, **277**, 28948-28958.

Zhang, Y., Nijbroek, G., Sullivan, M.L., McCracken, A.A., Watkins, S.C., Michaelis, S. and Brodsky, J.L. (2001) Hsp70 molecular chaperone facilitates endoplasmic reticulum-associated degradation of cystic fibrosis transmembrane conductance regulator in yeast. *Mol. Biol. Cell*, **12**, 1303-1314.

Zhong, X., Shen, Y., Ballar, P., Apostolou, A., Agami, R. and Fang, S. (2004) AAA ATPase p97/valosin-containing protein interacts with gp78, a ubiquitin ligase for endoplasmic reticulum-associated degradation. *J. Biol. Chem.*, **279**, 45676-45684.

Zielenski, J. (2000) Genotype and phenotype in cystic fibrosis. *Respiration*, **67**, 117-133.

Zielenski, J. and Tsui, L.C. (1995) Cystic fibrosis: genotypic and phenotypic variations. *Annu. Rev. Genet.*, **29**, 777-807.

APPENDICES

Note: published as a chapter in Methods in Molecular Biology.

Carlson, E., Bays, N., David, L., Skach, W.R. Reticulocyte lysate as a model system to study ER membrane protein degradation. Patterson, C. and Cyr D.M. editors. Methods in Molecular Biology, Humana Press, 301: 185-205. 2005.

The appendices describe detailed protocols for reconstituting ERAD in RRL using *de novo* synthesized substrates, manipulation of cytosolic and membrane components using proteolysis and alkylation of microsomes, affinity depletion of RRL with His-tagged proteins, and reconstitution of microsomes and lysates with recombinant proteins.

APPENDIX A

Preparation of RRL

The following procedure, used routinely in our laboratory, is based on a protocol previously described by Jackson et al. (Jackson and Hunt, 1983) and takes roughly 1 week from start to finish. Typically 5-10 rabbits are processed simultaneously. Preparing RRL *de novo* permits the composition and quality of reaction conditions to be controlled and optimized. Different preparations may vary significantly in terms of activity. Lysate from each animal is processed and stored separately and assayed independently for efficiency in translation and degradation reactions. We have found that the best preparations for degradation are often the least suitable for translation. The reason for this is unknown, but likely reflects biological differences between animals and/or the amount of endogenous free hemin present in RRL (see Note A1).

Commercial preparations of RRL are available for *in vitro* translation (Promega (TNT systems, L2080; Nuclease treated RRL, L4960; and Untreated RRL, L4151). However, if large numbers of experiments are to be performed it is often more economical to prepare this reagent since one rabbit yields between 20-40 ml of RRL. It should be emphasized that with the exception of Untreated RRL (Promega, L4151) these commercial products contain exogenous hemin, which stimulates RRL translation but is also a potent proteasome inhibitor. The concentration of hemin in commercial preparations is not specified, but based on preparation of Untreated RRL (Promega, L4151)(TM 232) for use in protein synthesis, it seems that 20 uM hemin is Promega's standard treatment. Because most commercial products are optimized for translation they are generally not suitable to study degradation. (see Note A2).

A. Reagents and supplies for reticulocyte induction

1. New Zealand White rabbits (~6 months old, ≥ 3kg)
2. 3 cc syringes (# of rabbits x 3)

3. 26 gauge needles

4. Clinical Centrifuge with rotor suitable for hematocrit determination (e.g. IEC rotor #927)

5. Hematocrit reader, hematocrit tubes, and clay to plug tubes

6. Acetyl phenyl hydrazine (APH) solution: Add 2.5 g of APH to 20 ml of EtOH then add 50 ml of water. pH to 7.0 with ~1 ml of 1 M KOH, and bring to 100 ml with water. Filter solution (0.22 μm), aliquot and store at –20 ^{o}C.

B. Reagents and supplies for processing of reticulocyte lysate

1. Rabbit restrainer

2. Pentobarbital /Nembutal, 50 mg/ml (4-5 ml per rabbit)

3. Heparin, 1000 units/ml (2 ml per rabbit)

4. 70% isopropanol

5. IV tubing (e.g. extension set # ET-20L (472010) from B/Braun – 21" long tubing)

6. Reticulocyte wash buffer: 5 mM Glucose, 0.14 M NaCl, 0.05 M KCl, 5 mM $MgCl_2$ (~500 ml per rabbit).

7. Micrococcal nuclease, 15 U/μl: dissolve in 10 mM Tris, pH 8.0 or RNAse free water. Store in aliquots at –80 ^{o}C. (US Biochemicals, Cleveland, OH).

8. 0.1 M $CaCl_2$

9. 0.1 M EGTA

10. 1 mM hemin stock solution. Combine reagents in the following order: 6.44 mg hemin (bovine crystalline type I, Sigma, St. Louis, MO), 0.25 ml 1 M KOH, 0.5 ml 0.2 M Tris-HCl, pH 7-8, 8.9 ml ethylene glycol, 0.19 ml 1 N HCl, 0.05 ml H_20. Filter (0.22μm) and store at –20 ^{o}C.

C. Procedure

1. All steps involving the handling and care of animals should be approved by the institutional animal review board.

2. Inject rabbits subcutaneously in scruff of neck on three consecutive days (days 1, 2 and 3) with 2 ml of APH solution.

3. On days 4 – 7 monitor animals for health, activity, and food intake. Hematocrits should be measured in selected animals by collecting blood samples in a capillary tube (via ear vein puncture). Centrifuge blood at ~8,000 x g for 5 minutes and read hematocrit directly. The hematocrit should normally not fall below 20%.

4. On day 8, place rabbits in a restrainer, cannulate an ear vein and inject 2 ml of heparin (2000 U) followed by a lethal dose of pentobarbital (200-250 mg) one minute later. When rabbit has lost eyelid reflex and respiration has ceased, remove the animal from restrainer, transect left ribs with a scalpel, open chest cavity and puncture left ventricle directly with 16 gauge needle attached to IV extension tubing. Collect blood in a 250 ml centrifuge bottle on ice. Perform all subsequent steps on ice.

5. Centrifuge blood at 2,500 x g at 4^{o}C for 10 min and discard supernatant (aspirate buffy coat layer of white blood cells). Wash cells three times with 150 ml of ice cold reticulocyte wash buffer followed by centrifugation at 2,500 x g for 10 min. After the third wash resuspend cells in small volume of wash buffer, transfer to 50 ml conical tube, centrifuge at 3,000 x g for 10 minutes and remove supernatant. Add one volume of ice cold H_2O and shake very vigorously for 30 sec to lyse cells. Repeat shaking every 5 minutes 3 times. Centrifuge lysate at 15,000 x g for 10 minutes and carefully decant supernatant. Lysate can be frozen in liquid nitrogen at this stage and stored at -80^{o}C for several years with minimal loss of activity. Set aside several small samples (0.5 ml) to test relative activity in translation and/or degradation assays.

6. For degradation reactions the lysate is used without further modification. This

is untreated RRL (not to be confused with Promega's product of the same name. See Note A2).

7. For translation, hemin is added to a final concentration of 40 μM, and RRL RNA is digested by nuclease treatment. To perform the latter, a 1ml aliquot of RRL is quickly thawed in a 25°C water bath. 10 μl of 0.1 M $CaCl_2$ and 10 μl of micrococcal nuclease are added. The sample is incubated for 8-10 minutes at 25°C, and 20 μl of 0.1 M EGTA is added. Samples are aliquoted, frozen in liquid nitrogen and stored at -80°C for 2-3 months.

D. Notes

A1. Repeated freeze-thaw cycles will decrease RRL activity. 3-4 cycles are generally well tolerated as long as samples are thawed quickly, and refrozen in liquid nitrogen. The quality of RRL may vary between rabbits due to slight variations in cytosolic factors such as endogenous hemin, and age and maturity of the reticulocytes. Therefore we process lysate from each rabbit separately. The most active preparations for translation and/or degradation are stored and used appropriately. Lower yields can result from failure to completely exanguinate the animal or inefficient lysis of reticulocytes. The latter problem is usually due to inadequate shaking of the lysate and will be manifest by a very large pellet in the second 15,000 x g spin in the RRL protocol.

A2. Most commercial RRL preparations are designed for performing translations and, therefore, contain added hemin (Promega TnT system and nucleased RRL). These preparations are incompatible with proteasome degradation assays because hemin inhibits ATPase activity of the 19S subunit (Hoffman and Rechsteiner, 1996). Promega's "untreated" RRL appears to contain no hemin. However, different lots may need to be tested to find one with optimal activity. In the presence

of hemin, degradation is inhibited but ubiquitination is not, so degradation substrates usually accumulate as ubiquitinated intermediates. It should be noted that unsupplemented RRL may also contain some endogenous free hemin. This may account for differences in degradation efficiency observed for different rabbits. The best RRL preps in our hands will convert 60-70+% of *in vitro* synthesized CFTR into TCA soluble fragments in 4 hr at 37^{o}C.

APPENDIX B

Preparation of ER microsomal membranes

Our canine pancreas microsome preparation is based on the procedure described by Walter and Blobel (Walter and Blobel, 1983).

A. Reagents and supplies

1. Pancreas tissue
2. 50 ml Potter-Elvehem tissue homogenizer with Teflon pestles (one loose fitting and one snug)
3. 25 ml Potter-Elvehem tissue homogenizer (Teflon pestle)
4. Hand held food grinder
5. 10X stock buffer (100 ml): 0.5 M KoAc, 60 mM $Mg(oAc)_2$, 10 mM EDTA, 0.5M triethanolamine-acetate, pH 7.5.
6. Buffer A: 1/10 dilution of 10X stock buffer containing 0.25 M sucrose, 1 mM dithiothreitol (DTT), 0.5 mM phenylmethylsulfonyl fluoride (PMSF). Add DTT and PMSF immediately before use.
7. Buffer B: 1/10 dilution of 10X stock buffer containing 1.3 M sucrose
8. Buffer C (100 ml): 0.25 M sucrose, 1 mM DTT, 50 mM triethanolamine-acetate, pH 7.5. Add DTT immediately before using.
9. 1% SDS, 0.1 M Tris-HCl, pH 8.0

B. Procedure

All procedures are carried out on ice in a $4^{o}C$ cold room.

1. Quickly remove pancreas from euthanized animal and immediately place into 100 ml of ice cold Buffer A (see Note B1). Trim away fat, connective tissue and blood vessels, and record weight. Grind pancreas by hand using a coarse grinder until a

pulpy consistency is achieved. Collect fragments together with 4 volumes (4 ml/gram of original tissue) of ice cold Buffer A.

2. Homogenize this mixture in a 50 ml Potter-Elvehem tissue homogenizer attached to a high speed motor with 3-4 passes of a loose fitting teflon pestle, and return homogenate to ice. Homogenize solution a second time with 1-3 passes of a tight fitting teflon pestle. Sample must be kept ice cold during the entire procedure.

3. Divide homogenate into 50 ml polyallomer tubes and centrifuge at 600 x g for 10 minutes. Decant supernatant into fresh 50 ml polyallomer tubes and centrifuge at 10,000 x g for 10 min. Decant the resulting supernatant into a 150 ml beaker taking care not to contaminate the supernatant with the loose pellet.

4. Carefully layer ~15-20 ml of this supernatant fraction over a 5-7 ml cushion of Buffer B and centrifuge at 150,000 x g for 3 hours. Aspirate supernatant and gently resuspend pellets (by hand in a 25 ml homogenizer) in Buffer C (1/2 ml per gram of starting material). When the solution is uniform, aliquot and freeze 1 ml aliquots in liquid nitrogen. Microsomes are stable for several years when stored at $-80^{\circ}C$.

5. Determine the OD_{280} by dissolving 10 µl of membrane suspension in 990 µl of 1% SDS, 0.1 M Tris-HCl, pH 8.0. This provides a useful reference based on crude protein content. OD_{280} concentration of the final membrane prep should be ~50-100.

6. Prior to use, digest endogenous mRNA with micrococcal nuclease as described for RRL (see section 3.1, item 7). Typically, 1 ml of microsomes are treated, frozen in liquid nitrogen as 50-100 µl aliquots, and stored at $-80^{\circ}C$ for up to 3 months.

7. Test microsomes for translocation and glycosylation (see Note B2).

C. Notes

B1. Traditionally canine pancreatic microsomes have been used to study *in vitro* translation of secreted and transmembrane proteins. However, preparations can also be made from pig or sheep pancreas by following essentially the same procedure

(Kaderbhai et al., 1995). Proteolysis or autolysis of the pancreas can be a significant problem so the pancreas should be removed as quickly as possible following euthanasia.

B2. Like RRL, canine pancreas membrane preparations vary widely in their efficiency of translocation, and it may take several attempts to achieve a satisfactory preparation. A suitable preparation, however, generates 10-30 ml of microsomes and is sufficient for thousands of typical translation and/or degradation reactions. Optimal preparations yield $\geq$ 90% translocation and ~ 80% core glycosylation efficiency at a final OD_{280} concentration of 4-10 in the translation reaction.

APPENDIX C

In vitro transcription/translation

We routinely assemble reactions *de novo*, which allows us to control conditions for both synthesis and degradation. All reagents, including RRL and microsomal membranes, and containers used for transcription and translation must be kept RNAse free. Transcription reactions can be made up fresh or stored at -80°C. The following conditions are used for SP6 RNA polymerase, which usually gives better results for translation than T7 RNA polymerase in our lab. Our vector (~4000 bp plasmid) has been optimized for use in RRL by adding a 5' UTR from *Xenopus laevis* globin gene (TCTTGTTCTTTTTGCAGA AGCTCAGAATAAACGCTCAACTTTGGCAGATCTGAACATG) immediately upstream of the ATG start site (Melton et al., 1984). DNA constructs are put into this vector after removing the endogenous 5' UTR to place the start codon as close as possible to the end of the *X. laevis* 5' UTR.

A. Transcription reagents

1. 5X transcription buffer: 30 mM $MgCl_2$, 10 mM spermidine, 200 mM Tris-HCl, pH 7.5.
2. 10X NTP's: 5 mM ATP, 5 mM CTP, 5 mM UTP, 1 mM GTP, 20 mM Tris-HCl, pH 8.0. (Nucleotides from Roche Molecular Biochemicals, Indianapolis, IN).
3. Diguanosine triphosphate (Promega, Madison, WI): Dissolve 25 U in 300 µl sterile, ddH_2O (~ 5 mM) and store at -80° C.
4. 0.1 M DTT (Roche Molecular Biochemicals, Indianapolis, IN))
5. tRNA, 10 mg/ml (bovine liver type XI, Sigma, St. Louis, MO)
6. RNAse inhibitor, 20 U/ml (Promega, Madison, WI)
7. SP6 polymerase, 10 U/ml (Epicenter, Madison, WI)

B. Translation reagents

1. 20X translation buffer: 2M KoAc, 16 mM $Mg(oAc)_2$, 40 mM Tris-acetate, pH 7.5.

2. 5X Emix: 5 mM ATP, 5 mM GTP, 60 mM creatine phosphate, 1 mM mixture of 19 amino acids except methionine, and 5 μCi/μl Trans^{35}S-label (ICN, Costa Mesa, CA). Aliquots are typically made in 100-200 μl volumes, adjusted to pH 7.5 with Tris base and stored at -80C.

3. RRL (hemin and nuclease treated - see Appendix A)

4. tRNA, 10 mg/ml (bovine liver type XI, Sigma, St. Louis, MO)

5. RNAse inhibitor, 20 U/ml (Promega, Madison, WI)

6. Creatine kinase, 4 mg/ml (CK) (Sigma, St. Louis, MO): Dissolve in 50% glycerol, 10 mM Tris-acetate, pH 7.5.

7. Microsomal membranes (nuclease treated - see Appendix B)

8. SDS loading buffer (SDS-LB): 4% SDS, 2 mM EDTA, 10% sucrose, 0.05% bromophenol blue, 1M DTT, 100 mM Tris-HCl, pH 8.9.

9. 1-2 mM aurin tricarboxylic acid (ATA) (Sigma, St. Louis, MO). adjust to pH ~7.0 with Tris base.

Procedure

C. Transcription

1. Assemble a 20 μl transcription reaction, by combining the following reagents on ice: 4 μl of 5X transcription buffer, 2 μl of10X NTP's, 2 μl of 0.1 M DTT, 2 μl of GpppG, 0.4 μl tRNA, 0.8 μl of RNAse inhibitor, 0.8 μl of SP6 polymerase, 4 μg of plasmid DNA and 4 μl of mH2O. For larger constructs such as CFTR (4400 bp) use 8 μg of plasmid DNA. mH2O is substituted for DNA in mock transcription reactions. Incubate for 1 hour at 40°C (37°C for T7 polymerase) and transfer to ice.

D. Translation

1. Translation reactions are usually linked to transcription so that no purification or extraction of RNA is necessary. The composition of translation buffers thus takes into account the ionic contributions of the transcript. Assemble a 100 μl translation reaction by combining 5 μl of 20X translation buffer, 20 μl 5X Emix, 40 μl RRL (nucleased and treated with hemin), 1 μl RNAse inhibitor, 1 μl CK, and 20 μl transcription mixture. The volume of microsomes is determined empirically based on translocation and glycosylation activity (see Appendix B). Most translations are performed at 24°C for 1 hour. For proteins > 80 kD, ATA (an inhibitor of translation initiation) is added to increase the ratio of full length protein to partially synthesized fragments. Add ATA typically after 15 minutes (0.05-0.1 mM final concentration) and continue incubating at 24°C until maximal expression is achieved (up to 2 hrs). Transfer reaction to ice (see Note C1).

D. Optimization

1. Certain components may need to be titrated for optimal translation. Typical concentrations for potassium and magnesium vary between 50-150 mM and 0.5-2.5 mM, respectively. High concentrations of microsomes inhibit translation, whereas low concentrations yield low translocation and glycosylation efficiencies. Optimal concentration of Mg^{2+}, K^{+}, and the timing of ATA addition should be determined empirically to maximize translation efficiency (see Note C2).

E. Notes

C1. Ubiquitination of membrane proteins generally does not occur at 24°C (temperature used for translation). However, ubiquitin ladders rapidly form cotranslationally when polytopic membrane proteins are translated at a higher temperature or in the absence of microsomes (our unpublished observations). For example, CFTR translated without microsomes is cotranslationally incorporated into a covalent high molecular weight complex, and aquaporin translated in the absence

of microsomes forms clear ubiquitin ladders. Co-translational ubiquitination of CFTR has been reported to occur at 30°C but was observed for only a small fraction of total protein (Sato et al., 1998).

C2. A common problem in translating large proteins (e.g. CFTR) is the generation of incomplete translation products. This can occur if, a) insufficient ATA is added, b) ATA is added too late or c) transcript concentration is too high. In addition to inhibiting translation initiation, ATA has been shown to inhibit the ATPase activity of the 26S proteasome (Hoffman and Rechsteiner, 1996). Additional articles by Jackson and Hunt (Jackson and Hunt, 1983) and Promega's technical manual part# TM232 (downloadable through their web site) contain further information concerning the optimization of RRL translation.

APPENDIX D

In vitro degradation and membrane release assays

A. Reagents

1. 10X degradation buffer: 10 mM ATP, 120 mM creatine phosphate, 30 mM DTT, 50 mM $MgCl_2$, 100 mM Tris-HCl, pH 7.5.
2. 0.1M sucrose buffer: 0.1M sucrose, 100 mM KCl, 5 mM $MgCl_2$ 1mM DTT, 50 mM HEPES-NaOH, pH 7.5.
3. 0.5M sucrose cushion: 0.5 M sucrose, 100 mM KoAc, 5 mM $Mg(oAc)_2$, 1 mM DTT, 50 mM Hepes-NaOH, pH 7.5.
4. RRL (untreated. See Appendix A).
5. Creatine kinase, 4 mg/ml (see Appendix C)
6. 20% trichloroacetic acid (TCA)
7. Ready-Safe scintillation fluid (Beckman, Fullerton, CA)
8. 10 mM MG132 (in DMSO). (Sigma, St. Louis, MO. listed as "*n*-cbz-leu-leu-leu-al")

Procedure

B. Collection and resuspension of microsomal membranes

Following translation, membrane proteins are isolated by pelleting microsomes through a sucrose cushion to remove unincorporated radiolabel. This isolation step should reduce background counts to $\leq$ ~20%. Isolated microsomes are then used to reconstitute degradation reactions.

1. Dilute translation mixture with two volumes of 0.1 M sucrose buffer and layer mixture onto 3-4 volumes of 0.5 M sucrose cushion. Centrifuge at 180,000 x g for 10 min. Aspirate the supernatant and resuspend the pellet in twice the original translation

volume in 0.1 M sucrose buffer by physically dislodging the membrane pellet with a 200 µl pipette tip. Vigorously titurate the solution with the end of the pipette tip placed tightly against the bottom of the tube so that the buffer (and pellet) slowly squeezes through the opening. It is critical resuspend the pellet uniformly. Re-cool the tube on ice if necessary (see Note D1).

2. Layer the resuspended pellet on 0.5 M sucrose cushion, and centrifuge at 180,000 x g for 10 min. The final resuspension of the membrane pellet is done in 1/2 the original translation volume in 0.1 M sucrose buffer.

C. *In vitro* degradation assay

Substrate degradation can be monitored by two techniques, a) direct visualization by SDS PAGE or b) scintillation counting. The former will indicate the disappearance of full-length protein which occurs either by ubiquitination or cleavage, whereas the latter can be used to determine the rate and extent to which substrate is converted into TCA soluble fragments (i.e. end products of proteasome-mediated degradation).

1. For a 100 µl reaction, combine on ice: 10 µl of 10X degradation buffer, 72 µl of untreated RRL (see Appendix A), 2 µl of creatine kinase, and 18 µl of resuspended membranes. Use one reaction as a control (no additions) and others to test various experimental conditions (e.g. depleted RRL (see Appendix E), proteasome inhibitors, and/or treated membranes (see Appendix F). It is critical to set up a parallel degradation reaction containing membranes from a mock translation for each membrane treatment tested.
2. Prior to the start of the reaction (T_0), remove 3 µl aliquots from each reaction mixture and place one in 2.5 ml of scintillation fluid (duplicates are usually done for total counts), another in 300 µl of 20% TCA (on ice), and a third in 30 µl of SDS-LB (see Note D2).

3. Incubate at 37°C. At desired time points, remove 3 µl aliquots and place one in SDS-LB and the other into 300 µl of 20% TCA. Reactions usually proceed for 3-4 hrs or until maximum degradation is achieved.

4. Precipitate TCA samples on ice (minimum of 30 min) and centrifuge at 16,000 x g for 15 minutes (4°C). Transfer 250 µl of supernatant to 2.5 ml of scintillation fluid and count in a scintillation counter.

5. Samples collected into SDS-LB are incubated for 30 minutes at 37°C, centrifuged at 16,000 x g for 2 minutes, separated on polyacrylamide gels, and processed for autoradiography.

Calculating percent of protein degraded: Determine total ^{35}S in the degradation reaction by counting 3 µl of reaction mixture directly in scintillation fluid. Because TCA supernatants contain 250/300 of the sample, counts are corrected by a factor of 1.2 to yield "corrected TCA soluble counts." Calculate the percent of protein degraded at each time point using the following formula:

$$\% \text{ degraded} = \{((T_n - T_0) - (M_n - M_0))/((T - T_0) - (M - M_0))\}*100$$

T_n = corrected TCA soluble counts in samples taken at time point, n.

T_0 = corrected TCA soluble counts measured at time 0 (i.e. background TCA soluble counts).

T = total counts in degradation reaction.

M_n=corrected TCA soluble counts from mock samples taken time point, n.

M_0 = corrected TCA soluble counts from mock degradation at time 0 (i.e. background TCA soluble counts present in mock degradation).

M = total counts in mock degradation reaction. (The factors (M_n-M_0) and $(M-M_0)$ represent nonspecific counts). (see Notes D3 and D4).

D. ER release of integral membrane proteins during ERAD

The membrane release assay is similar to the degradation assay, except that each sample is pelleted through a sucrose cushion, and the supernatant is analyzed for total counts and/or TCA soluble counts released from the membranes. Protein fragments can be analyzed by SDS PAGE as well. Without proteasome inhibitors, all released counts are usually TCA soluble, but TCA insoluble fragments are generated with progressive proteasome inhibition.

1. Before starting the degradation reaction (T_0), mix a 7 µl aliquot from each reaction with 13 µl of 0.1 M sucrose buffer. 5. Layer sample on 30 µl of 0.5 M sucrose cushion. Centrifuge at 180,000 x g for 10 min.
2. Remove supernatant and aliquot 10 µl into 2.5 ml of scintillation cocktail, 20 µl into 20 µl of SDS-LB (see note D5), and 10 µl into 300 µl of 20% TCA (see Note D2).
3. Keep TCA precipitated samples on ice a minimum of 30 min and centrifuge at 16,000 x g for 15 minutes (4°C). Transfer 250 µl of supernatant to 2.5 ml of scintillation fluid and count in a scintillation counter.
4. Solubilize the membrane pellet in 50 µl of 1% SDS, 0.1 M Tris-HCl, pH 8 and add 20 µl to 20 µl of SDS-LB. (see Note D5).
5. Incubate reactions at 37°C for 3-4 hrs and process 7 µl samples as in steps 1-4 at desired time points.

Calculating ERAD-mediated substrate release from membranes: Count 3 µl of degradation mixture directly in scintillation fluid to determine total ^{35}S in the reaction. Total ^{35}S in the supernatant is determined by counting 10 µl of supernatant after pelleting 7 µl of degradation mixture. Because 10 µl of supernatant contains 1.4 µl of degradation mixture ((10 µl/50 µl)*7 µl), the counts are corrected by a factor of 2.14, giving "corrected total counts in the supernatant." Calculate the percent substrate released into the supernatant at each time point using the following formula:

% protein released = $\{((TS_n - TS_0) - (MS_n - MS_0))/((T - TS_0) - (M - MS_0))\} * 100$

TS_n = corrected total counts in supernatant at time point, n.

TS_0 = corrected total counts in supernatant at time 0 (i.e. background).

T = total counts in degradation reaction.

MS_n = corrected total counts in mock supernatant at time point, n. (mock degradation reaction).

MS_0 = corrected total counts in mock supernatant at time 0 (i.e. background in mock degradation reaction).

M = total counts in mock degradation reaction. (The factors (MS_n-MS_0) and (M – MS_0) represent nonspecific counts). (see Note 9).

Calculating TCA soluble counts released from membranes: Correct the TCA soluble counts from supernatant samples by a factor of 2.14 as noted above. An additional correction by a factor of 1.2 is made because only 250/300 of the sample in TCA supernatants is counted. Using the "corrected TCA soluble counts", calculate the percent TCA soluble fragments released into the supernatant using the following formula:

% TCA soluble fragments released = $\{((A_n - A_0) - (B_n - B_0))/TC\} * 100$, where

A_n = corrected TCA soluble counts in supernatant samples taken at time points, n.

A_0 = corrected TCA soluble counts in supernatant samples at time 0 (i.e. background).

B_n = corrected TCA soluble counts in mock supernatant samples taken time points, n (mock degradation).

B_0 = corrected TCA soluble counts in mock supernatant sample at time 0 (i.e. background in mock degradation). (B_n-B_0) represents nonspecific counts).

TC = total insoluble counts in the reaction at T=0. Calculated as in section C: $(T–T_0) – (M–M_0)$. (see note D3).

E. Notes

D1. Uniform resuspension of microsomes is necessary to avoid scatter in experimental results. This is one of the most difficult steps in the degradation procedure and may require significant practice. When resuspension is complete, the solution should appear faintly opalescent and there should be no particulate membrane clumps visible. If foaming of the solution occurs, transfer the liquid portion to a fresh tube. If the resuspended microsomes have significantly less radiolabeled protein than the original translation (as determined by SDS-PAGE autoradiography), the following should be considered. a) A significant fraction of the microsomal pellet may have been lost during resuspension. b) protein was synthesized but did not insert into the membranes. The latter can occur if microsomes are sub-optimal or if the translation reaction was not mixed sufficiently.

D2. Because RRL is so concentrated, the protein will rapidly precipitate in 20% TCA. Therefore, expel the sample from the pipette with the tip pressed against the bottom of the tube, break up large pieces of precipitate with the tip, and vortex immediately after addition of sample to TCA to assure adequate dispersion of TCA-soluble peptide fragments. Periodically vortexing the samples during the 30 min incubation on ice is also recommended.

D3. Radioactivity released from membranes in the absence of ATP results from nonspecific association of Trans^{35}S-Label to microsome components and a small amount of background translation in RRL. The relative contribution of ATP-independent release is assessed by comparing standard (containing transcript) and "mock" translations. Nonspecific counts also vary depending on the membrane prep (from 15% - 60%), and several preps may be evaluated before finding one with a low background. Nucleasing microsomes for up to 20 minutes may help reduce the background without affecting activity. Also, EDTA stripping of microsomes ((Walter and Blobel, 1983)) may reduce background. Incubate microsomes in 25

mM EDTA for 15 min on ice, pellet through a 0.5 M sucrose cushion, and resuspend in Buffer C. When analyzed under reducing conditions by SDS-PAGE, microsomes from mock translations appear largely devoid of radiolabeled protein. Release of non-specific counts into the TCA soluble fraction is also independent of ATP and RRL, and is likely due to reversible association of components in Trans^{35}S-Label with components of microsomal membranes. Release of TCA-soluble radioactivity from mock reactions is thus equivalent to the ATP-independent release of radioactivity from standard translations. In other words, nonspecific release is not related to substrate degradation, and can be subtracted from each corresponding sample.

D4. Under optimal conditions, 50-70% of total CFTR is converted to TCA soluble fragments in 4 hours. Factors affecting degradation include a) the RRL prep (does it contain hemin), b) the membrane prep, c) ATP regenerating system, and d) translation efficiency. RRL degradation activity can also be easily assessed using commercially available radiolabeled substrates such as ^{14}C-lysozyme (Xiong et al., 1999).

D5. Release of proteins from the ER membrane can also be followed by SDS PAGE. However, unless a proteasome inhibitor such as MG132 is being used the fragments in the supernatant will be too small to visualize.

APPENDIX E

Affinity adsorption of RRL ERAD components

RRL can be manipulated by affinity adsorption using immobilized recombinant proteins. One approach is to deplete components necessary for ERAD using ubiquitin conjugating proteins as bait. For example, an N-terminal ubiquitin fusion of UbcH5a (Ub-UbcH5a) depleted > 95% of Ufd1 from RRL in a single adsorption step (Figure E1A). His-tagged bait is first adsorbed onto Ni-NTA resin, which is then incubated in RRL to remove endogenous binding partners. Adsorbed proteins can be identified by elution and mass spectrometry. Using this approach, we found that RRL contained numerous Ub-UbcH5a binding proteins including Ufd2 (an E3 ubiquitin ligase), Isopeptidase T (a deubiquitinating enzyme), and p97 (an AAA-ATPase involved in ERAD) (Figure E1B). (see Note E1).

A. Reagents and supplies for purification of His-tagged recombinant proteins

1. Ni-NTA agarose (e.g. Qiagen, Inc., Valencia, CA)
2. *E. coli* strain BL21(DE3)
3. Expression vector (e.g. pET, pTrc, pQE)
4. L-broth: 7.5 g NaCl, 7.5 g tryptone, 15 g yeast extract. Bring to a volume of 1.5 L with water. Autoclave.
5. Ampicillin, 8 mg/ml (stock)
6. 20% glucose
7. 1 M IPTG (Sigma, St. Louis, MO)
8. Buffer D: 300 mM NaCl, 5% glycerol, 0.5 mM PMSF, 2 mM β-mercaptethanol, 50 mM Tris-HCl, pH 7.5. Add PMSF and β-ME prior to using.
9. Buffer E: Buffer D with 500 mM imidazole.
10. French Press (e.g. SLM-Aminco)

11. Econo-column (1 cm x 10 cm; cat # 737-1011) and flow adaptor (1 cm x 1-7 cm ; cat # 738-0014) (e.g. Biorad, Hercules, CA)

12. FPLC (e.g. Pharmacia model 500) with fraction collector

13. Dialysis tubing (e.g. Spectra/Por 12-14 kD MWCO; Spectrum Laboratorie Inc., Rancho Dominguez, CA)

14. Dialysis buffer: 100 mM NaCl, 1 mM β-mercaptoethanol, 25 mM Tris-HCl, pH 7.5

15. Centriplus concentrators (e.g. Amicon, Millipore Corp., Bedford, MA)

B. Reagents for RRL Affinity depletion

1. Ni-NTA agarose (Qiagen, Inc., Valencia, CA)
2. His-tagged recombinant protein
3. RRL (not nucleased, +/- hemin)
4. TNB buffer: 100 mM NaCl, 1 mM β-mercaptoethanol, 25 mM Tris-HCl, pH 7.5.
5. Wash buffer: TNB buffer + 20 mM imidazole.
6. High salt elution buffer: 1 M NaCl, 1 mM β-mercaptoethanol, 25 mM Tris-HCl, pH 7.5.
7. Imidazole elution buffer: TNB buffer + 500 mM imidazole

C. Purification of His-tagged recombinant proteins

Our lab uses several different expression vectors that include the pET family (Novagen), pTrc (Invitrogen), and the pQE family (Qiagen) and which allow the inducible expression (with IPTG) of the recombinant protein in *E. coli*. They also contain either an N- or C-terminal His tag. A T7 promoter allows the protein to be expressed in RRL or other cell free systems.

1. Transform BL21(DE3) *E. coli* with the plasmid containing your construct by heat shock (42°C for 1 min) and plating on LB/Amp plates (37°C).

2. Pick one colony and inoculate a 40 ml overnight culture: 39 ml LB + ampicillin (200 μg/ml final). Incubate in a 37°C shaker.

3. The next day inoculate a 1 L culture containing ~950 ml LB, ampicillin (200 μg/ml), 10 ml of 20% glucose, and 20 ml of overnight culture. Incubate at 37°C with continuous shaking until the OD_{600} is between 0.4 and 0.5. Induce expression of the recombinant protein by adding 400 μl of 1M IPTG and ampicillin (200 μg/ml) to the culture. Incubate at 37°C for 3 hours, and immediately place on ice.

4. Pellet bacteria by centrifuging at 2,400 x g for 10 min. Resuspend the pellets in ~80 ml of 1X PBS and then centrifuge at 2,000 x g for 30 minutes. Decant the supernatant and freeze the pellets at –20°C overnight.

5. Resuspend the pellets in lysis buffer (Buffer D + 10% Buffer E) and lyse using a French press (1250 psi; lyse twice). Pellet the membrane debris from the lysate by centrifuging at 19,000 x g for 40 minutes. Decant the cleared lysate into a 50 ml conical tube.

6. Load the lysate at a flow rate of 1 ml/min using either a peristaltic pump or FPLC onto a Ni-NTA column (5 ml beads in a 1 x 10 cm column) equilibrated in 10% Buffer E. After loading, wash the column with 50 ml of 5% Buffer E, followed by a 125 ml elution with a linear imidazole gradient (5% Buffer E to 100% Buffer E). Collect 25 x 5 ml fractions of the elution. Typically proteins elute between fractions 3-8. Analyze 10 μl of each fraction by SDS-PAGE followed by Coomassie Blue staining. Pool the fractions containing your protein (typically 5-6 fractions or 25-30 ml) and dialyze overnight at 4°C in 4 L of dialysis buffer.

7. Concentrate the dialyzed material using Centriplus concentrators with an appropriate MWCO. Store at –80°C in aliquots of 10 μl to 500 μl. Quantitate the recombinant protein using a suitable assay (i.e. Bradford or Lowry). Typically,

we obtain 10 mg/L culture, but actual yield varies significantly depending on expression and purification efficiency. (see Note E2).

D. RRL Affinity Depletion

1. Wash 100 µl of Ni-NTA beads with 2 x 1 ml of TNB buffer. Add 10 mg of His-tagged protein and bring volume to 1 ml with TNB buffer. Leave the control beads in 1ml of TNB buffer. Rotate the beads at 4°C for at least 30 minutes to bind the His-tagged protein. Then wash the beads with 6 x 1ml TNB buffer. (see Note E3).

2. After final wash remove as much buffer as possible from the beads, and add 500 µl of RRL. Rotate at 4°C at least 4 hours. Centrifuge briefly (16,000 x g for ~10 sec) and remove ~400 µl of the affinity depleted RRL (be careful to avoid contaminating the depleted RRL with beads containing the bait protein). Store at –80 °C in 100-200 µl aliquots. Efficiency of RRL depletion can be tested by immunoblotting and/or silver staining.

3. To identify bound proteins, remove the remaining supernatant and wash the beads 6-8 x 1 ml of wash buffer.

4. Elute the beads with 500 µl of elution buffer. We use two methods of elution. Imidazole elution buffer will elute virtually all bound RRL proteins and His-tagged bait. Because the excess His-tagged bait (and globin from RRL) often poses a problem in subsequent identification, we also elute with graded concentrations of high salt (0.5M, 1M, 1.5M, and 2M KCl or NaCl). 1 M salt is sufficient to disrupt many protein-protein interactions and release RRL proteins (Figure 1B).

5. To prepare eluates for analysis by mass spectrometry, the eluted proteins are concentrated by TCA precipitation (20% TCA, centrifuged at 16,000 x g for 10 min, washed with 50% acetone, and resuspended in SDS-LB, analyzed by SDS-

PAGE and silver stained (see Note E4). Selected protein bands are manually excised from the gel and trypsinized, and the resulting fragments are analysed by LC-MS-MS or MALDI-TOF MS and identified by mass fingerprinting. Specific conditions for sample preparation should be determined in conjunction with a suitable MS facility.

E. Notes

E1. For RRL depletion, the smallest bead volume possible should be used because degradation activity decreases significantly with dilution. We use a 5:1 (RRL:bead volume) ratio as a starting point. This causes less < 20% loss of degradation for the substrate CFTR. Control RRL is always "depleted" in parallel using empty Ni-NTA beads. Depleted RRL can then be compared with a mock depletion in standard degradation assays (see section 3.4.2) to determine if depleted factors are involved in substrate degradation.

E2. We typically purify only soluble proteins because of the likelihood of forming inclusion bodies with membrane proteins. Removing transmembrane segments from single spanning membrane proteins (e.g. ubc6) has also worked. Qiagen's manual, the QIAexpressionist, and references therein provide a good source of information on solubilizing inclusion bodies, various buffer conditions, etc.

E3. It may be necessary to titrate the amount of bait protein to load on the Ni-NTA beads. Qiagen indicates that the beads have a 10 mg/ml binding capacity for a 20 kD protein. Our lab has used primarily small monomeric proteins as bait, but larger or multimeric proteins (e.g. p97 and p47) may require much less material to saturate the beads.

E4. Not all silver staining protocols are compatible with MS. Typically, gluteraldehyde is used during the sensitization step, and formaldehyde is a component of the silver impregnation buffer. However, if MS analysis is desired the

protocol used for staining must be modified by omitting these reagents at the indicated steps. Additionally, 0.05% formaldehyde is used during the development step (Yan et al., 2000).

Figure E-1. Affinity depletion of RRL. RRL was depleted with Ub-UbcH5a or Ni-NTA beads (section 3.5.2). (A.) The depleted RRL was immunoblotted for ufd1. Essentially complete depletion of ufd1 was obtained from a single adsorption step. (B.) The beads used to deplete RRL were washed and eluted with either 0.5 M imidazole or 1 M KCl. The proteins were separated by SDS PAGE on a 7-12% gel and silver stained. Bands were excised, trypsinized and identified by MS analysis.

A.

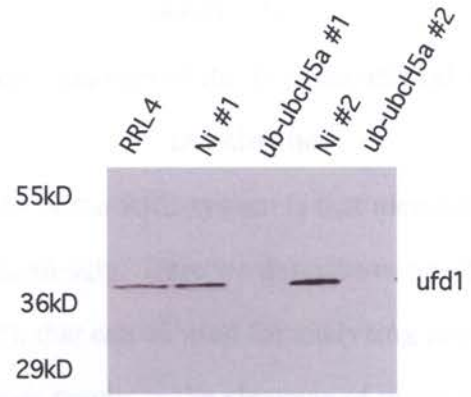
RRL 4
Ni #1
ub-ubcH5a #1
Ni #2
ub-ubcH5a #2
55kD
36kD
29kD
ufd1

B.

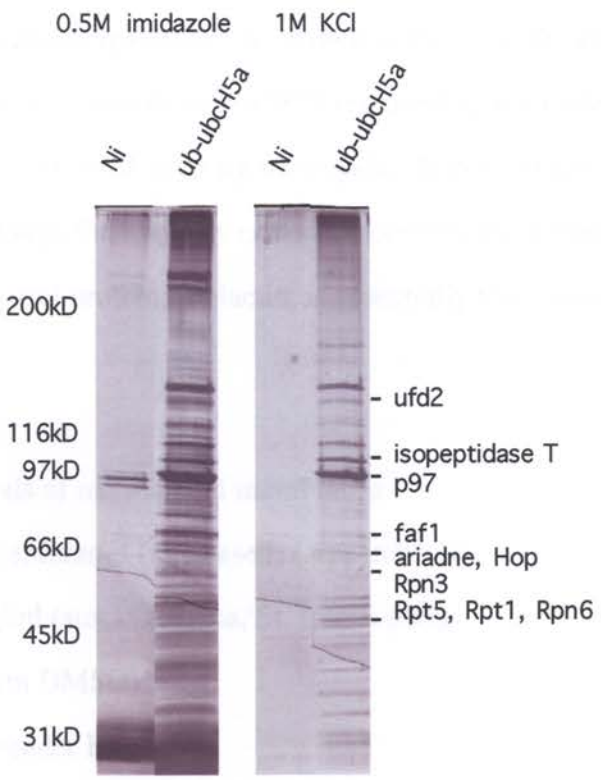
0.5M imidazole
1M KCl
Ni
ub-ubcH5a
Ni
ub-ubcH5a
200kD
116kD
97kD
66kD
45kD
31kD
ufd2
isopeptidase T
p97
faf1
ariadne, Hop
Rpn3
Rpt5, Rpt1, Rpn6

APPENDIX F

Inactivation and reconstitution of the translocational activity of microsomal membranes

One of the strengths of the RRL system is that membrane component parts can also be manipulated biochemically. Here we describe two techniques, proteolysis and alkylation (Gilmore, 1982), that can be used for analyzing membrane components of the ERAD pathway. Proteolysis results in the cleavage of many peripheral and integral membrane proteins, and alkylation modifies accessible cysteines. For example, microsomes are rendered incompetent for translocation when SRP receptor α subunit (SRα) is cleaved or alkylated (Andrews, 1989). Up to 80% of translocation activity can be restored, however, by adding recombinant SRα to treated membranes. The treated membranes can then be tested for release and removal of other endogenous membrane proteins and used in degradation reactions. As shown in Figure 2, the E2 enzyme, ubc6, is extremely sensitive to trypsinization with > 90% removed by incubation in 1 μg/ml trypsin, and more than 95% cleaved in 25 μg/ml trypsin. *In vitro* expressed Cue1 is slightly less sensitive although the majority is also cleaved from membranes by 1 μg/ml trypsin. The secretory control protein, prolactin, is essentially fully protected within the microsomal lumen.

A. Reagents for proteolysis of microsomal membranes

1. Microsomal membranes (nucleased) (Appendix B)
2. Trypsin, 4 mg/ml (stock) (Sigma, St. Louis, MO)
3. 0.1 M PMSF (in DMSO)
4. Buffer C (Appendix B)
5. Buffer F: 1 mM DTT, 50 mM triethanolamine-acetate, pH 7.5.
6. 4M KoAc

7. PK cushion: 0.5 M sucrose, 500 mM KoAc, 0.5 mM PMSF, 5 mM $Mg(oAc)_2$, 1 mM DTT, 50 mM Hepes-NaOH, pH7.5. Add PMSF just before using.
8. 0.5 M sucrose cushion (Appendix D)

B. Reagents for alkylation of microsomal membranes

1. Microsomal membranes (nucleased) (Appendix B)
2. 0.5 M sucrose cushion (-DTT): Appendix D. Do not add DTT.
3. Buffer C (-DTT): Appendix B. Do not add DTT.
4. 50 mM N-ethylmaleimide (NEM) (Sigma, St. Louis, MO)
5. 1 M DTT

C. Reagents for SRα repopulation of treated microsomal membranes

1. proteolysed or alkylated microsomal membranes (see below, sections D and E).
2. recombinant SRP receptor alpha subunit (Appendix E)
3. Buffer C: see Appendix B.
4. 0.5 M sucrose cushion: see Appendix D.

D. Proteolysis of microsomal membranes

This procedure is performed on ice and in a cold room. It is necessary to empirically determine the optimal concentration of protease for a given microsomal membrane preparation. We have obtained similar results with both trypsin and proteinase K.

1. Dilute 100 µl of membranes in Buffer F followed by the addition of 0, 1, 2, 5, 10, and 25 µl of 100 µg/ml trypsin for a total volume of 1ml. Mix thoroughly and incubate on ice for 1 hour.
2. Add 10 µl of 50 mM PMSF (0.5mM final concentration) to each reaction and incubate on ice for 15 minutes to inactivate the protease.
3. Add 144 µl of 4M KoAc (0.5 M final concentration) to each reaction and then layer the mixture on 1.2 ml of PK cushion. Centrifuge for 10-15 minutes at

180,000 x g. Resuspend the membrane pellet in 200 µl Buffer C (see Appendix D, sections B and Note D1).

4. Layer the resuspended pellet on 300 µl of 0.5 M sucrose cushion and centrifuge at 180,000 x g for 10-15 minutes.

5. Resuspend the pellets in 100 µl Buffer C. Freeze in liquid nitrogen and store at –80°C in 20-25 µl aliquots. SRα repopulation can also be done at this time (see below, section F).

6. To determine the amount of protein remaining associated with the membranes, remeasure the OD_{280} as described in Appendix B.

E. Alkylation of microsomal membranes

1. Layer 50 µl of membranes on 300 µl of 0.5 M sucrose cushion (-DTT) and centrifuge for 10 minutes at 180,000 x g. Resuspend the pellet in 50 µl of Buffer C (-DTT).

2. Split the resuspended membranes into two 25 µl aliquots. To one add 1 µl of 50 mM NEM (2mM final) and to the other add 1 µl of ddH2O. Incubate at 24 °C for 30 minutes.

3. Add 0.5 µl of 1M DTT (20 mM final) to each tube to quench the reaction. Freeze in liquid nitrogen and store at –80°C in 10-25 µl aliquots. SRα repopulation can be done also be done at this time (see below, section F). The final step of the repopulation protocol is pelleting the membranes through a 0.5 M sucrose cushion and resuspending in Buffer C, so the high concentration of DTT is not maintained. Also, it has been shown that excess DTT does not affect translocation (Gilmore, 1982).

F. SRα repopulation of treated microsomal membranes

Both treatments described above disrupt ER targeting due to cleavage or modification of SRα (Walter and Blobel, 1981). By adding recombinant SRα to the treated membranes, this activity can be restored (Figure F1). We use a soluble His-tagged fragment missing

the N-terminal 152 amino acids that is equivalent to the fragment produced by trypsinization (Andrews, 1989). The concentration of SRα needed to repopulate a particular membrane preparation must be determined empirically as excess SRα will inhibit translation. This can be tested by repopulating mock treated membranes with recombinant SRα.

1. To repopulate 20 μl of membranes add 1 μg of recombinant SRα/ μl of membranes. Incubate on ice for 30-60 min.
2. Bring the volume up to 100 μl with Buffer C, and layer the mixture on 300 μl of 0.5M sucrose cushion. Centrifuge at 180,000 x g for 10 minutes to remove unbound SRα.
3. Resuspend the pellet in 20 μl of Buffer C. Freeze in liquid nitrogen and store at $-80^{\circ}C$.

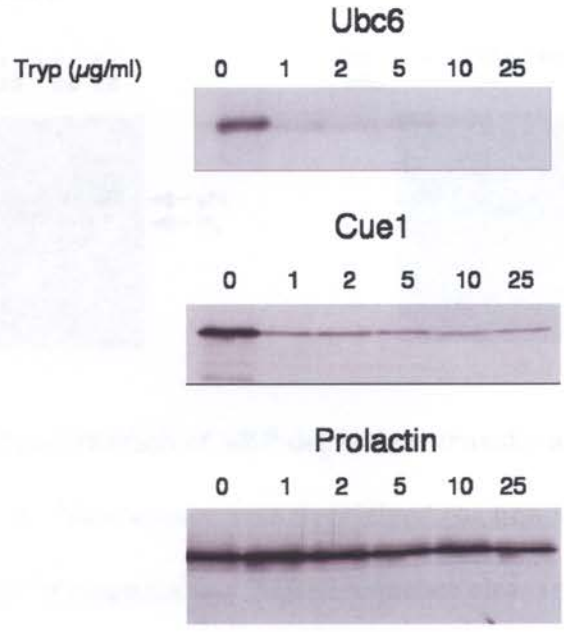

Figure F-1. Trypsinization of microsomal membranes. The indicated proteins were translated *in vitro* in the presence of ER microsomes (section 3.3.2). The membranes were pelleted through a 0.5 M cushion and subjected to limited proteolysis with increasing concentrations of trypsin (section 3.6.1). The membranes were then solubilized in SDS-LB and resolved by SDS PAGE and autoradiography. Ubc6, an ER-localized E2 enzyme, is highly sensitive to trypsinization, even at 1mg/ml of trypsin. Cue1 is slightly less sensitive, and the secretory protein, prolactin, is protected within the lumen of the ER.

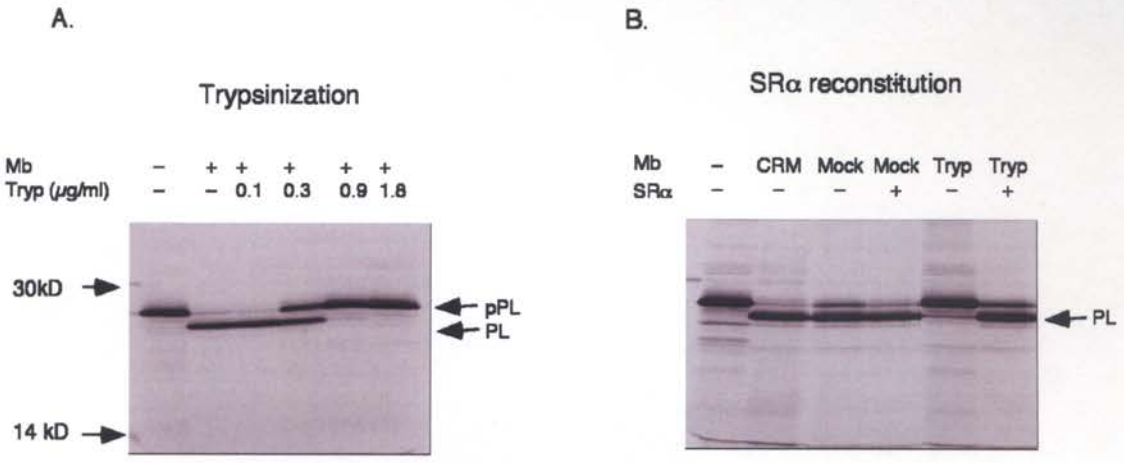

Figure F-2. Reconstitution of SRP dependent translocation in proteolyzed microsomes. (A.) Microsomes were trypsinized (section 3.6.1) and used for *in vitro* translations of preprolactin. Signal sequence cleavage no longer occurs at 0.9 μg/ml trypsin, indicating microsomes are incompetent for translocation. (B.) Adding recombinant SRα to trypsinized microsomes (section 3.6.3) restores translocation activity as demonstrated by signal sequence cleavage of preprolactin.